Theses and Dissertations   1. Thesis and Dissertation Collection, all items

1997-09

Extratropical transition of Western North Pacific tropical cyclones

Klein, Peter M.

Monterey, California. Naval Postgraduate School

http://hdl.handle.net/10945/8384

NAVAL POSTGRADUATE SCHOOL
Monterey, California

THESIS

EXTRATROPICAL TRANSITION OF WESTERN NORTH PACIFIC TROPICAL CYCLONES

by

Peter M. Klein

September, 1997

Thesis Co-Advisors: Russell L. Elsberry
                        Patrick A. Harr

Approved for public release; distribution is unlimited.

REPORT DOCUMENTATION PAGE

Form Approved OMB No. 0704-0188

1. AGENCY USE ONLY *(Leave blank)*	2. REPORT DATE September 1997.	3. REPORT TYPE AND DATES COVERED Master's Thesis

4. TITLE AND SUBTITLE EXTRATROPICAL TRANSITION OF WESTERN NORTH PACIFIC TROPICAL CYCLONES	5. FUNDING NUMBERS
6. AUTHOR(S) Peter M. Klein	

7. PERFORMING ORGANIZATION NAME(S) AND ADDRESS(ES) Naval Postgraduate School Monterey CA 93943-5000	8. PERFORMING ORGANIZATION REPORT NUMBER

9. SPONSORING/MONITORING AGENCY NAME(S) AND ADDRESS(ES)	10. SPONSORING/MONITORING AGENCY REPORT NUMBER

11. SUPPLEMENTARY NOTES The views expressed in this thesis are those of the author and do not reflect the official policy or position of the Department of Defense or the U.S. Government.

12a. DISTRIBUTION/AVAILABILITY STATEMENT Approved for public release; distribution is unlimited.	12b. DISTRIBUTION CODE

13. ABSTRACT *(maximum 200 words)*

Extratropical transition (ET) of a tropical cyclone (TC) often results in a mid-latitude storm that threatens maritime and coastal interests. Cases of ET between 1 July through 31 October during 1994-1996 are reviewed using Navy Operational Global Atmospheric Prediction System (NOGAPS) analyses and hourly geostationary satellite imagery. Current conceptual models are found to be inadequate to explain the physical processes in ET. ET is redefined to have two stages: *transformation*, where the TC is transformed from a warm-core vortex into a baroclinic, cold-core extratropical cyclone, and *re-intensification*, where the transformed TC either deepens or dissipates, depending on the existence of upper-tropospheric support for extratropical cyclogenesis. ET is further defined in terms of two characteristic mid-latitude synoptic patterns: *meridional*, in which the cyclones have meridional tracks and tend to re-intensify less vigorously than *zonal*, which have zonal tracks and may deepen explosively. Review of NOGAPS 500-mb anomaly correlation scores in 1996 demonstrated that ET may be associated with significant NOGAPS errors. Sea-level pressure forecasts during ET events involving a merger tend to be too deep. In ET cases of rapidly deepening storms, NOGAPS tends to overforecast their intensity during transformation, and then underforecast during re-intensification. Rules of thumb are provided to assist forecasters in improving predictions of the track and intensity of storms undergoing ET.

14. SUBJECT TERMS Extratropical transition, Transformation, Re-Intensification, Meridional transitions, Zonal transitions, Extratropical transition forecast error.	15. NUMBER OF PAGES 101
	16. PRICE CODE

17. SECURITY CLASSIFICATION OF REPORT Unclassified	18. SECURITY CLASSIFICATION OF THIS PAGE Unclassified	19. SECURITY CLASSIFICATION OF ABSTRACT Unclassified	20. LIMITATION OF ABSTRACT UL

NSN 7540-01-280-5500

Standard Form 298 (Rev. 2-89)
Prescribed by ANSI Std. 239-18 298-102

EXTRATROPICAL TRANSITION OF WESTERN NORTH PACIFIC TROPICAL CYCLONES

Peter M. Klein

Lieutenant Commander, United States Navy

B.S., Cornell University, 1988

Submitted in partial fulfillment
of the requirements for the degree of

MASTER OF SCIENCE IN METEOROLOGY AND PHYSICAL OCEANOGRAPHY

from the

NAVAL POSTGRADUATE SCHOOL

September 1997

ABSTRACT

Extratropical transition (ET) of a tropical cyclone (TC) often results in a mid-latitude storm that threatens maritime and coastal interests. Cases of ET between 1 July through 31 October during 1994-1996 are reviewed using Navy Operational Global Atmospheric Prediction System (NOGAPS) analyses and hourly geostationary satellite imagery. Current conceptual models are found to be inadequate to explain the physical processes in ET. ET is redefined to have two stages: _transformation_, where the TC is transformed from a warm-core vortex into a baroclinic, cold-core extratropical cyclone, and _re-intensification_, where the transformed TC either deepens or dissipates, depending on the existence of upper-tropospheric support for extratropical cyclogenesis. ET is further defined in terms of two characteristic mid-latitude synoptic patterns: _meridional_, in which the cyclones have meridional tracks and tend to re-intensify less vigorously than _zonal_, which have zonal tracks and may deepen explosively. Review of NOGAPS 500-mb anomaly correlation scores in 1996 demonstrated that ET may be associated with significant NOGAPS errors. Sea-level pressure forecasts during ET events involving a merger tend to be too deep. In ET cases of rapidly deepening storms, NOGAPS tends to overforecast their intensity during transformation, and then underforecast during re-intensification. Rules of thumb are provided to assist forecasters in improving predictions of the track and intensity of storms undergoing ET.

TABLE OF CONTENTS

ACKNOWLEDGMENT

I. INTRODUCTION

Extratropical transition (ET) of western North Pacific tropical cyclones (TCs) often results in the development of powerful, mid-latitude cyclones capable of causing significant damage to property and loss of life. Optimum Track Ship Routing (OTSR) recommendations take into account the climatologically benign winds and waves typically observed during summer and early autumn in the western North Pacific. Therefore, many trans-ocean voyages are planned at higher latitudes, which minimizes distances while avoiding TCs and foul weather. The hazards associated with a TC are typically well understood and respected. Often, little expectation exists that a TC beginning an ET may result in a rapidly deepening, mid-latitude cyclone with gale- or storm-force winds that pose a serious threat to maritime and coastal interests at higher latitudes. Furthermore, the thermodynamic and dynamical processes responsible for ET are poorly understood and not well defined. Numerical weather prediction (NWP) models often fail to properly forecast the transition timing and subsequent evolution of the mid-latitude cyclone, and thus may have significant motion and intensity errors. In summary, forecasters often have difficulty anticipating, recognizing, and forecasting ET, which impacts their ability to disseminate accurate high wind, high seas, or flash flood warnings when warranted.

Matano and Sekioka (1971; hereafter MS) defined two characteristic types of ET, which they labeled as "complex" and "compound" transformations.[1] A complex transfor-

---

[1] Replacement of the term "transformation" with "transition" will be described later.

1
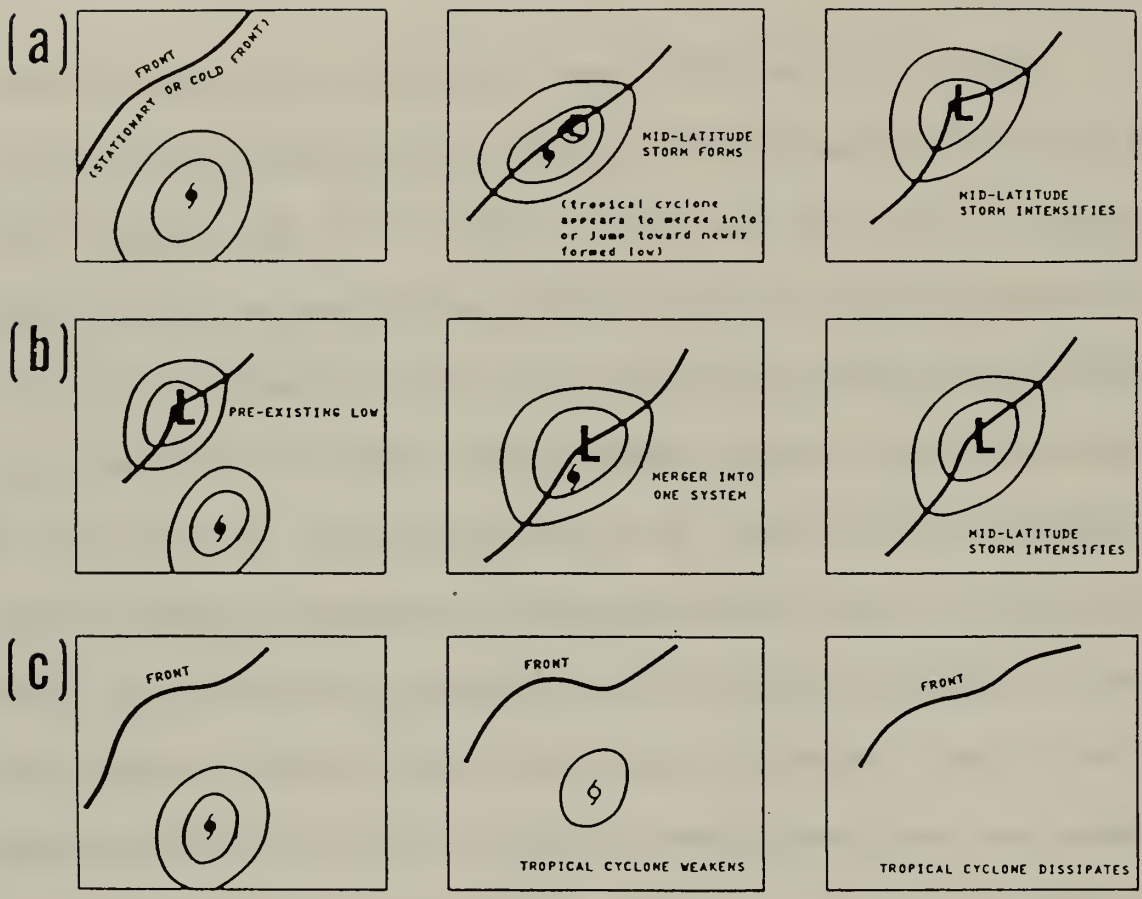
Fig. 1. The three types of ET, including (a) complex, (b) compound, and (c) dissipating transformations (Brand and Guard 1978).

mation (Fig. 1a) occurs when a pre-existing mid-latitude front or trough interacts with a TC to produce a new extratropical cyclone on the front or trough. A compound transformation (Fig. 1b) results when a pre-existing mid-latitude cyclone appears to merge with a TC such that the mid-latitude low usurps the TC and intensifies.

Brand and Guard (1978) defined a third type of transformation in which the TC simply dissipates after recurvature into extratropical latitudes (Fig. 1c). Willoughby (1979) described

a process in which a TC moving over colder water experiences a decrease in central convection organization due to decreasing equivalent potential temperature (θ_e) of air entering the eyewall clouds. As the eyewall clouds dissipate, air converging in the friction layer may only ascend to the top of the boundary layer before diverging outward in the lower troposphere. This process decouples the lower part of the TC from the upper circulation, and ultimately results in the decay of the warm-core aloft and a spin-down of the upper portion of the TC.

DiMego and Bosart (1982) studied the complex transformation of Hurricane Agnes in 1972 as Agnes moved into a baroclinic zone over land. They suggested low-level heating and cyclonic vorticity associated with the remnants of Agnes combined with upper-level positive vorticity advection (PVA) above the baroclinic zone to permit the complex transformation of Agnes into an extratropical cyclone through archetypal Petterssen "Type B" development. Based on a case study of Tropical Cyclone Patsy in the western South Pacific, Sinclair (1993) suggested that the coupling of Patsy's remnants to a 200-mb subtropical jet streak played a significant role in the ET of Patsy. Foley and Hanstrum (1994) identified two types of ET along the west coast of Australia. Those TCs caught in the pre-cold frontal westerlies were said to be "captured" (a category similar to what MS defined as complex). Those that translated poleward (southward) while remaining in a synoptic pattern with easterly flow to poleward were said to be "cradled." This category has no analog with the definitions of MS.

Harr et al. (1996) demonstrated through the use of empirical orthogonal functions (EOFs) and principal component (PC) analysis that ET is influenced by characteristic 500-mb

circulation patterns into which a TC is translating. Specifically, the third EOF (EOF-3) featured high (low) PC amplitudes that corresponded to a more zonal (meridional) track during transition (see Chapter III). Furthermore, it was shown that transitioning TCs can greatly impact the accuracy of Navy Operational Global Atmospheric Prediction System (NOGAPS) forecasts.

The terms "transformation" and "transition" have been used interchangeably in the literature to refer to the types of ET defined by MS. Because this results in confusion, the term "transition" will be used here to describe the three types of ET defined above (Fig. 1), while the term "transformation" will refer to the process by which a TC changes from a tropical, warm-core system to a baroclinic, extratropical low.

Storms resulting from ET pose a unique threat to vessels using high latitude shipping routes during the summer and early autumn months. In this study, all ETs that occurred in the western North Pacific from 1 July through 31 October during 1994-1996 were examined using NOGAPS analyses and Geostationary Meteorological Satellite (GMS) imagery. The complex transition of Typhoon Ivy during September 1994 (Fig. 2) is a classic example of the conceptual model of MS, while a textbook case of compound transition is depicted in Fig. 3 for Typhoon Joy during August 1996.

As in Fig. 1a, Ivy at the initial time (Fig. 2a) is located ahead of an approaching cold front. In Figs. 2b and 2c, Ivy starts the process of transformation into a baroclinic system while still downstream of the cold front. In Fig. 2d, the transformation of Ivy is nearly complete. It is important to note that the cold front never intersects or overtakes Ivy, and that Ivy does not transform on the front. Instead, Ivy draws cold, dry air from behind the
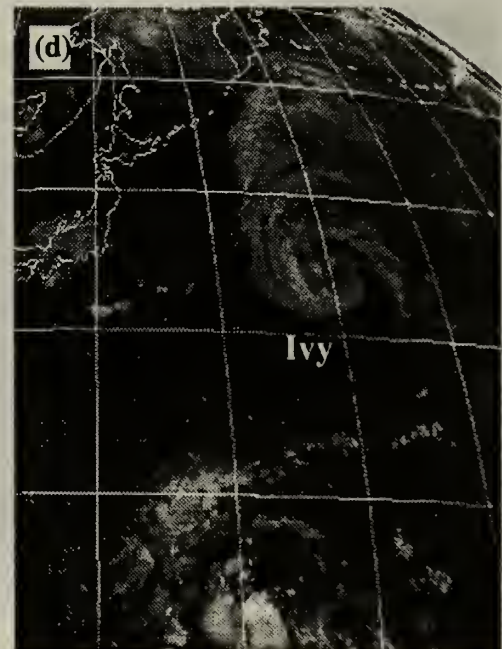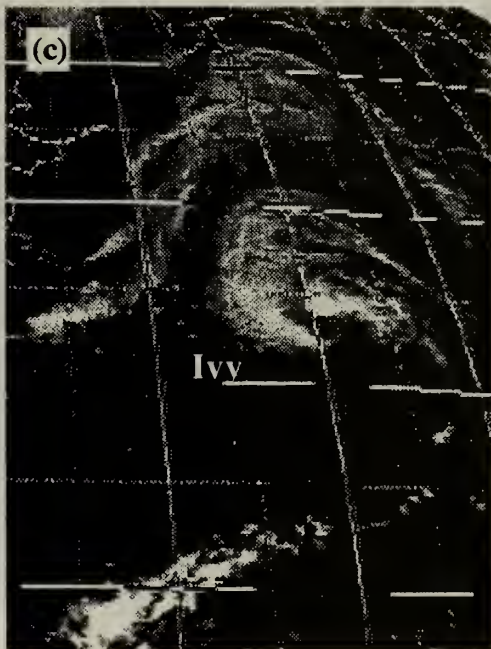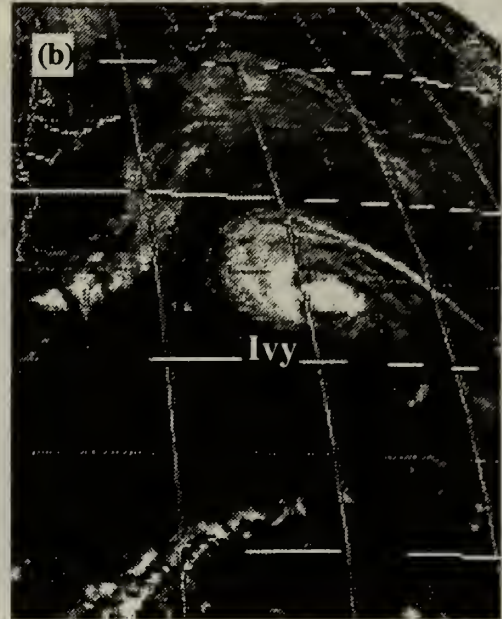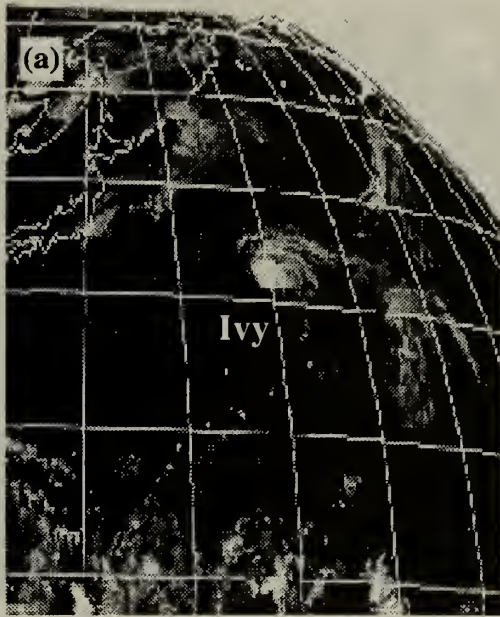
Fig. 2. Infrared imagery of the complex ET of Typhoon Ivy at (a) 1200
UTC 1 September, (b) 0300 UTC 2 September, (c) 0600 UTC 2 September,
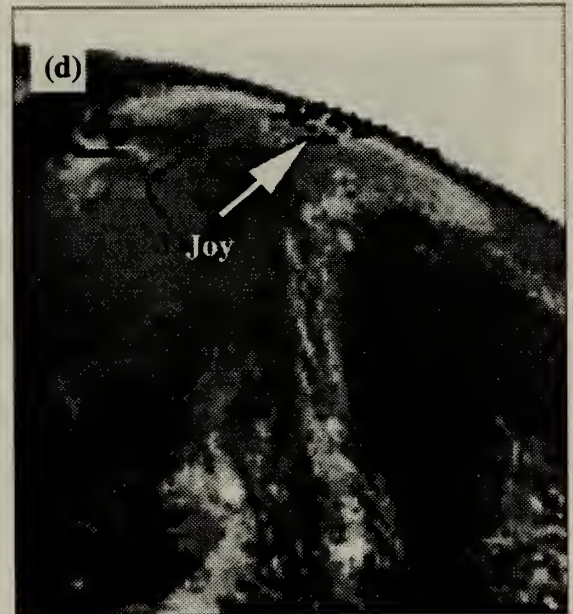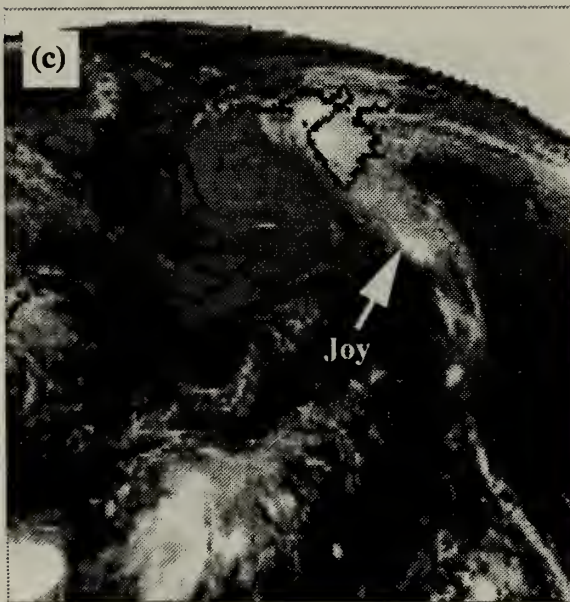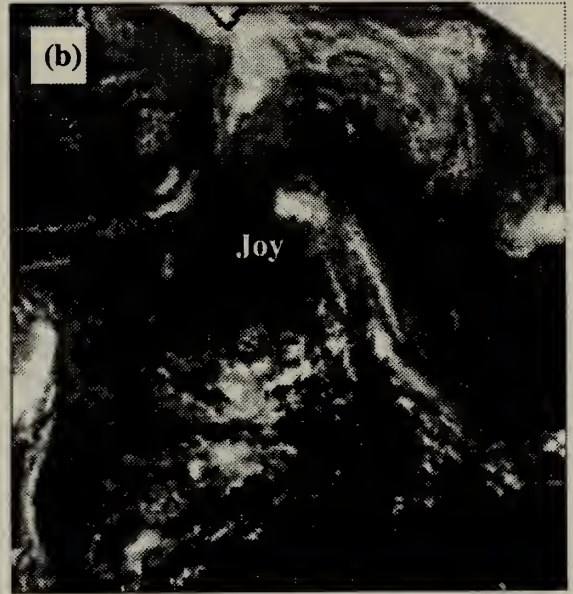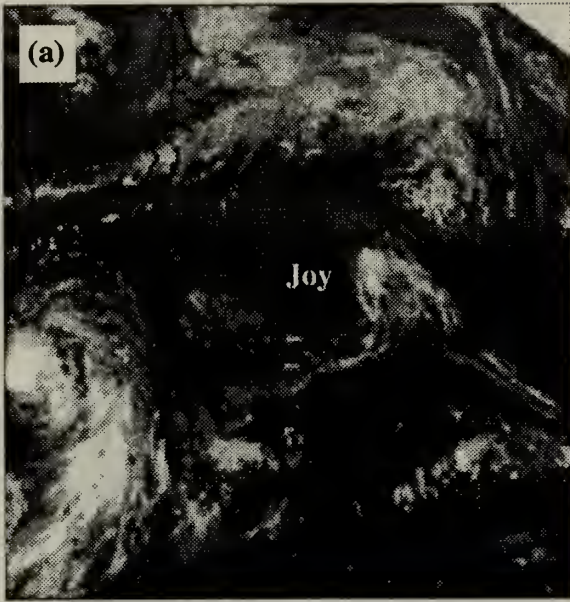and (d) 1200 UTC 2 September 1994.

5

Fig. 3. Infrared imagery of the compound ET of Typhoon Joy at (a) 0632
UTC 4 August, (b) 0632 UTC 5 August, (c) 0632 UTC
6 August, and (d) 0632 UTC 7 August 1996.

front into its surface circulation, with the resulting cross-frontal flow severing the front and sweeping it onto one of Ivy's rainbands (Fig. 2d). By contrast, Typhoon Joy at the initial time (Fig. 3a) is south and east of a pre-existing, mid-latitude low (compare to Fig. 1b). In Figs. 3b and 3c, Joy is translating poleward and overtaking the pre-existing low, while the beginning of a merger of Joy and the pre-existing low is depicted in Fig. 3d.

It became obvious early in this review of the 1994-1996 cases that the conceptual models of MS were inadequate in classifying, describing, and understanding ET. Many transitions that occurred during the period did not resemble in appearance or description those defined by MS, as represented in Figs. 1 through 3. For instance, many transitions occurred in the absence of any surface fronts or mid-latitude cyclones, which makes classification using the definitions of MS difficult. Some transitions occurred downstream of a 500-mb trough, in a baroclinic zone (e.g., near the coast of Japan), or over the open ocean. None of these possibilities are well represented by the conceptual model of MS. In another case (Typhoon Kirk) during 1996, the 500-mb circulation of a pre-existing mid-latitude cyclone coupled with the intact surface circulation of Kirk to form one new, extratropical low. Not one complex transition was observed to occur on a cold front, and no surface fronts were observed to have intersected with or cut through a TC as suggested in the complex transition conceptual model of MS (Fig. 1a). Furthermore, MS describes the phenomena in terms of surface pressure patterns only, which does not explicitly acknowledge the contributions of the mid- and upper-tropospheric circulations to ET. All of these deficiencies illustrate that the conceptual model of MS does not describe or explain in a satisfactory way the key dynamics and thermodynamics that are responsible for ET.

The resistance to radial deflections in a TC may be expressed in terms of the inertial frequency

$$I^2 = (f_o + \zeta)(f_o + 2v/r) , \qquad (1.1)$$

where f_o is the Coriolis parameter, ζ is the relative vorticity, v is the tangential velocity, and r is the radius. Because lower-troposphere I^2 values are high near the center of a mature TC, the TC exhibits high resistance to radial motions until it begins to decay. Therefore, TCs should be expected to resist direct momentum interaction with surface fronts and troughs. Thus, these surface features should not penetrate, intersect, or cut through the TC, which is consistent with the TCs observed during this period. Rather than directly interact with surface fronts during complex transition as in Fig. 1a, the TCs remained in the pre-frontal flow ("captured" using the terminology of Foley and Hanstrum). The TC then drew cold, dry air from behind the front into the storm. In cases where no cold front is present upstream of the TC, the TC may still ingest colder, drier air from a continental source, or from oceanic regions with low sea-surface temperatures (SSTs). Inflow of cold, dry air should be expected to weaken the convective clouds that induce or sustain the TC warm core, and the subsequent reduction in lower-tropospheric winds will decrease the I^2 values and diminish the resistance to radial deflections. This sequence would then permit accelerated intrusion of cold, dry air, which further reduces lower-tropospheric I^2 values and hastens the decay of the TC. As the TC translates poleward and moves over still lower SSTs, the continued cold, dry inflow into the TC should make it impossible for the TC to sustain its warm core. In the presence of a baroclinic zone, the TC may be transformed from a warm-core vortex into an extratropical, low, with cold, dry air to the west and warm, moist inflow to the east, and baroclinic tilt from

8

the surface to 500 mb and 200 mb (Klein et al. 1997). This stage of ET will be referred to in this thesis as the *transformation* stage.

With the completion of transformation into a baroclinic low, it is hypothesized that a new source of upper-level divergence and momentum is required if this system is to continue to deepen and intensify through baroclinic processes. The phasing of the mid-latitude upper-tropospheric flow that is favorable for extratropical cyclogenesis is to have PVA and upper-tropospheric divergence above the transformed low-troposphere circulation, which facilitates further surface pressure decreases. If large PVA and upper-level divergence become superposed over the low-level baroclinity of the transformed TC, an explosive, Petterssen "Type-B" extratropical cyclogenesis may result. Without this, the transformed TC remnants may only slowly deepen or may dissipate. Such an upper-troposphere influence in ET was demonstrated in the case studies by DiMego and Bosart (1982) and Sinclair (1993). This stage of ET will be referred to in this thesis as the *re-intensification* stage. Those storms that lack upper-tropospheric support and do not re-intensify will be described as having failed ET and will continue to be referred to as dissipators.

In compound cases, the TC would transform as described above, and then approach a pre-existing mid-latitude low. The transformed TC would serve as a source of low-level vorticity and warm advection south and east of the pre-existing low, which is hypothesized to maintain or increase its intensity. The pre-existing low might appear to completely absorb the transformed TC, or the mid- and upper-level circulation of the low could couple with the low-level circulation of the transformed TC (Klein et al. 1997).

Chapter II describes the definitions and methods used to examine ET in this period and includes a discussion of the statistics of each type of transition. In Chapter III, the thermodynamics and dynamics of ETs that occurred during this period of study are described, leading to the definition of ET as having two stages (transformation and re-intensification). The critical role of the upper-tropospheric flow in ET will also be emphasized. Results of EOF analysis will be used to suggest two types of transitions (*meridional* and *zonal*) based on characteristic, synoptic 500-mb patterns. In Chapter IV, the potentially negative impact of ET on NOGAPS forecast accuracy in the middle latitudes is described, with a detailed review of forecast track and sea-level pressure (SLP) errors during ET cases from 1 July through 31 October 1996. In Chapter V, the results of this study will be summarized. In addition, conclusions and recommendations, including forecast rules of thumb, NOGAPS model tendencies observed during ET, and suggested areas for future research will be presented.

II. DATA AND ANALYSIS PROCEDURES

A. DEFINITIONS

A TC is defined here to have become extratropical based on the Joint Typhoon Warning Center (JTWC) criteria, which consider both the latitude and the intensity of the TC. These criteria include a shearing of the central dense overcast (CDO) observed in the satellite imagery, and requires that the TC move into the axis of the polar jet. All TC track and location information in this study are derived from JTWC verifying ("best track") positions. Generally, ET follows recurvature of the TC, which is defined in this study to occur when the motion direction changes from westward to eastward as the TC passes through the subtropical ridge axis. The ET process can begin before recurvature and before JTWC determines that the TC has become extratropical.

B. METHOD

Archived NOGAPS analyses and forecasts at 12-h intervals for sea level, 500 mb and 200 mb with 2.5° latitude/longitude resolution were available throughout the study. After 1 September 1996, 1° latitude/longitude resolution NOGAPS analyses and forecasts were also available. A new data source was water vapor winds for the 1996 NOGAPS analyses. Each TC that completed ET was studied using GMS-4 and -5 imagery at 12-h intervals (00 UTC and 12 UTC). Each analysis began no less than 48 h before the TC became extratropical according to JTWC, and continued until at least 24 h after the transition appeared to be complete.

11

Classification of all ET cases was initially attempted using the definitions of MS. As discussed in Chapter I, this was impossible due to the flaws that existed in the conceptual model of MS. Thus, one aim of this study was to use the model of MS anyway so that all of its shortcomings could be identified and exploited to produce an improved conceptual model of ET. This required modification of the definitions so that all cases of ET studied could be forced into the classification scheme based on the conceptual model of MS. Cases in which a transformed TC coupled or merged with a pre-existing mid-latitude low were described as a compound ET. Any transition beginning ahead of a cold front, over a baroclinic zone, or over decreasing SSTs that eventually resulted in à re-intensified extratropical cyclone was classified as complex. Any transition that failed to re-intensify after transforming into a baroclinic system (i.e., SLPs continually increased after transformation) was classified as a dissipator.

This classification effort highlighted those cases in which the definitions of MS failed to describe properly or classify a case of ET. These cases were investigated further, especially in terms of dynamic and thermodynamic processes that might be similar. In this way, representative stages of ET were described and new classifications of transition types were defined. Unlike the surface-based definitions of MS, three-dimensional aspects of the physical processes were sought to better describe observations of the transition of the TC.

The NOGAPS analysis and forecast fields were compared to determine forecast errors associated with ET. This comparison included a review of Fleet Numerical Meteorology and Oceanography Center (FNMOC) NOGAPS 500-mb height anomaly correlation scores over the North Pacific region from 20°N to 80°N and 120°E to 180°. The hypothesis was that

improper handling of the complex interactions during ET contributed to NOGAPS forecasts of ET that were particularly poor, i.e., one standard deviation below the mean monthly anomaly correlation score.

C. STATISTICS

Using the definitions of MS modified as described in section B of Chapter II, cases of ET from 1 July through 31 October during 1994-1996 were classified. During this period, 73 TCs of tropical storm intensity or greater occurred. Twenty-six (36%) of these TCs completed ET. Of these 26 cases of ET, 14 were complex, three were compound, and nine were dissipators. At least during this three-year period, compound transitions occur infrequently. In the nine dissipator cases, five failed to complete a complex transition, one unsuccessfully attempted a compound transition, and the remaining three dissipated quickly after becoming extratropical (one of them over land). These statistics are stratified below by month (Table 1) and year (Table 2). Notice in Table 1 that most ET cases occur in September, which is when TCs are most numerous. Half of all complex cases (seven of 14) also occurred during September, which is when transiting mid-latitude lows begin to translate farther south than in summer months, which allows deeper equatorward intrusions of cold air. Notice in Table 2 that the relative distribution of ET cases is the same each year of the study. That is, complex transitions occurred most frequently, with fewer dissipators and fewer, if any, compound cases. Ten cases occurred in 1994 and 1996, while only six occurred in 1995. This suggests that there is interannual variability in the number of cases of ET.

	July	August	September	October
Complex	2	2	7	3
Compound	0	2	1	0
Dissipator	2	2	3	2
Total	4	6	11	5

Table 1. Number of cases of ET stratified by month, 1994-1996.

	1994	1995	1996
Complex	5	4	5
Compound	1	0	2
Dissipator	4	2	3
Total	10	6	10

Table 2. Number of cases of ET during 1 July through 31 October, stratified by year.

Carr and Elsberry (1994) developed a systematic approach to TC track forecasting that included classification of TCs based on synoptic patterns and regions. Characteristic tracks were found in each synoptic pattern and region. Of the 26 cases of ET during this period, 12 were in the Poleward pattern/Accelerating Westerlies region (P/AW) prior to commencing transition, and seven were in the Standard pattern/Accelerating Westerlies region (S/AW). A total of 19 cases (73%) were therefore in an AW region. Another six cases were in the Poleward pattern/Poleward-Oriented region (P/PO).

During the period of study, 19 (86%) of the 22 TCs that were in the AW region completed ET. A TC often commences ET after recurvature, where interaction with the westerlies and the polar jet should be expected. For this reason, it is not surprising that a majority of TCs that enter the AW region also complete ET, and that most of the cases of ET studied herein came from the AW region.

III. GENERAL CHARACTERISTICS OF EXTRATROPICAL TRANSITION

A. TRANSFORMATION

Using procedures described in Chapter II, each TC that completed ET was studied using both satellite imagery and NOGAPS analyses. In 24 of the 26 cases of ET, a similar sequence of events associated with the onset and progress of transformation was identified in the GMS-4 and -5 IR imagery. This sequence is depicted in Fig. 4 in the case of Super Typhoon (STY) Oscar in September 1995. As Oscar began to ingest cold, dry air from the north and west, convection in the southeastern quadrant of the storm began to weaken, with a characteristic dry slot forming (Fig. 4b). Continued inflow of cold, dry air resulted in accelerated weakening of convection as the dry slot wrapped farther around Oscar (Fig. 4c), until deep convection in the eastern and southern quadrants of the storm almost ceased (Fig. 4d). Finally, an overrunning, hook-shaped pattern of convection to the north and west was all that remained of Oscar's circulation (Fig. 4e).

The appearance of these events is similar in the cases of Typhoon Dan in July 1996 (Fig. 5), Typhoon Joy in August 1996 (Fig. 6) and Typhoon Zane in October 1996 (Fig. 7). Oscar and Dan were complex cases, while Joy was a compound case, and Zane was a dissipator. Whereas Oscar was a large and intense super typhoon, Zane was average in size and intensity, Dan was average in size but not very intense, and Joy was both small and weak. The general characteristic evolution illustrated in these four cases was therefore not unique to a certain size or intensity of TC, or type of ET, and was observed in all but two cases of ET as mentioned above. This implies that satellite imagery cannot be used effectively to dis-
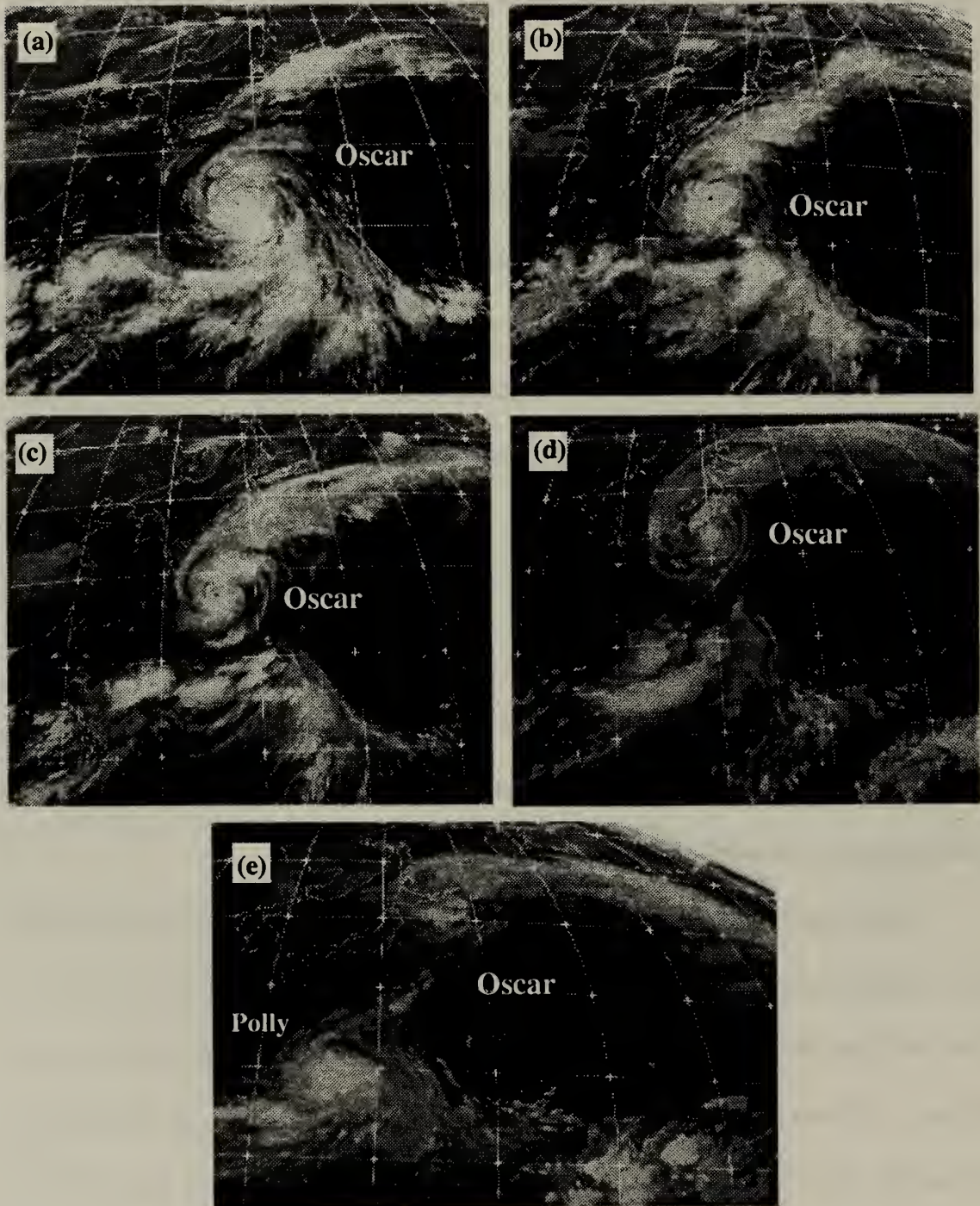
Fig. 4. Infrared imagery of Super Typhoon Oscar at (a) 0000 UTC 15 September, (b) 1200 UTC 15 September, (c) 0000 UTC 16 September, (d) 0000 UTC 17 September, and (e) 1200 UTC 17 September 1995. The start of transformation is depicted in (b).
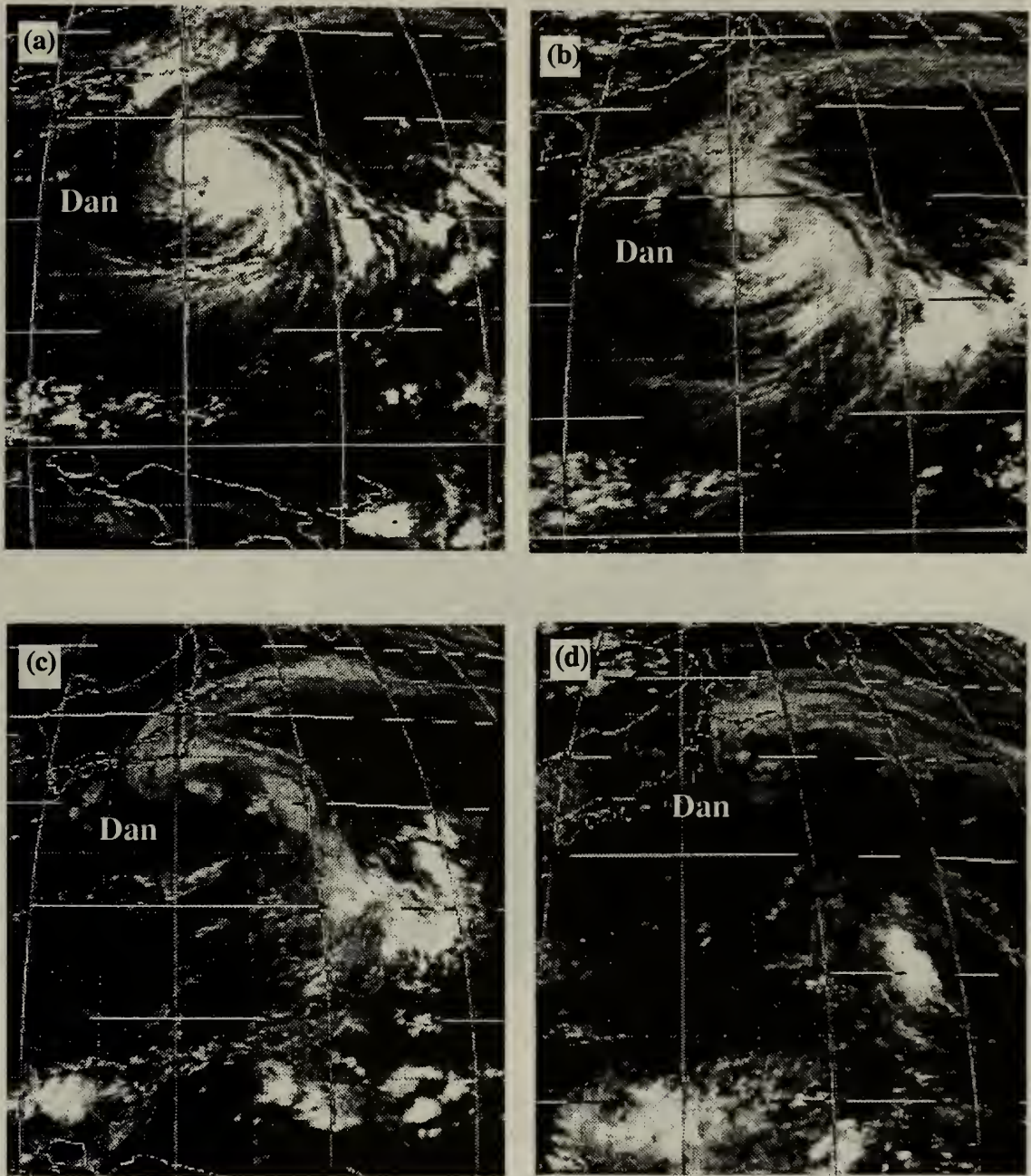
Fig. 5. As in Fig. 4, except for transformation of Typhoon Dan at (a) 0033 UTC 9 July,
(b) 0933 UTC 9 July, (c) 0033 UTC 10 July, and (d) 0033 UTC 11 July 1996.
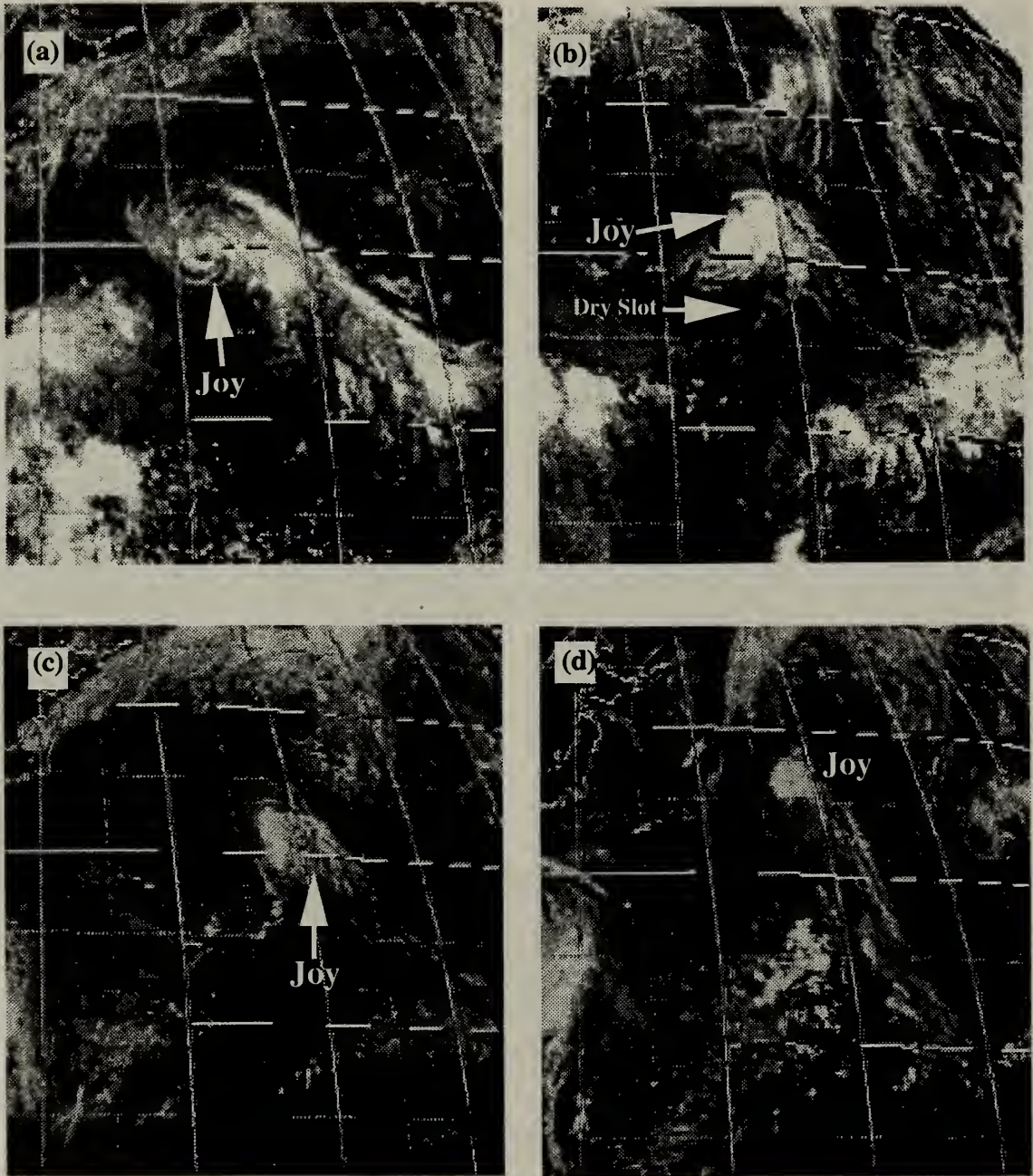
19

Fig. 6. As in Fig. 4, except for transformation of Typhoon Joy at (a) 0933 UTC
1 August, (b) 0933 UTC 3 August, (c) 0933 UTC 4 August, and
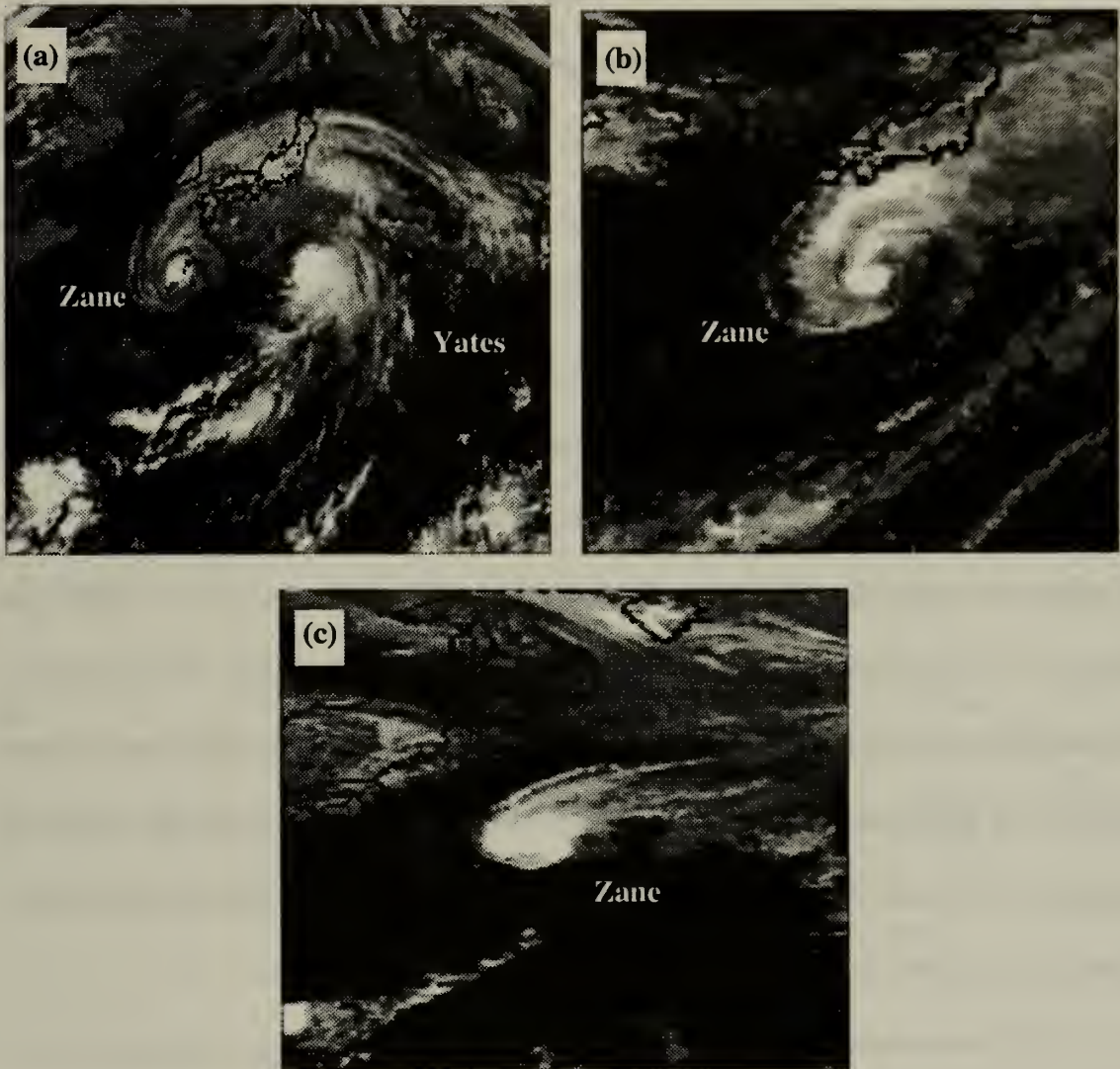0933 UTC 5 August 1996. Note dry slot in (b).

Fig. 7. As in Fig. 4, except for transformation of Typhoon Zane at (a) 0033 UTC 30 September, (b) 0633 UTC 1 October, and (c) 0633 UTC 2 October 1996.

tinguish between different intensities once ET has begun. It is important to note that the two cases that did not fit this general pattern began transformation over land, and resulted in a distinct departure from the sequence of events described earlier.

Compare the sequence of events depicted in Fig. 4 with the conceptual model illustrated in Fig. 8, which begins in the mature typhoon stage (Fig. 8a). In Fig. 8b, ET begins with the transformation stage, when inflow of cold, dry air leads to formation of a characteristic dry slot and decreased deep convection. This area of decreased convection grows and the dry slot expands (Fig. 8c) until virtually all deep convection ceases in the outer bands to the east and south of the transforming TC (Fig. 8d). The hook-like appearance of an overrunning cloud shield (Fig. 8e), with transformation of the TC nearly completed, is the last step of this sequence. In this study, the idealized sequence depicted in Figs. 8b through 8e typically took approximately 36 h to 48 h to complete. Of the 24 cases that completed this sequence, 12 did so before JTWC considered the TC to be extratropical, and the other 12 completed the sequence after being designated extratropical. This suggests the method used by JTWC to determine when a TC becomes extratropical does not necessarily require the completion of the thermodynamic transformation that actually defines whether the TC is still a warm-core system, or has become a baroclinic, extratropical low.

This characteristic sequence was used to determine only that transformation had begun or was underway. After transformation was suspected to have begun based on satellite imagery and the conceptual model of Fig. 8, the NOGAPS analyses at sea level and 500 mb were reviewed to determine the progress and possible completion of transformation. Changes in the pressure and wind fields of the TC were monitored at both levels, with several distinct events evident in nearly every case of ET.[2] The most obvious event was a systematic increase

_____

[2]Correlation of these events observed in NOGAPS analyses with the conceptual model of Fig. 8 will be discussed later in this chapter.

CONCEPTUAL MODEL OF TRANSFORMATION IN EXTRATROPICAL TRANSITION

(a)

(b)

Dry Slot
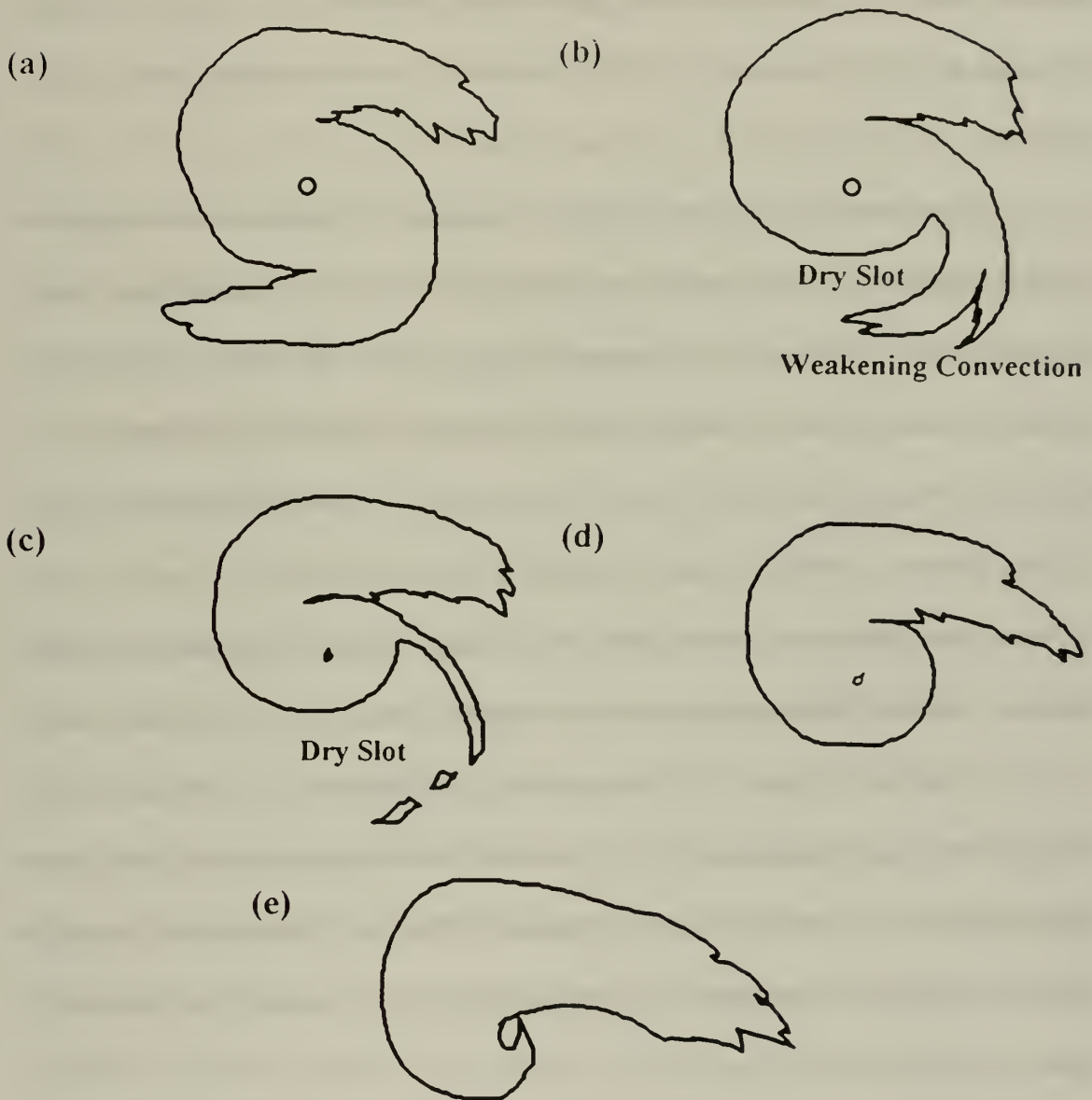
Weakening Convection

(c)

Dry Slot

(d)

(e)

Fig. 8. Conceptual model of transformation in cases of ET, to include (a) the TC late in the mature stage, (b) the start of transformation, with convection weakening in the south and east quadrants of the TC and formation of a characteristic dry slot, (c) continued decay of convection and growth of the dry slot, (d) cessation of all deep convection in the southern and eastern quadrants, and (e) hook-like appearance of overrunning convection to the north of the transforming TC.

in SLP and 500-mb heights at the center of the storm. Next, an "open wave" at 500 mb was detected above the surface circulation of the TC. Later, baroclinic tilt with height was observed, with the 500-mb low or trough located northwest of the center of surface circulation such that the vertical axis of the storm tilted toward the colder air mass to the northwest.

In every case of ET, winds at the surface diminished coincident with the changes in the pressure field noted above. Furthermore, a 500-mb wind maximum was observed in the southeast quadrant of the storm once the transforming TC interacted with the westerlies and entered the polar jet axis. As transformation progressed, this wind maximum grew in intensity, and remained downstream of the 500-mb trough or "open wave" described earlier. This wind maximum was always located at outer radii of the transforming TC, and not in the inner core as would be observed in a mature TC. Finally, wind speed appeared to increase with height such that 500-mb wind speeds now exceeded those directly below at the surface.

For example, Typhoon (TY) Orson at 0000 1 September 1996 was estimated by JTWC to have maximum winds of 80 kt. Note that the wind direction and speed at the surface (Fig. 9a) and 500 mb (Fig. 9b) are comparable.[3] This lack of vertical wind shear was observed in NOGAPS analyses prior to transformation of all TCs studied. On 0000 UTC 3

---

[3]It could be argued that synthetic TC observations ensured that a symmetric vortex displaying little vertical wind shear would exist in this NOGAPS analysis field. However, NOGAPS combines synthetic observations with previous model 6 h forecasts of the TC vortex that exist in the first-guess field, as well as current observations to develop the TC vortex in the analysis. Furthermore, NOGAPS analyses of 1996 cases of ET (which include Orson) used water vapor winds as a data source. For these reasons, it is believed that NOGAPS will properly represent the lack of vertical wind shear in a mature TC, and that such a representation is not solely the result of synthetic TC observations.

September (not shown), JTWC had classified Orson as a TS with maximum winds of 45 kt and a central SLP of 985 mb. Orson remained downstream of a 998 mb mid-latitude low and associated cold front, and had also ingested a strong, northwesterly flow of cold, dry air from over Manchuria, the Japan Sea, and Japan. By 0000 UTC 4 September (Fig. 9c), Orson had filled to 994 mb, and continued to ingest colder, drier air from the northwest. Orson also features an open wave at 500 mb (Fig. 9d), a 500-mb wind maximum at outer radii south of the storm center, baroclinic tilt, and winds that increase with height from the surface (Fig. 9c) to 500 mb (Fig. 9d) south and east of the storm center.

Recall the relationship between temperature and vertical wind shear as described by the thermal wind equation

$$\partial u_g / \partial (\ln p) = R/f * (\partial T / \partial y)_p , \qquad (3.1)$$

where the term on the left side of (3.1) is the change in the geostrophic zonal wind with pressure, and the term on the right side is the meridional temperature gradient on a constant pressure surface. The thermal wind relationship in (3.1) requires that the temperature decreases to the north and west of the center of Orson. Thus, NOGAPS analyses in Figs. 9c-d may be used to infer that the transforming TC was now a baroclinic system that was beginning to acquire a cold core. At this stage, the transformation of Orson was nearly complete. These events could be used to diagnose the progress of the transformation despite the fact that the resolution of the NOGAPS analyses was inadequate to depict properly the wind velocity and structure present in the innermost radii of the TC.
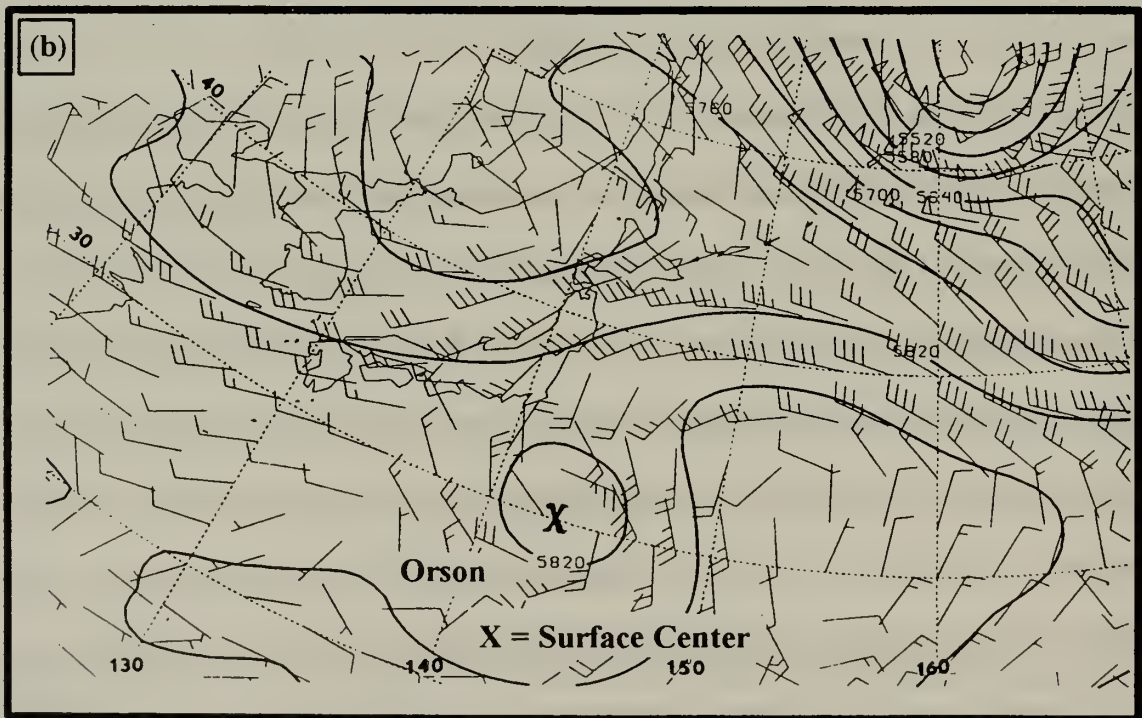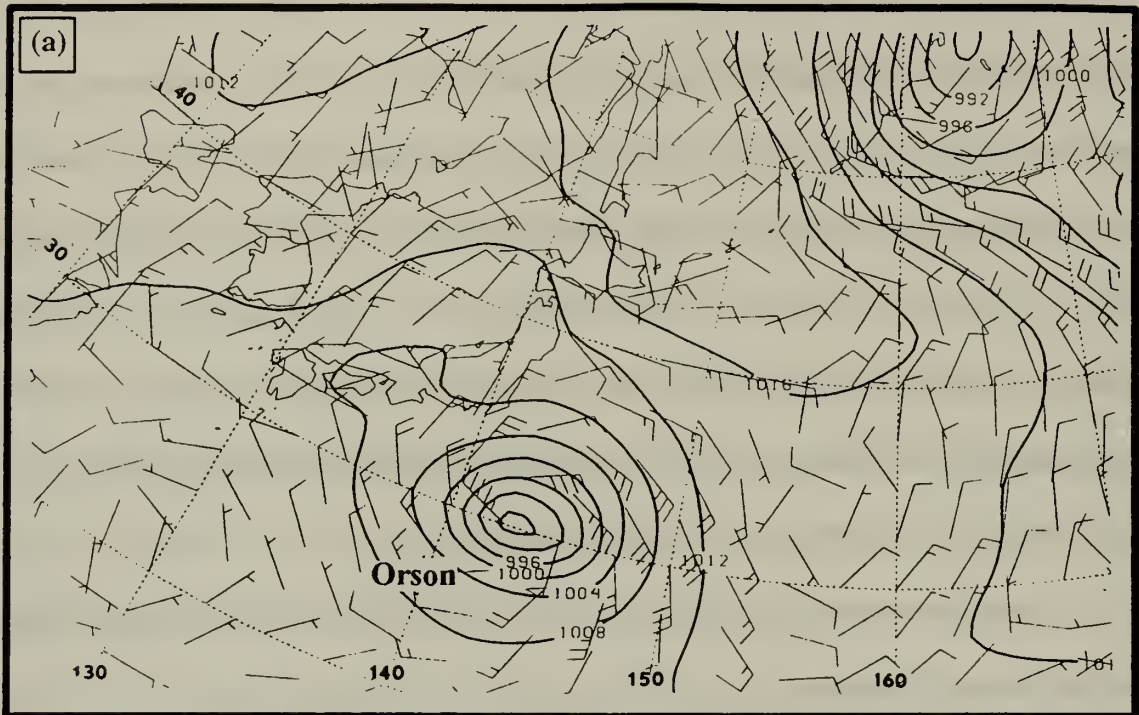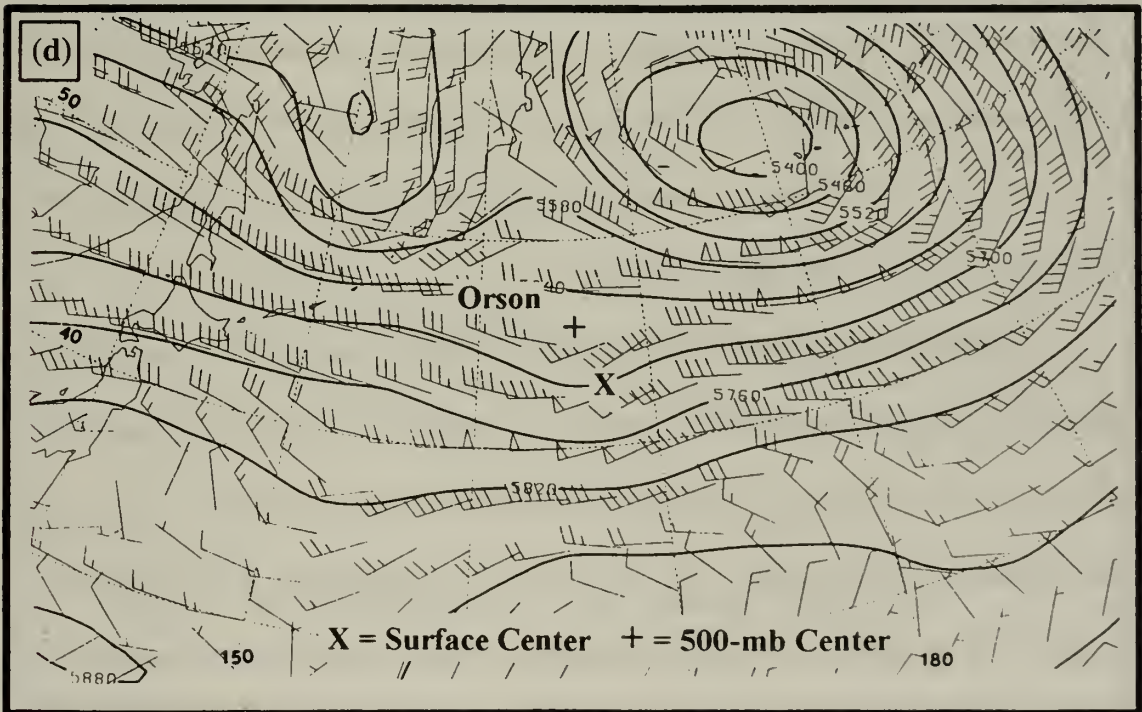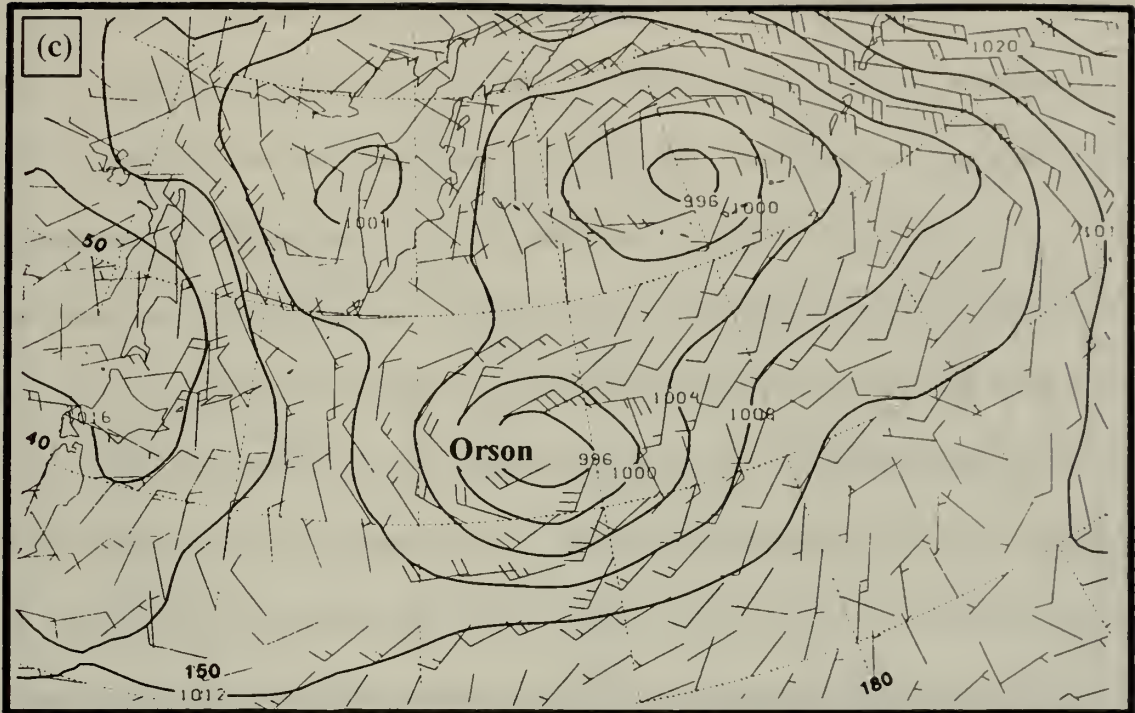
Fig. 9. Transformation of TY Orson depicted at 0000 UTC 1 September 1996 in NOGAPS (a) surface analysis, with SLP indicated by solid contours (4 mb intervals) and (b) 500-mb heights indicated by solid contours (60 m interval). Wind arrows shown with long (short) barbs are 10 (5) kt.

Figs. 9c-d (continued). Transformation of TY Orson as in Figs. 9a-b, except
at 0000 UTC 4 September 1996.

The surface and 500 mb NOGAPS analyses in Fig. 10 illustrate a similar process occurred during the transformation of TY Dan. At 1200 UTC 11 July 1996 (nearly 12 h after the imagery depicted in Fig. 5d), the central SLP associated with Dan has filled to 994 mb (Fig. 10a). Dan has ingested somewhat cooler, drier air from Asia that has been modified over the Japan Sea and Japan. The corresponding 500-mb analysis (Fig. 10b) has an open wave above Dan's surface circulation and 45 kt winds in the southeastern quadrant of Dan. Note that in the southern and eastern sections of the storm, the 500-mb wind speed is faster than that in the same location on the surface. At this time, JTWC had classified Dan as a tropical storm (TS). By 0000 UTC 12 July, TS Dan has the same central SLP (Fig. 10c), even though it continued to ingest cold, dry air as mentioned above. A significant increase in the intensity of the wind maximum to the southeast at 500 mb is consistent with the generally faster wind velocities at 500 mb than at the surface (Fig. 10d). Furthermore, notice the baroclinic tilt with height between the surface and 500 mb. At this time, the transformation of Dan was nearly completed.

A similar sequence also applied during the transformation of TS Tom, which was estimated by JTWC to have maximum winds of 55 kt at 0000 UTC 19 September 1996. By 1200 UTC, Tom's central SLP had filled to 986 mb as it began to ingest air from the north and west into its circulation (Fig. 11a). At 1200 UTC 20 September, Tom had filled to 998 mb (Fig. 11c). At 500 mb, the closed circulation of Tom at 1200 UTC 19 September (Fig. 11b) also decreased in intensity to an open wave by 1200 UTC 20 September (Fig. 11d). Notice that the wind maximum southeast of Tom had weakened from 1200 UTC 19 Sep-
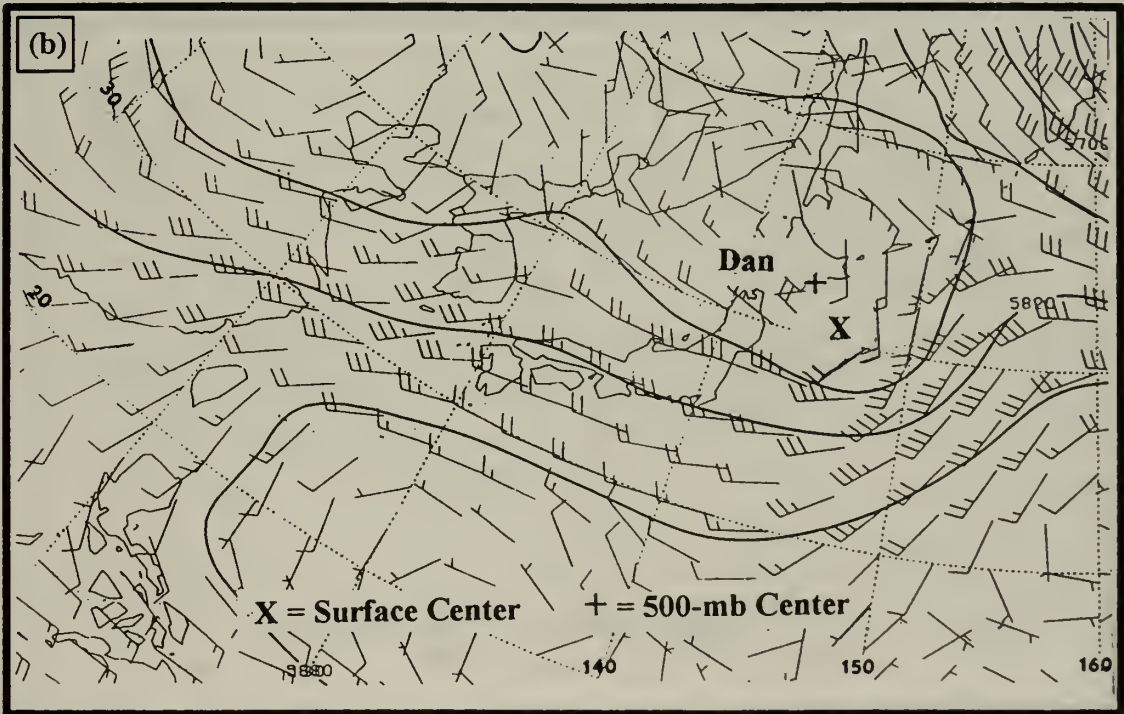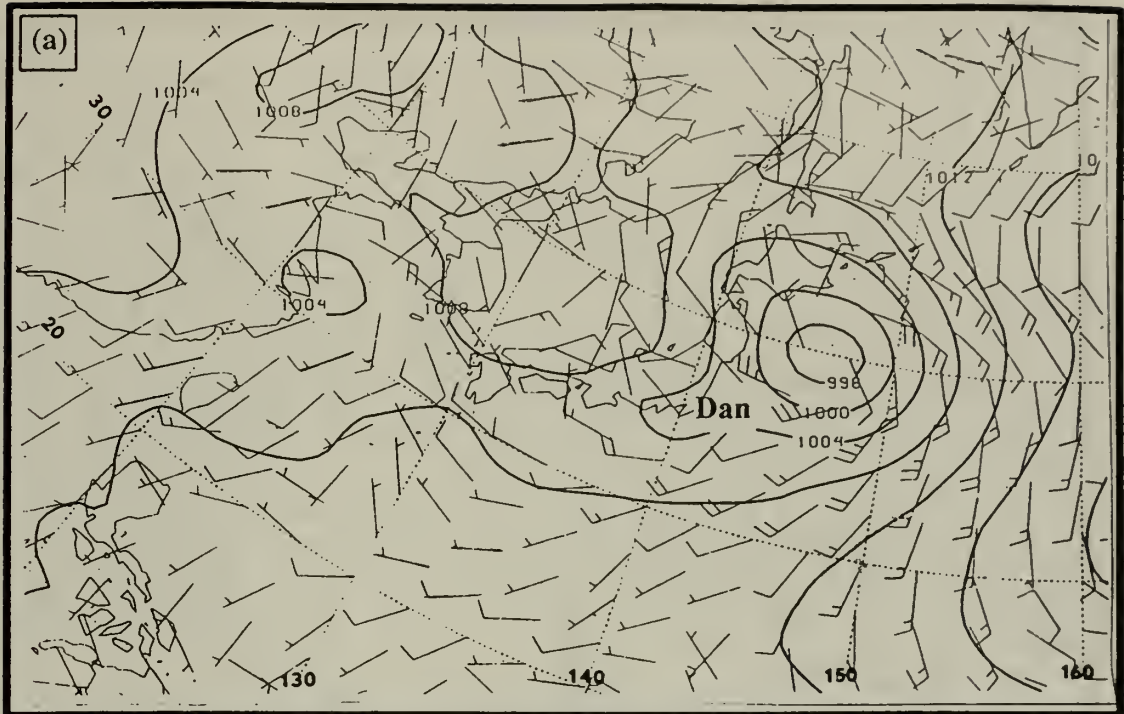
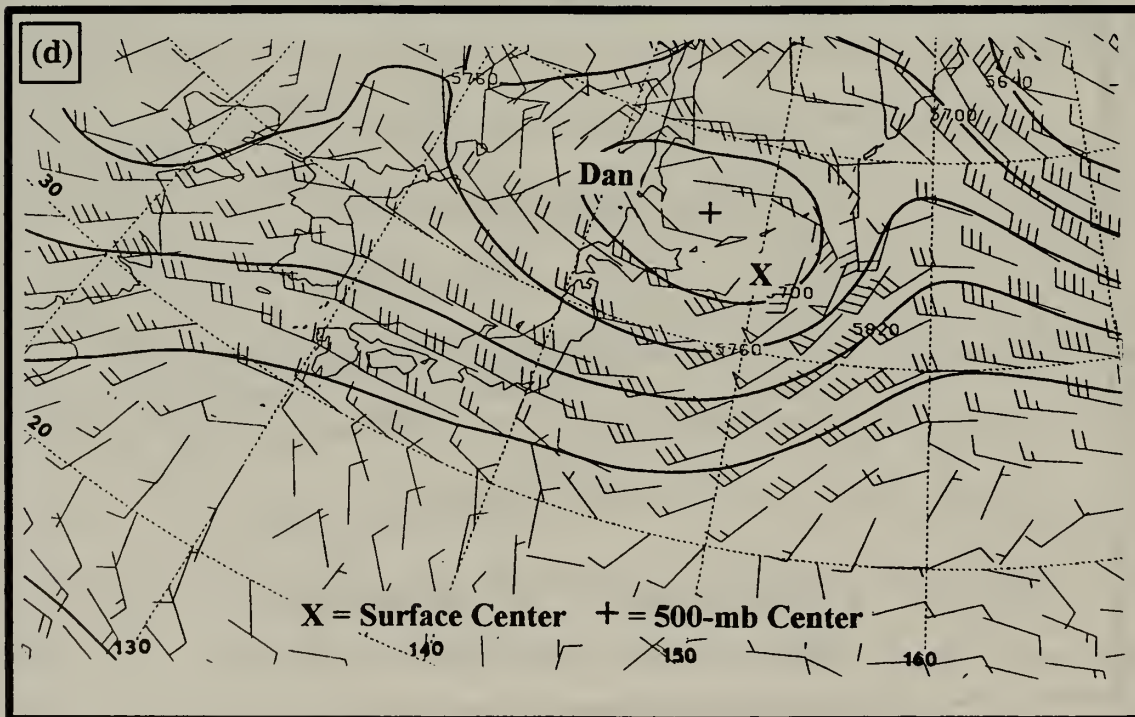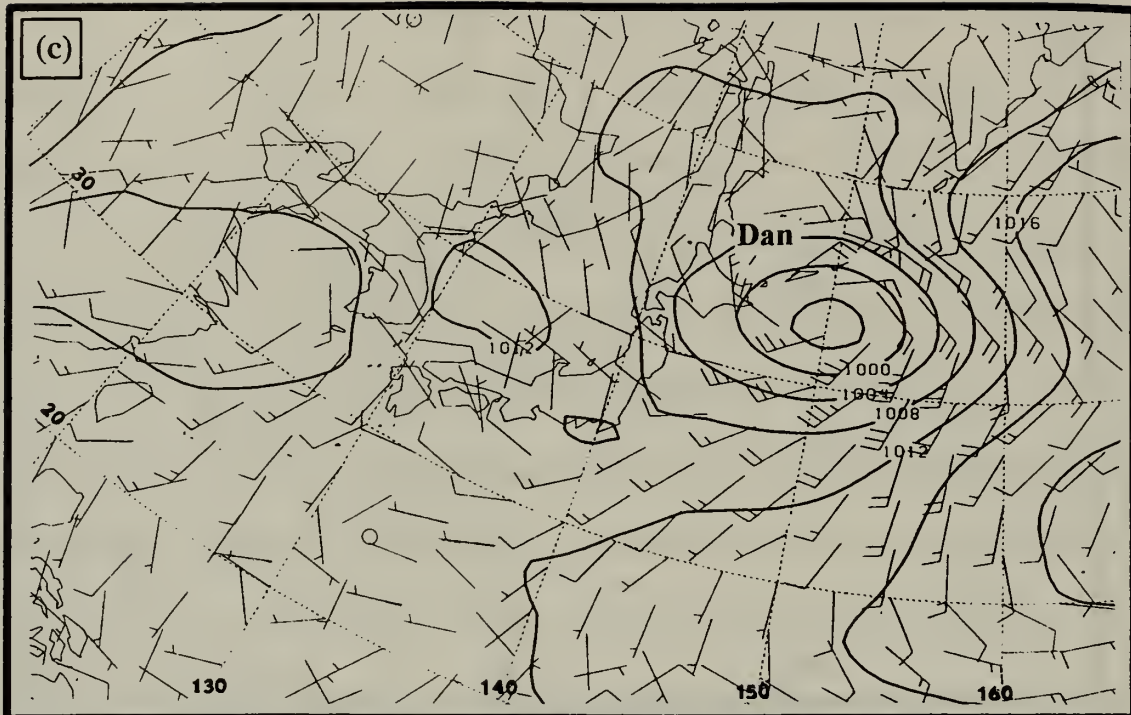Fig. 10. As in Figs. 9a-b, except for transformation of TY Dan at
1200 UTC 11 July 1996.

Figs. 10c-d (continued). Transformation of TY Dan as in Figs. 10a-b,
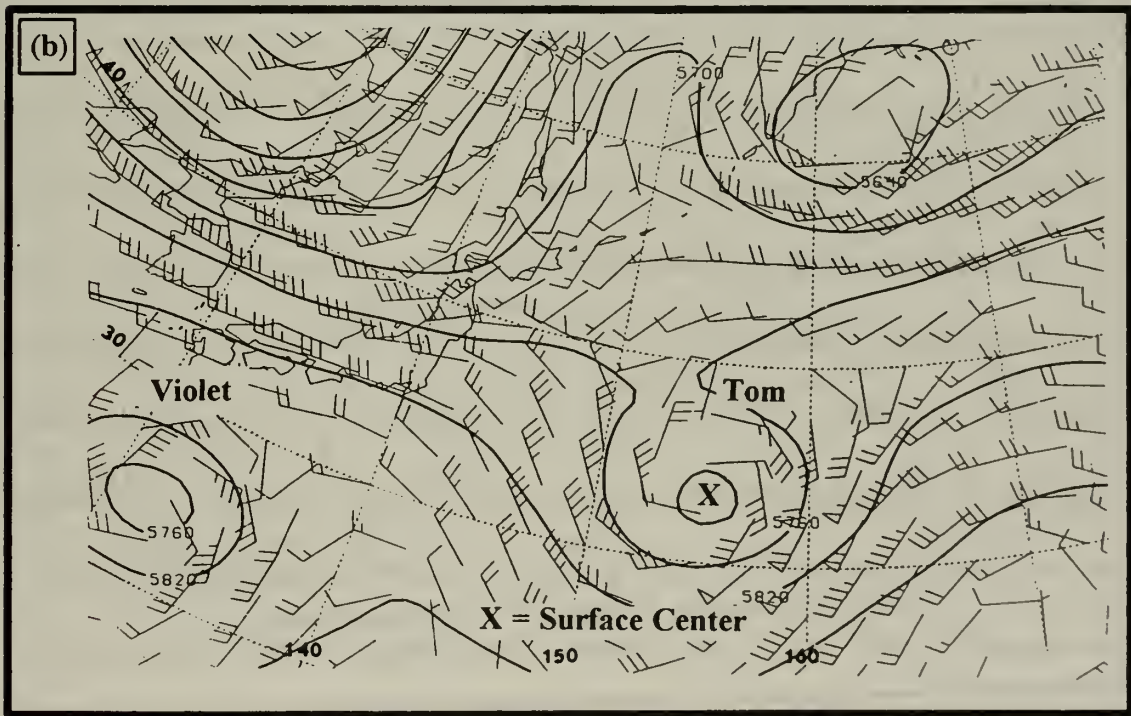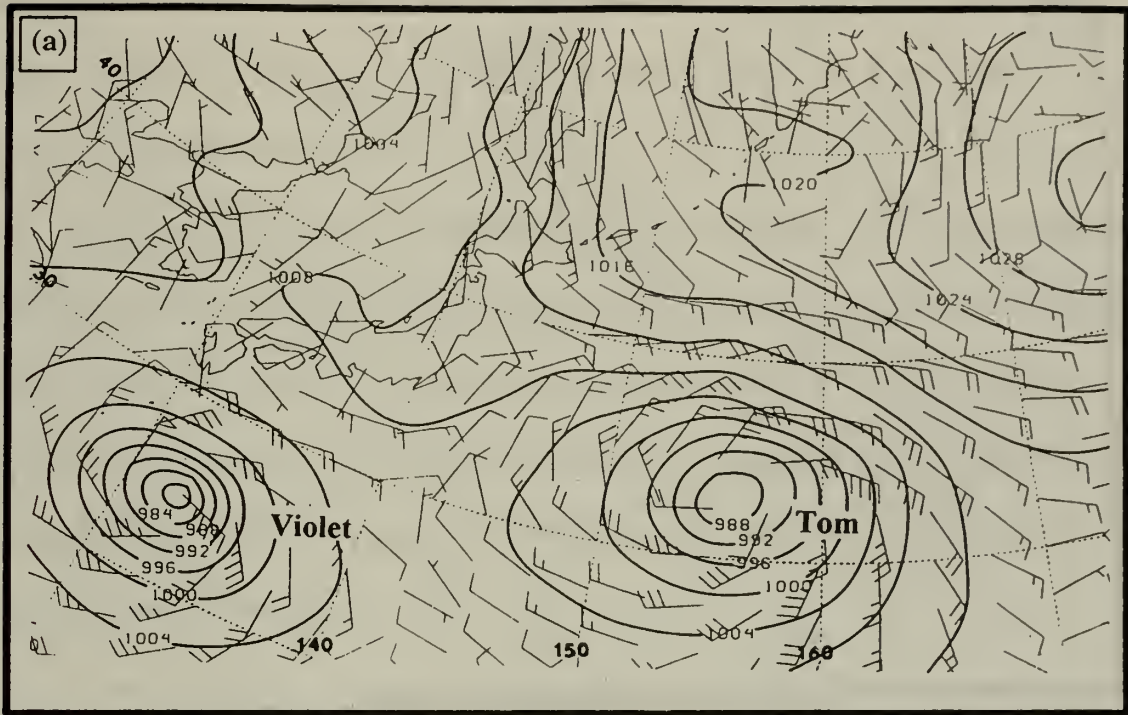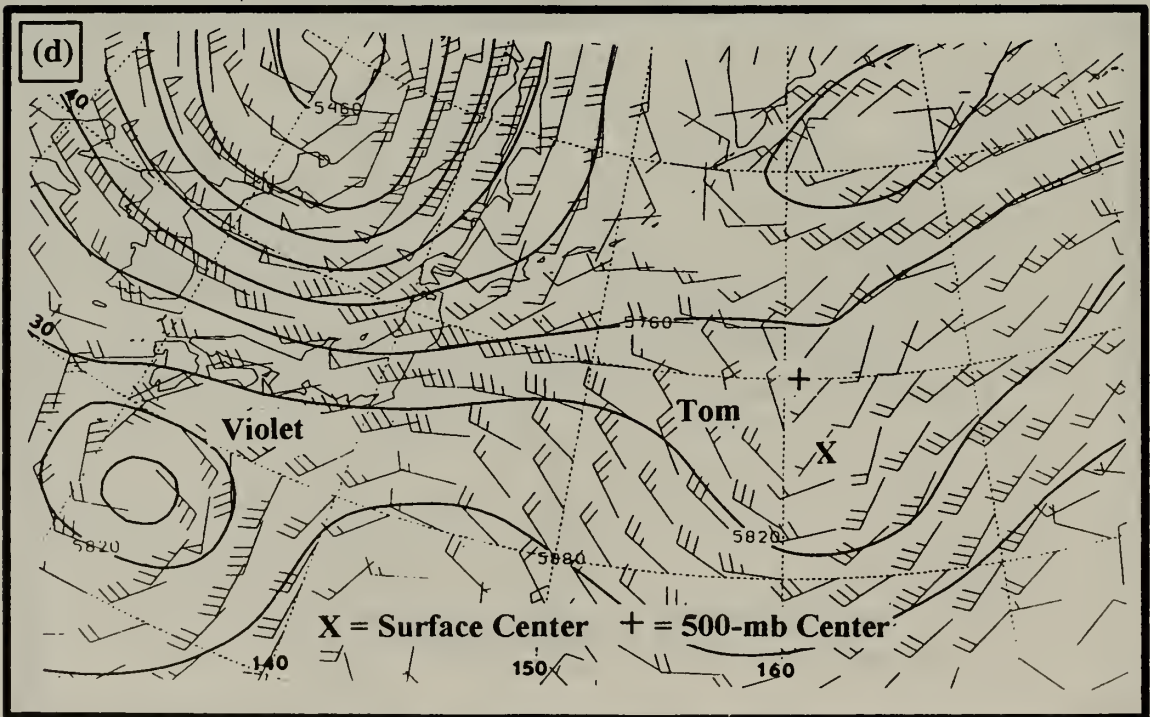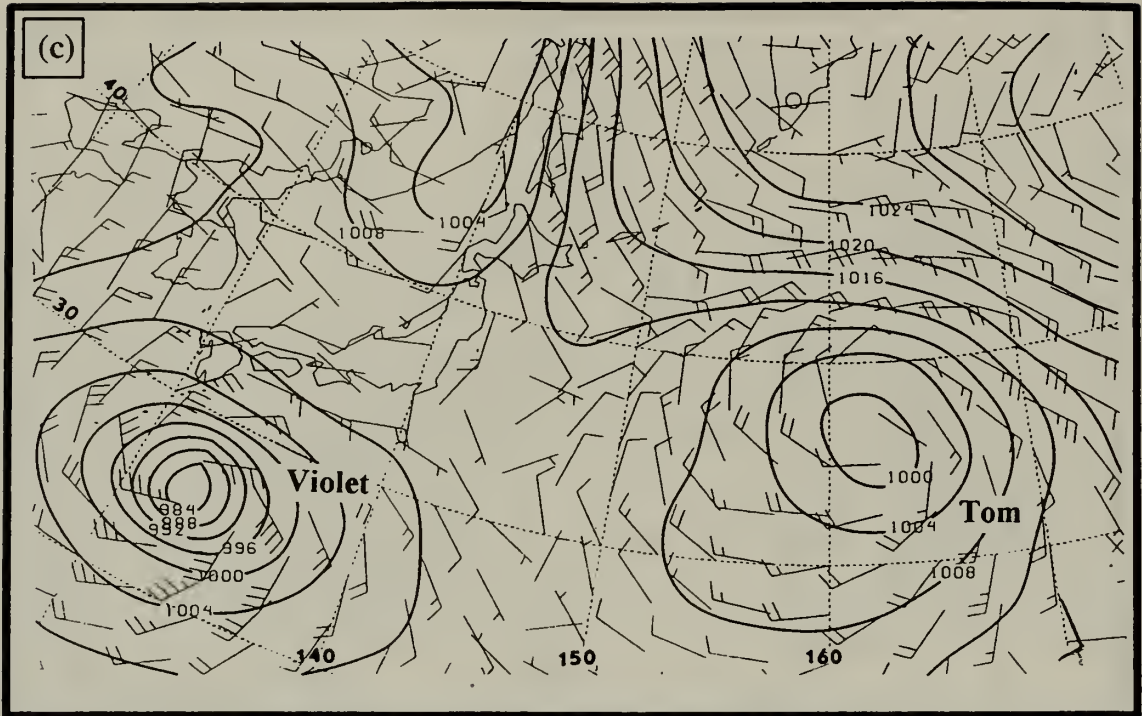except at 0000 UTC 12 July 1996.

Fig. 11. As in Figs. 9a-b, except for transformation of TY Tom at
1200 UTC 19 September 1996.

31

Figs. 11c-d (continued). As in Figs. 9c-d, except for transformation of TY Tom at 1200 UTC 20 September 1996.

tember (Fig. 11b), even though wind velocity generally increases from the surface to 500 mb in the baroclinically tilted open wave (Fig. 11d). By 1200 UTC 20 September, Tom has virtually completed transformation.

According to JTWC, Zane was classified a TY until 0000 UTC 2 October 1996. However, the NOGAPS analysis in Fig. 12a depicts Zane at 1200 UTC 2 October as having filled to 990 mb while ingesting colder air with a trajectory from the north and northwest. At 500 mb (Fig. 12b), note the characteristic wind maximum to the south and east, the baroclinic tilt, and the increase in wind velocity with height that was described in the previous three cases during transformation.

These cases illustrate a pattern of events that was evident in the surface and 500-mb NOGAPS analyses of each case of ET studied. Recall the conceptual model of TC transformation described earlier (Fig. 8). As the TC began to ingest cold, dry air from the north and west in each case of ET, deep convection was observed to diminish to the south and east (Fig. 8b). This apparently weakened the TC warm-core as diagnosed by an increase in central SLP, increase in 500-mb heights, and diminishing surface winds that were also observed in every case of ET. Transformation of the TC into a baroclinic system had begun. Reduction in lower-tropospheric winds should then have decreased I^2 values near the center, and resulted in weakened resistance to radial deflections, continued decrease of deep convection to the south and east, and accelerated intrusion of cold, dry air. This process is also consistent with the observations from the NOGAPS analyses and satellite imagery of the cases of ET described above, and corresponds to the stages of transformation illustrated in Figs. 8c and 8d. As this process continued, the TC translated northward into the polar jet
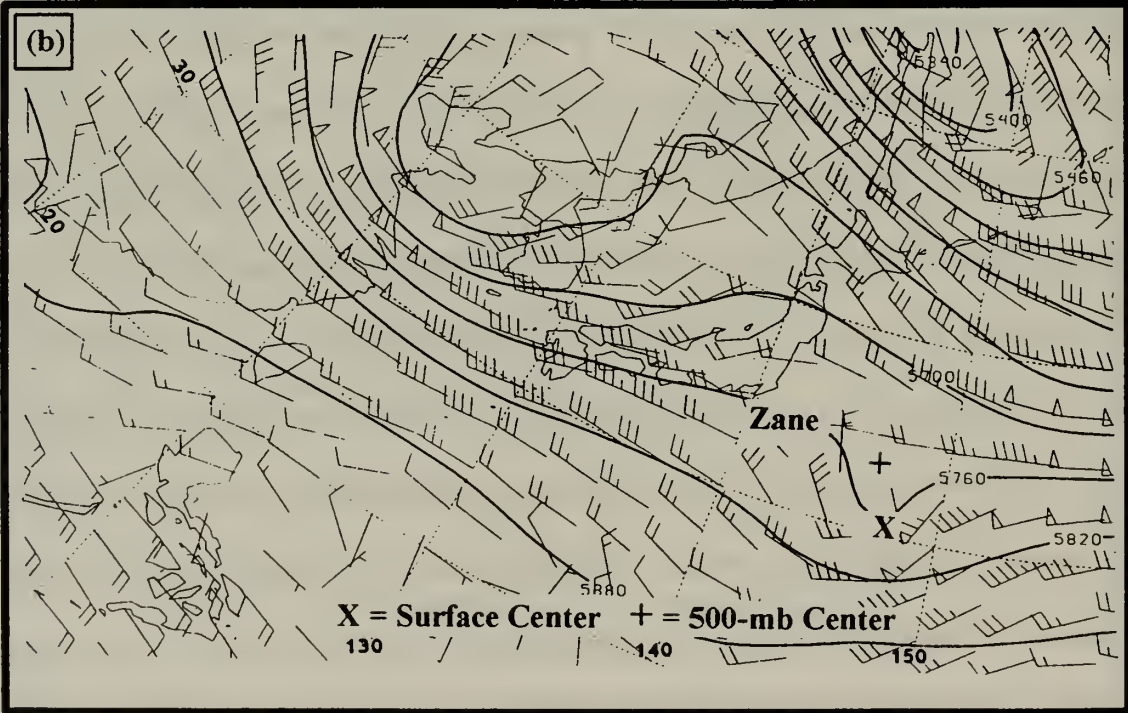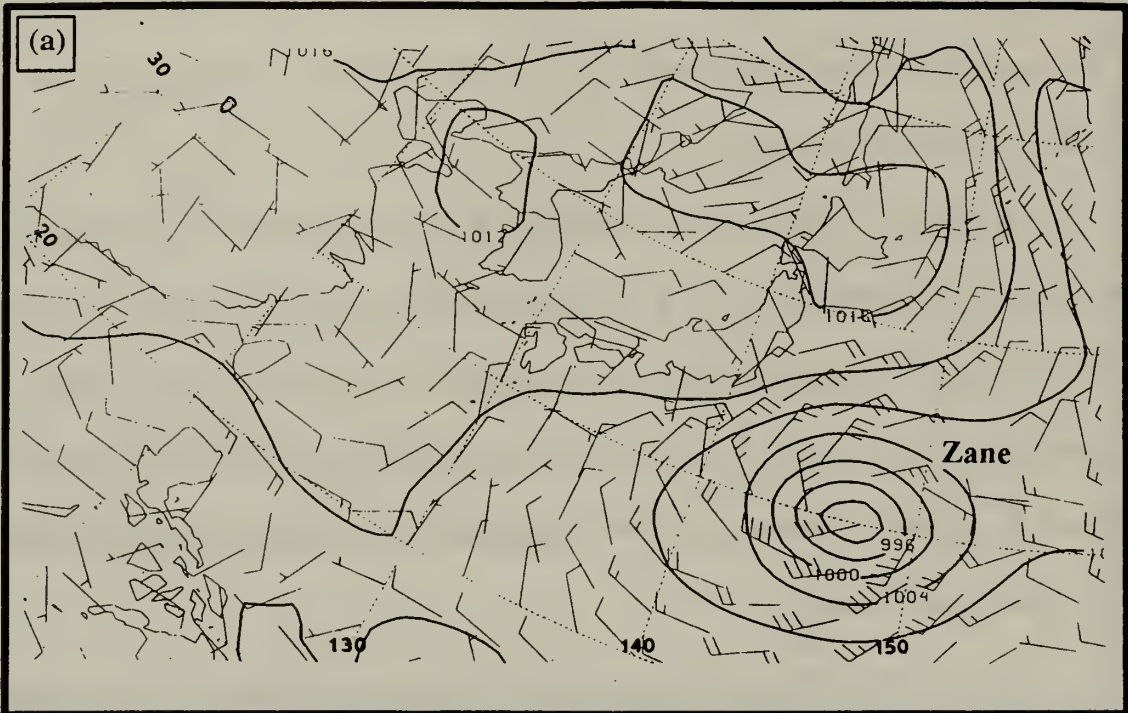
33

(a)

(b)

X = Surface Center   + = 500-mb Center

Fig. 12. As in Figs. 9a-b, except for transformation of TY Zane
at 1200 UTC 2 October 1996.

34

axis, which placed the TC adjacent to colder air north of the jet axis. At this time, the characteristic 500-mb wind maximum south and east of the center of the TC could be observed in the NOGAPS analyses. Continued intrusion of cold, dry air with subsequent further decrease in lower-tropospheric I^2 values is consistent with the eventual decay of the warm-core as diagnosed by further increases in SLP, weakening of surface winds, and the appearance of an "open wave" at 500 mb. This stage corresponds to the IR imagery in Fig. 4e, and to Fig. 8e of the conceptual model. With colder air north and west of the transforming TC, winds in the NOGAPS analyses were observed to increase with height from the surface to 500 mb, which suggests that the warm-core of the TC had been replaced by colder air according to the thermal wind relationship in (3.1). Final completion of transformation could be inferred from the baroclinic tilt in the NOGAPS analyses, and from IR imagery.[4] Typhoon Polly (Fig. 13a) and STY Violet (Fig. 13b) are shown after they have completed transformation. Both storms have begun to show a distinct cold front, and appear similar to mid-latitude cases of "instant occlusion." The final stages of Orson (Fig. 4e), Dan (Fig. 5d), and Zane (Fig. 7c) also appear to have similar characteristics.

This entire process, from the appearance of the dry slot in satellite imagery as depicted in Fig. 8b to the observation of baroclinic tilt in NOGAPS analyses, required from 36 to 72 h to complete in the cases studied. It is acknowledged that the resolution of 2.5° latitude/longitude NOGAPS analyses were inadequate to resolve completely the features near the center of the TC. However, recall that the cases presented in Figs. 9 through 12 were

---

[4]This suggests that baroclinic instability has replaced the TC convection as the source of energy for this transformed cyclone.
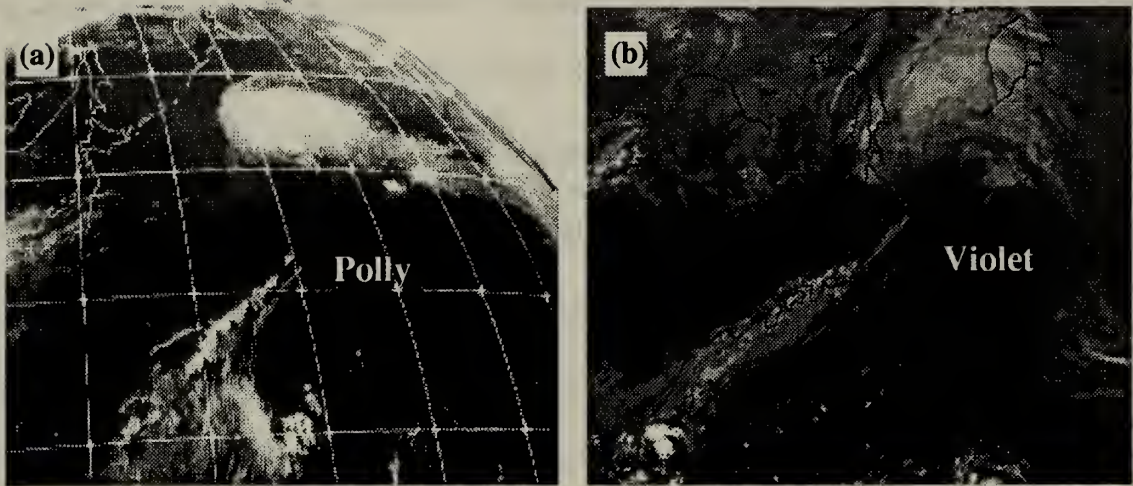
Fig. 13. Infrared imagery of completed transformation in the case of TY Polly at (a) 0000 UTC 22 September 1995, and STY Violet at (b) 1232 UTC 23 September 1996.

from 1996 and included water vapor winds as an important data source. The analyses were therefore judged to be of sufficient quality to assess the progress of transformation.

In the remainder of this thesis, transformation will be defined as starting with the appearance in satellite imagery of weakening convection and a dry slot to the south and east of the TC (as in Fig. 8b). Transformation will be defined to be complete when evidence of baroclinic tilt and cold-core characteristics are observed in the NOGAPS analyses and in the satellite imagery as depicted in Fig. 13.

B.   ROLE OF THE UPPER TROPOSPHERE IN ET

In all cases of ET in this sample, the 200-mb NOGAPS analyses are consistent with the 500-mb circulations described above during the later stages of transformation. As expected, polar jet wind speeds increase from 500 mb to 200 mb. Furthermore, the baroclinic tilt from the surface to 500 mb observed during the later stage continues up to 200 mb. This
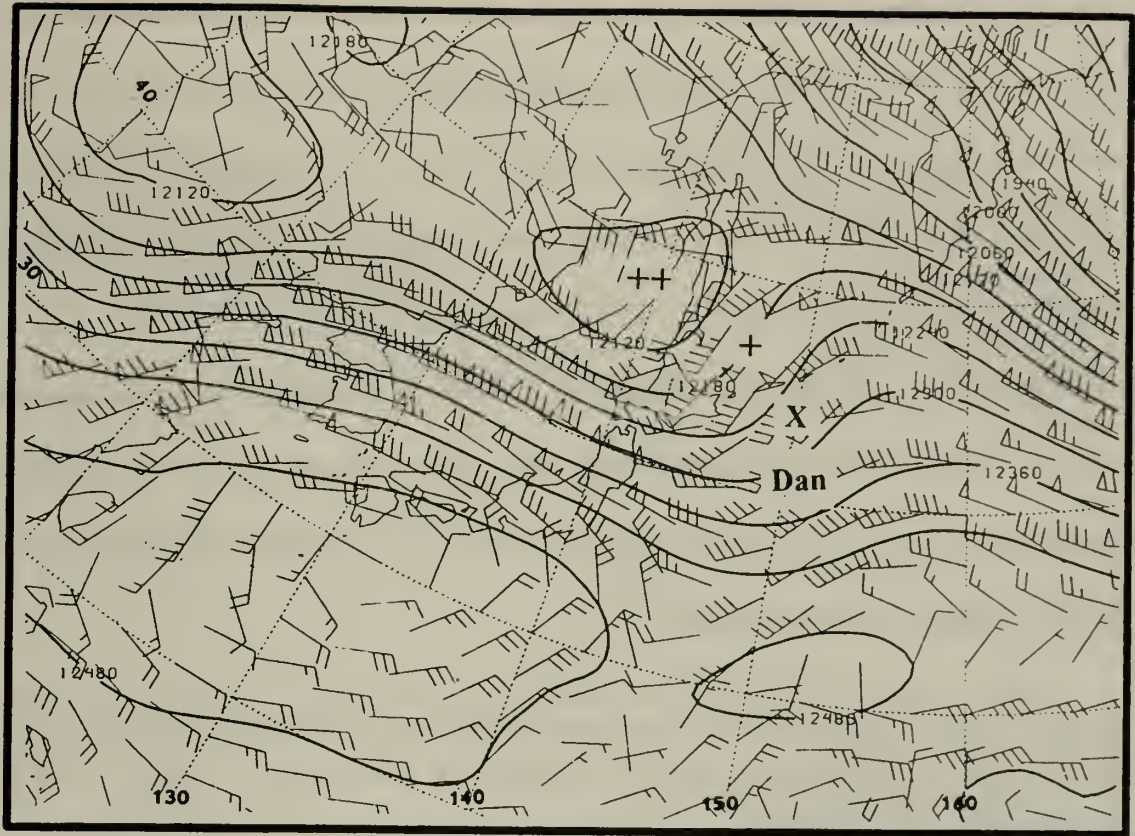
X = Surface Center   + = 500-mb Center   ++ = 200-mb Center

Fig.14. Transformation of TY Dan depicted in NOGAPS 200-mb height (contour interval 60 m) analysis at 0000 UTC 12 July 1996. Winds are depicted in knots.

tilt is evident for TY Dan in Fig. 14, which extends upward from the surface and 500-mb NOGAPS analyses in Figs. 10c and 10d, respectively. Thus, the NOGAPS surface, 500-mb, and 200-mb charts together proved effective in monitoring the progress of transformation.

Once the transformation had been completed, it was hypothesized that the TC was a baroclinic system that required PVA and upper-level divergence to re-intensify. In every case of ET that did re-intensify, significant upper-tropospheric support for extratropical

cyclogenesis was observed. For example, TY Dan at 0000 UTC 12 July 1996 (Fig. 15) was located near the left-exit region of an upstream jet streak, and the right-entrance quadrant of a downstream jet streak. Both of these jet streak regions may have contributed to divergence at 200 mb above TY Dan, and thus are believed to have had a critical role in the deepening of the central SLP to 986 mb by 1200 UTC 12 July (Fig. 15b).

In the case of TY Orson, a diffluent 200-mb trough above the transformed remnants of Orson at 0000 UTC 5 September 1996 (Fig. 16a) represents an area of upper-level divergence. Within 12 h, Orson re-deepens 13 mb to 977 mb while remaining under the diffluent trough at 200 mb (Fig. 16b).

Super Typhoon Yates after transformation on 0000 UTC 3 October 1996 had a central SLP of 994 mb (Fig. 17a) and a 200-mb jet streak was upstream. Within 12 h, Yates deepened 4 mb and moved east-northeast under the left-exit region of the upstream jet streak (Fig. 17b), where upper-tropospheric divergence favored continued intensification. Notice the relatively tight gradient from 50 kt to 110 kt in the left-exit region in Fig. 17b. By 0000 UTC 4 October, Yates deepened further to 982 mb (Fig. 17c), and remained under the tight gradient of winds in the left-exit region of an upstream jet streak. At 0000 UTC 5 October, Yates had deepened to 978 mb (not shown).

In Fig. 17c, the remnants of TY Zane at 160°E are just upstream of the right-rear quadrant of the jet streak that is upstream of Yates. The horizontal gradient of jet winds over Zane is not as large as in the left-exit region of the jet above Yates. By 1200 UTC 4 October (Fig. 18), Zane moved farther downstream toward the right-exit region of the jet where convergence existed. As a result, Zane failed to couple with the upper-troposphere circu-
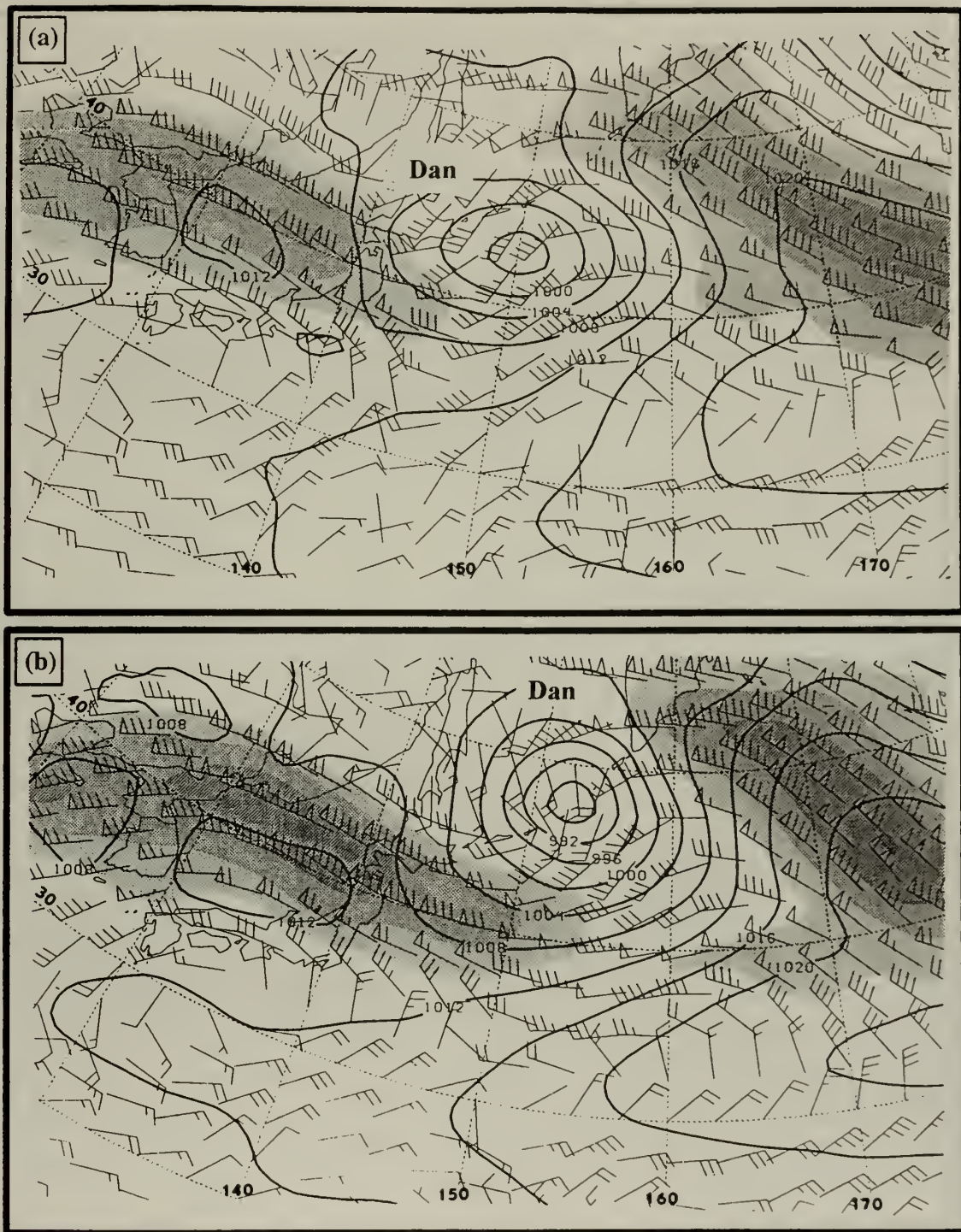
Fig. 15. Re-intensification of Dan at (a) 0000 UTC, and (b) 1200 UTC 12 July 1996 depicted in 200-mb NOGAPS analyses. Successively darker shades of gray at 20 kt intervals, beginning with 50 kt, represent jet streaks superposed above SLP contours (solid, interval 4 mb).
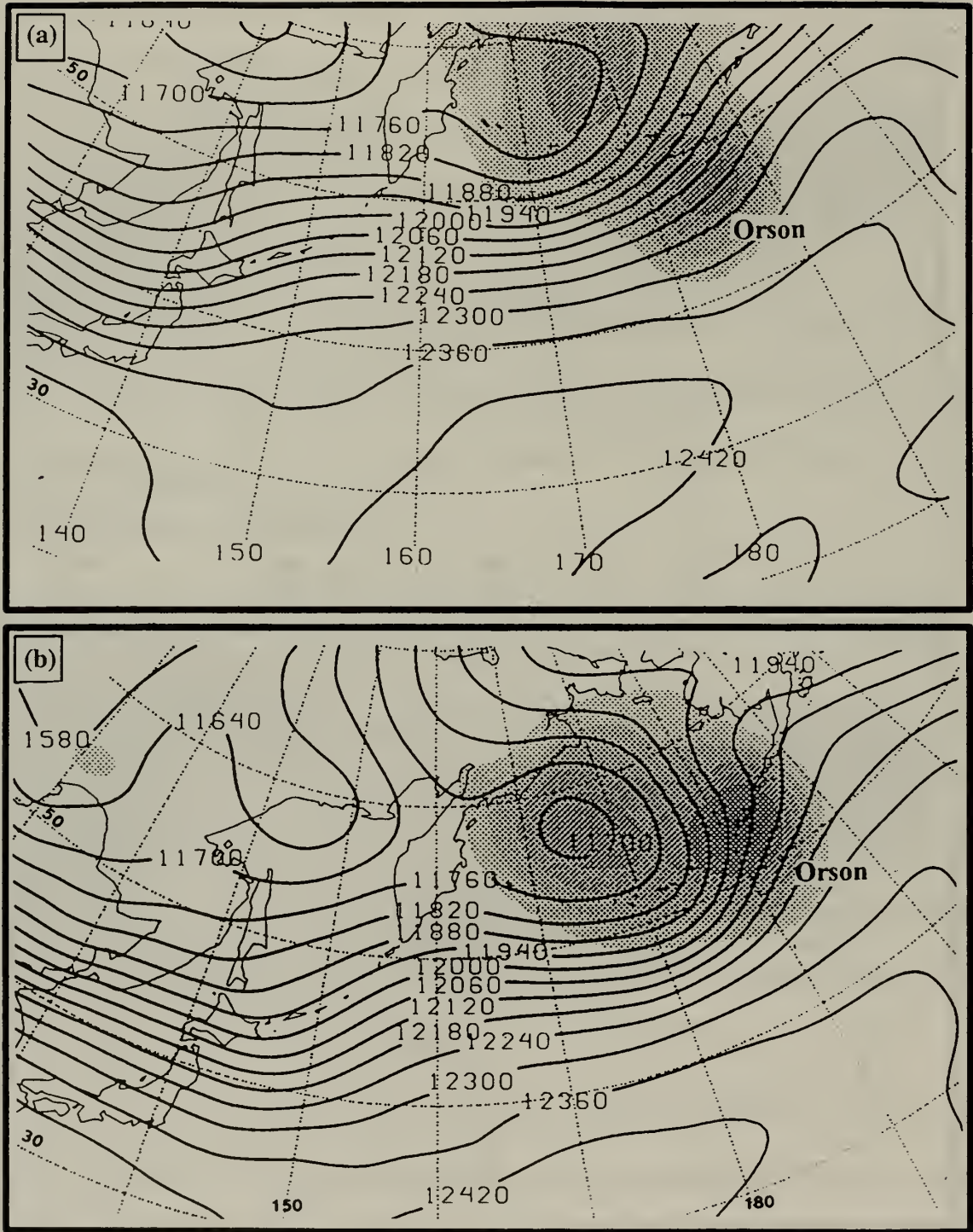
Fig. 16. Re-intensification of Orson depicted in NOGAPS analyses. Solid contours represent 200-mb heights (m), with gray shading indicating SLPs at 4 mb intervals, starting at 1004 mb at (a) 0000 UTC, and (b) 1200 UTC 5 September 1996.
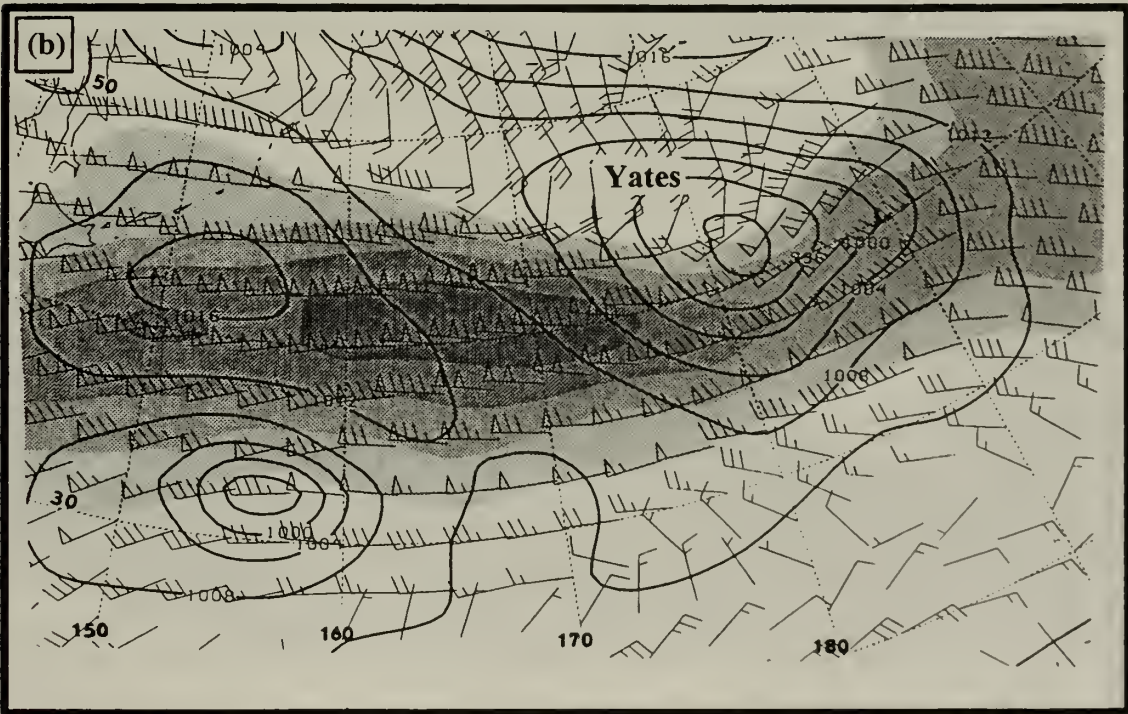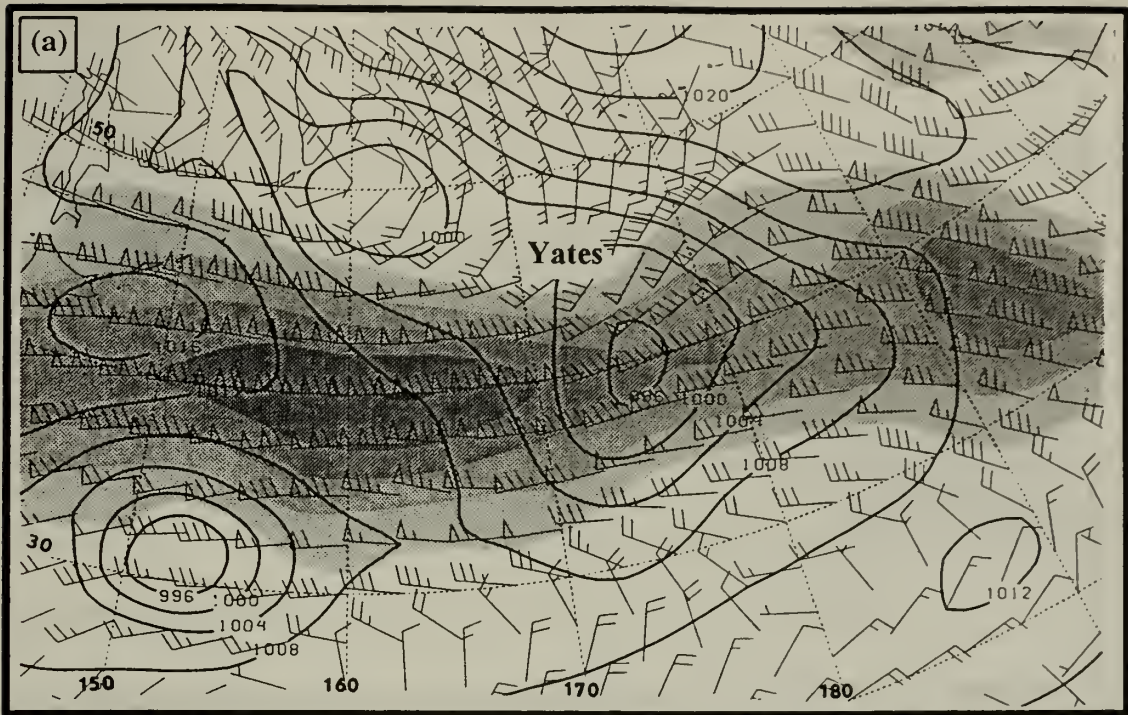
Fig. 17. As in Fig. 15, except for re-intensification of STY Yates at (a) 0000 UTC
and (b) 1200 UTC 3 October 1996.

41
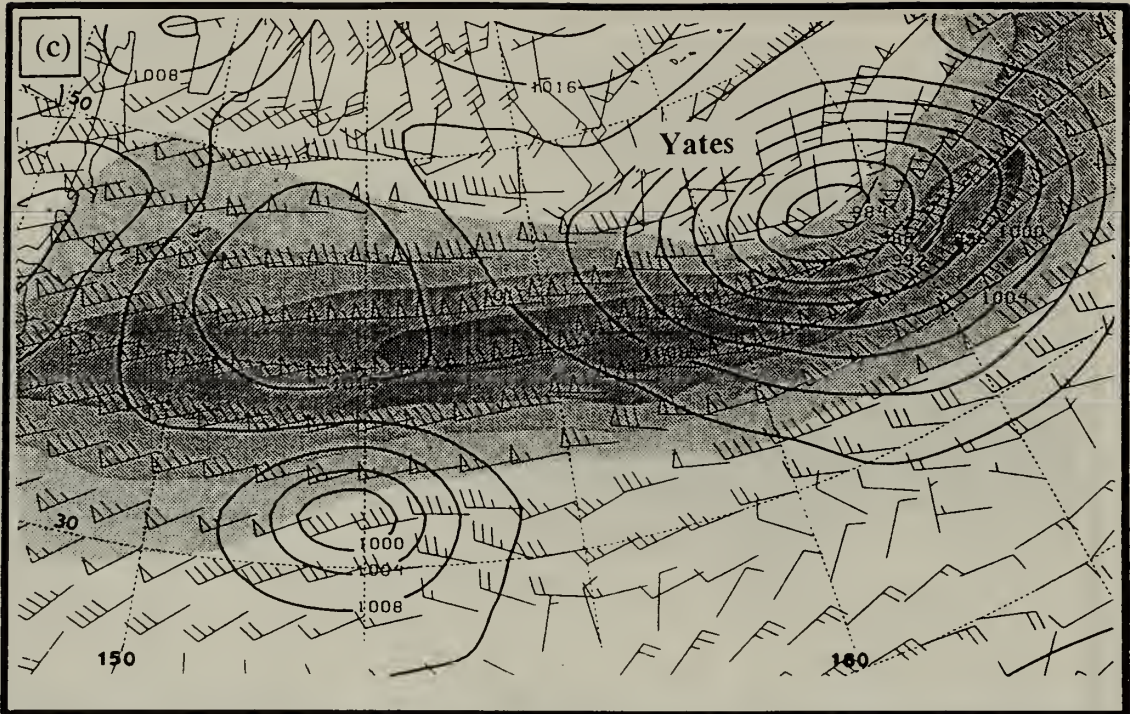
Fig. 17c. As in Fig. 15, except for re-intensification of STY Yates at
0000 UTC 4 October 1996.
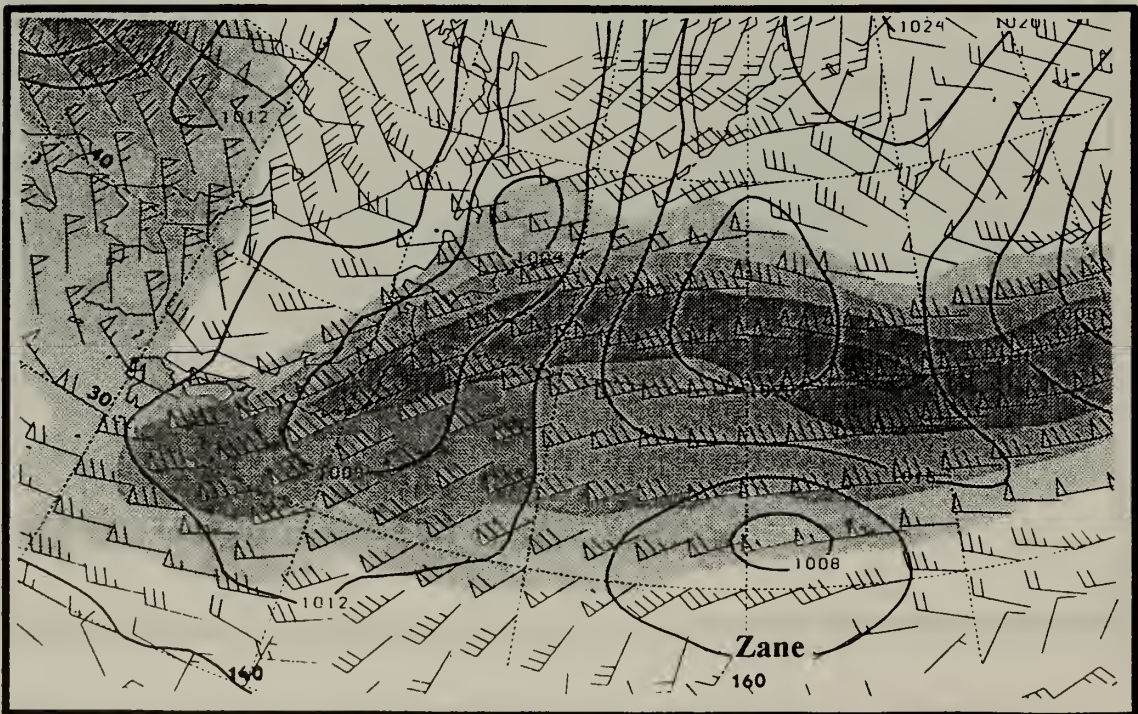
Fig. 18. As in Fig. 15, except for TY Zane at 1200 UTC 4 October 1996.

lation, and continued to dissipate over the next 12 h (not shown) beneath a 200-mb environment unfavorable for re-intensification.

In all dissipator cases of ET in this sample, the transformed TC never moved beneath a diffluent trough, region of speed divergence, or a favorable jet streak quadrant in the NOGAPS 200-mb analyses. Thus, these cases are considered to have never received upper-tropospheric support for re-intensification, which is consistent with their dissipation. The filling of Zane under an unfavorable 200 mb circulation, and these dissipation cases in "null" conditions, are a counter-point to the re-intensification cases under favorable upper-tropospheric support (as illustrated in the examples of Figs. 15 through 17).

The transitions of STY Oscar, TY Polly, and STY Ryan in September 1995 demonstrated how a TC, particularly a large one, may interact with and modify the 200-mb flow in such a manner that makes the upper-tropospheric support for re-intensification even more favorable. Oscar, Polly and Ryan formed in a sequence in a reverse-oriented monsoon trough (ATCR 1995), as depicted at 1200 UTC 16 September (Fig. 19a), 1200 UTC 18 September (Fig. 19b), and 1200 UTC 23 September 1995 (Fig. 19c), respectively. The NOGAPS analyses that correspond with this IR imagery are presented in Fig. 20. Oscar was a particularly intense and large TC whose outflow at 200 mb entered the polar jet. Notice the sharp cloud edge and anticyclonic curvature of this outflow pattern in Fig. 19a as it flows directly into the polar jet. An area of upper-level convergence (where the label "Oscar" appears) is associated with the peripheral anticyclone produced by Oscar, and a larger area of convergence exists to the east in the subtropical ridge, which is consistent with the subsidence that persisted throughout the sequence of images in Fig. 19. The poleward out-
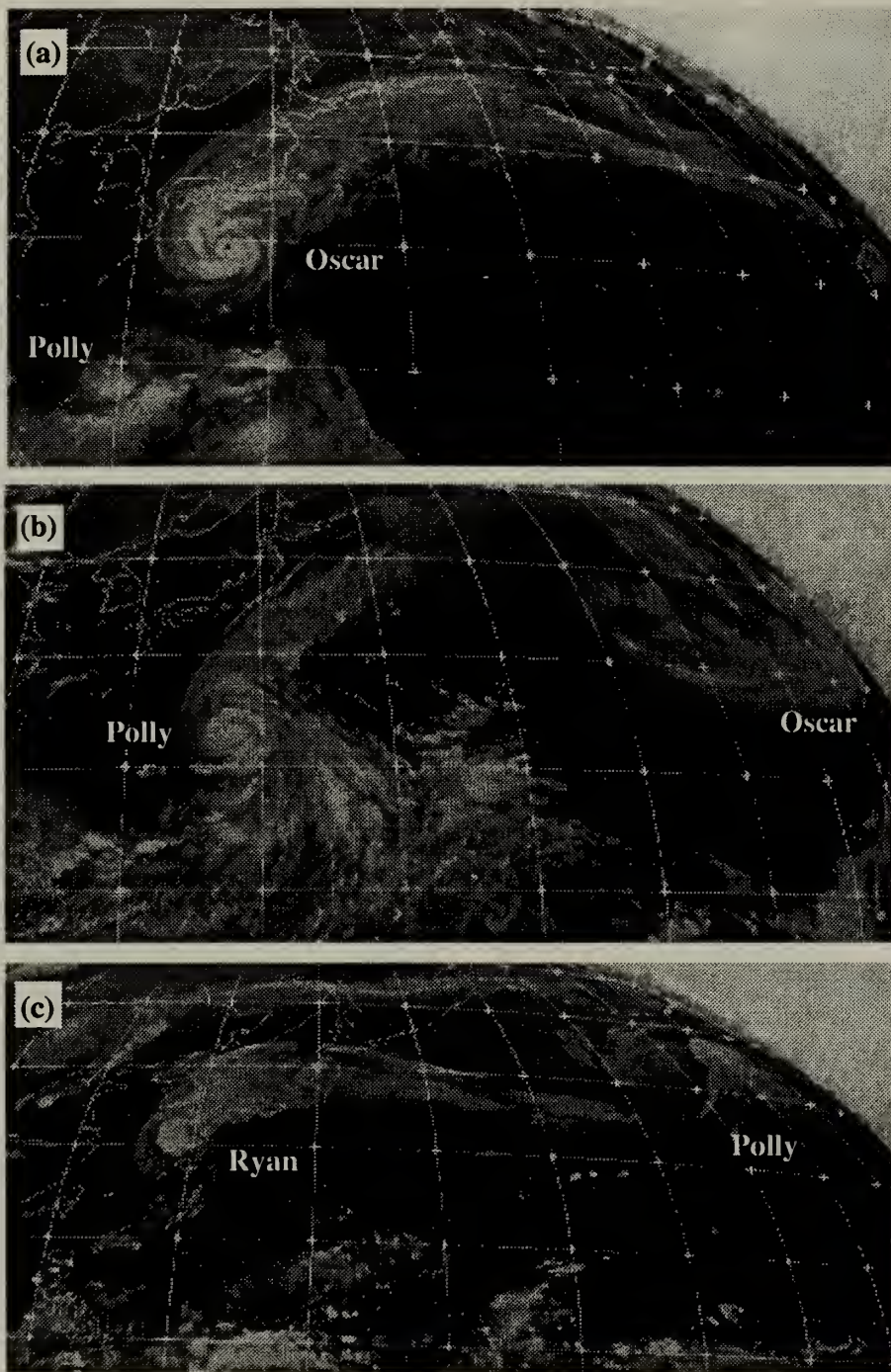
43

Fig. 19. Infrared imagery of the outflow patterns and polar jet associated with (a) STY Oscar at 1200 UTC 16 September, (b) TY Polly at 1200 UTC 18 September, and (c) STY Ryan at 1200 UTC 23 September 1995.
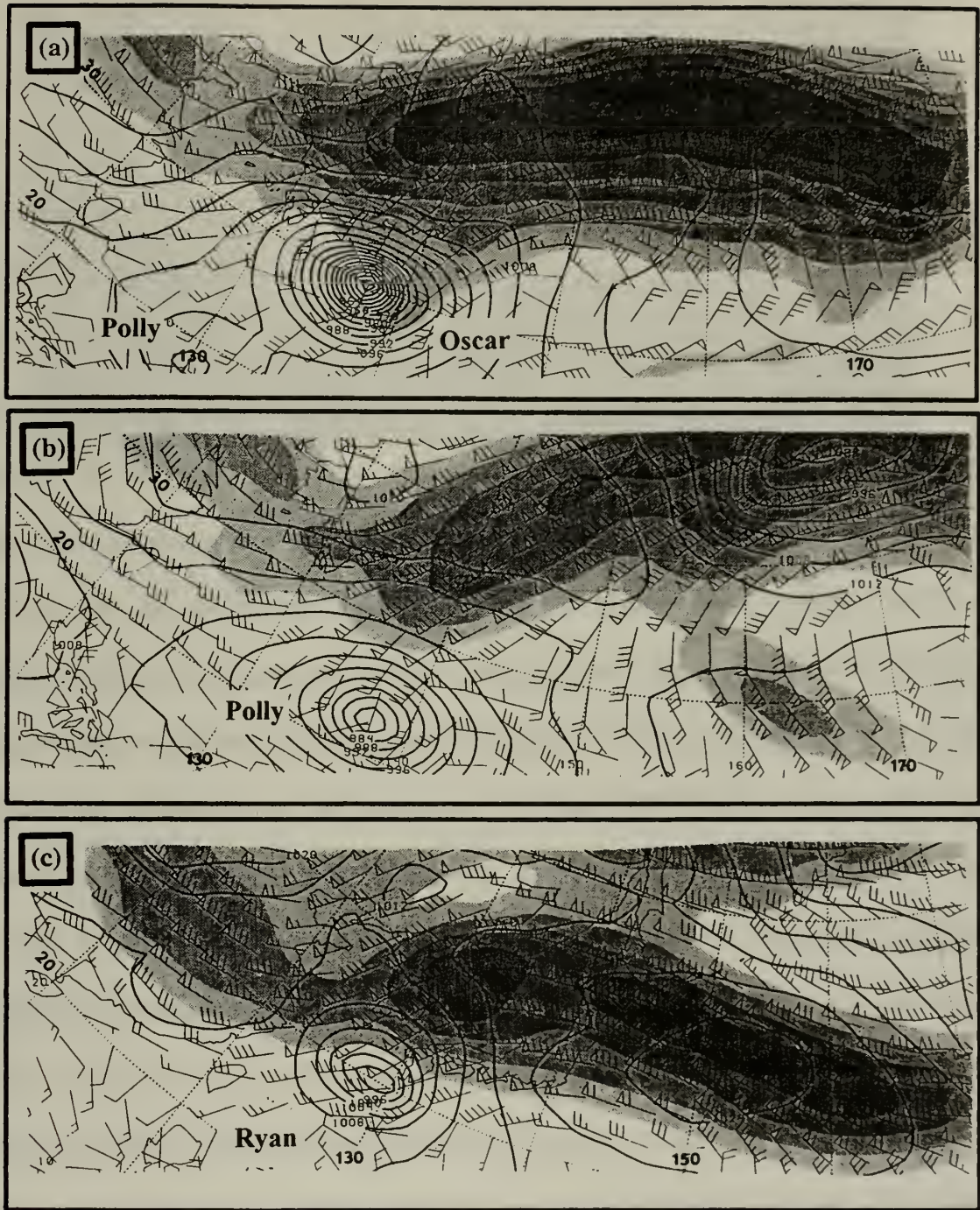
Fig. 20. As in Fig. 15, except for (a) STY Oscar at 1200 UTC 16 September, (b) TY
Polly at 1200 UTC 18 September, and (c) STY Ryan at 1200 UTC 23 September 1995.

flow of Oscar around this peripheral anticyclone appears to converge with the polar jet, and produce the sharp cloud edge shown in the imagery (Fig. 19a), and may contribute to the powerful (maximum winds of 165 kt) downstream jet streak depicted in Fig. 20a. Similarly, outflow of Polly (Fig. 19a) and Ryan (Fig. 19c) into the polar jet also appears to be associated with sharp cloud edges and large downstream accelerations into jet streaks (compare to Figs. 20b and 20c, respectively). Polly and Ryan were not nearly as large as Oscar, and their effect on the 200-mb flow was not as profound. That is, the outflow patterns of Polly and Ryan appear less vigorous in the imagery than that of Oscar, and the NOGAPS analyses have weaker downstream jet streaks associated with Polly and Ryan. After Oscar and Ryan completed transformation, they then re-intensified beneath the right- rear quadrants of the downstream jet streaks that their warm outflows appeared to have helped to build. Oscar's re-intensification continued under the left-exit region of an upstream jet streak that appeared to be enhanced by Polly's outflow. Similarly, Polly re-intensified beneath the left-exit region of an upstream jet streak that was associated with the outflow of Ryan. This sequence of re-intensifications was not forecast well by NOGAPS, which poorly predicted both the track and intensity of these storms during ET. Errors associated with NOGAPS forecasts of ET will be further discussed in Chapter IV.

The case of TY Tom in September 1996 also illustrated how the outflow of a TC, as well as the presence of another TC downstream, may create a 200-mb environment that is more favorable for re-intensification. In Fig. 21, Tom is shown approximately 1200 n mi east of STY Violet. By 1200 UTC 20 September, the outflows of both Tom and Violet have interacted with the polar jet and contributed to enhanced downstream jet streaks (Fig. 22a).
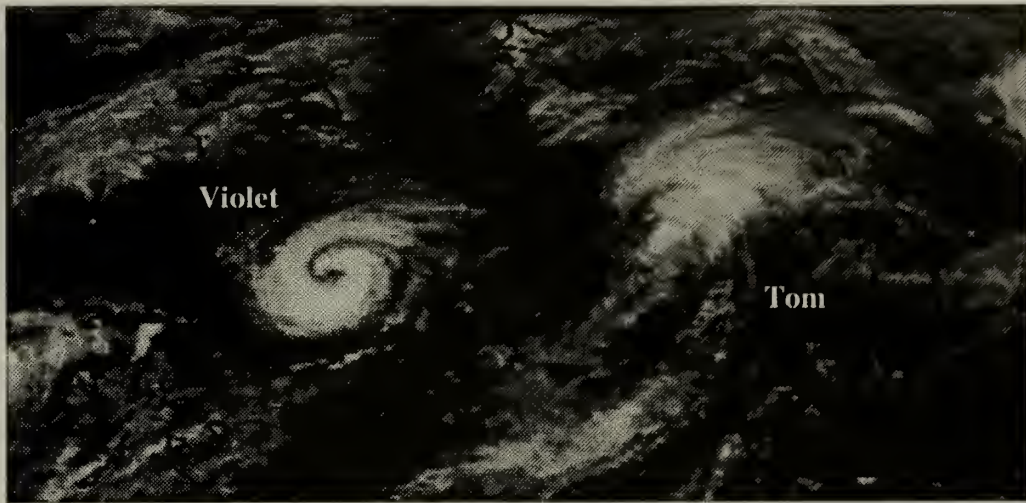
Fig. 21. Infrared imagery of TY Tom and STY Violet at 0632 UTC 18 September 1996.

Speed divergence associated with the downstream jet streak sustained Tom after transformation. At 1200 UTC 22 September, the left-exit region of the upstream jet streak enhanced by Violet's outflow is superposed above Tom (Fig. 22b). Tom quickly re-intensifies, and deepens 12 mb in 24 h (Fig. 22c).

A final example demonstrates the critical role played by the upper-troposphere circulation in the re-intensification of storms completing ET. In September 1994, STY Melissa completed transformation upstream of a characteristic omega blocking pattern (Fig. 23). As Melissa translated south of the blocking pattern from 19 through 21 September, it filled to 1002 mb, and nearly dissipated. Once the remnants of Melissa moved downstream of the blocking pattern, Melissa re-intensified beneath the right-rear quadrant of a downstream jet streak at 0000 UTC 22 September (Fig. 24a). Melissa then translated north-

47
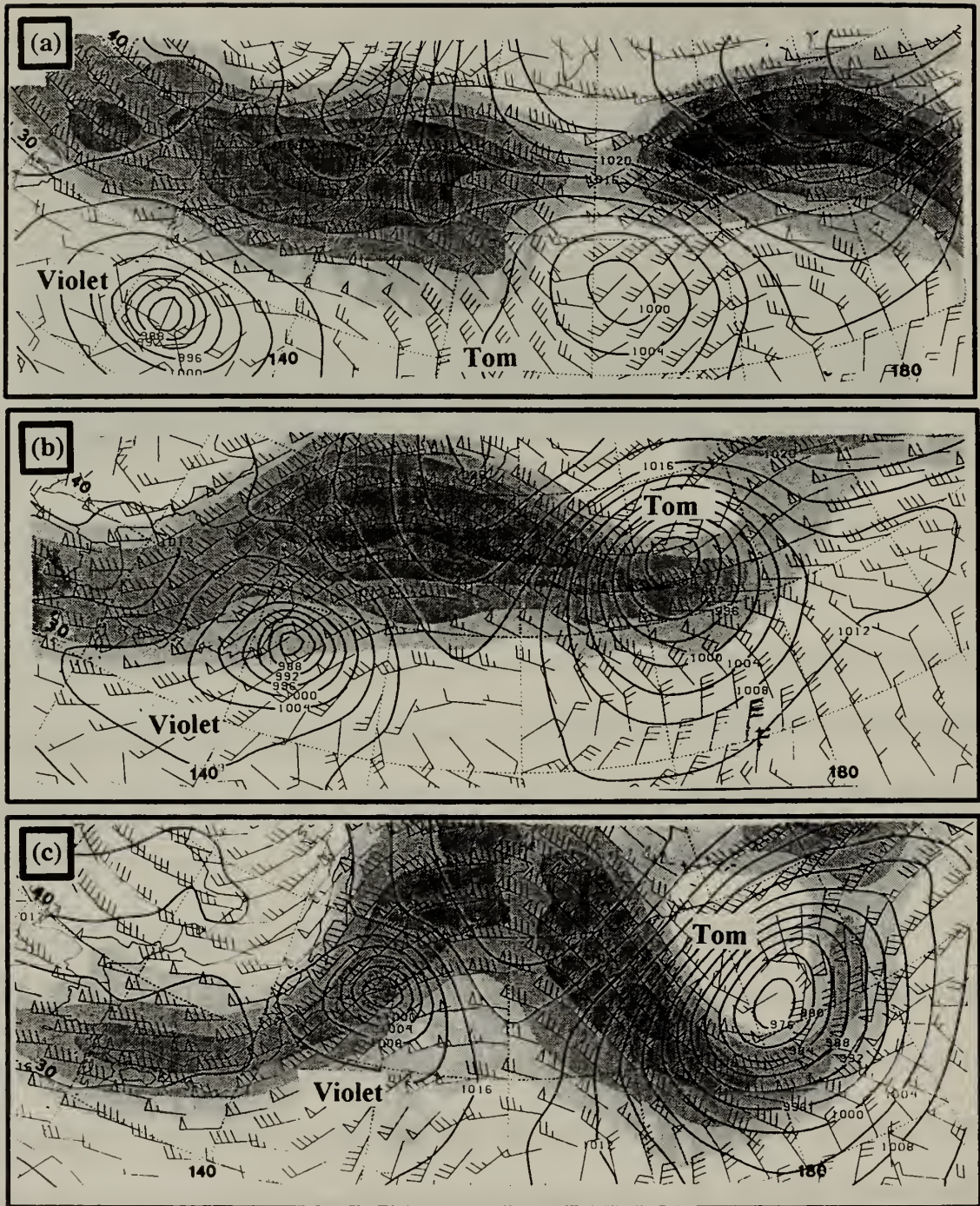
Fig. 22. As in Fig. 15, except for TY Tom and STY Violet at (a) 1200 UTC 20 September, (b) 1200 UTC 22 September, and (c) 1200 UTC 23 September 1996.

Fig. 23. Transformation of STY Melissa depicted in NOGAPS 500-mb height analyses (60 m contours) with superposed SLPs at 4 mb intervals indicated by gray shades decreasing from 1004 mb at (a) 1200 UTC 19 September, (b) 1200 UTC 20 September, and (c) 1200 UTC 21 September 1994.
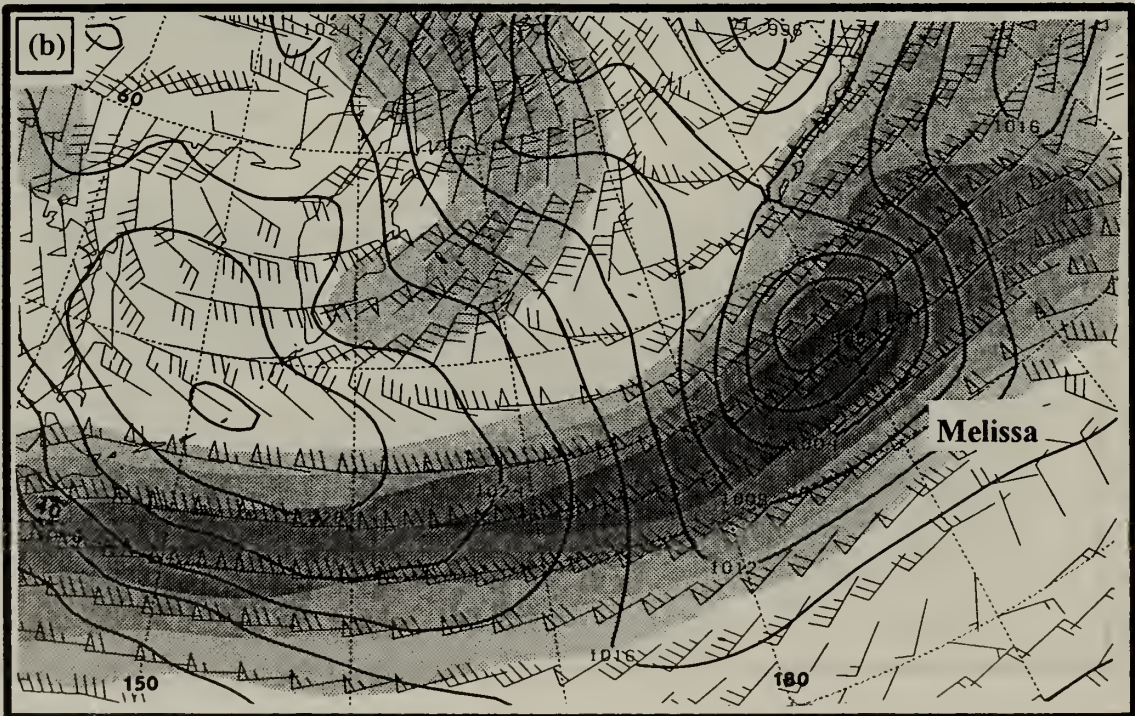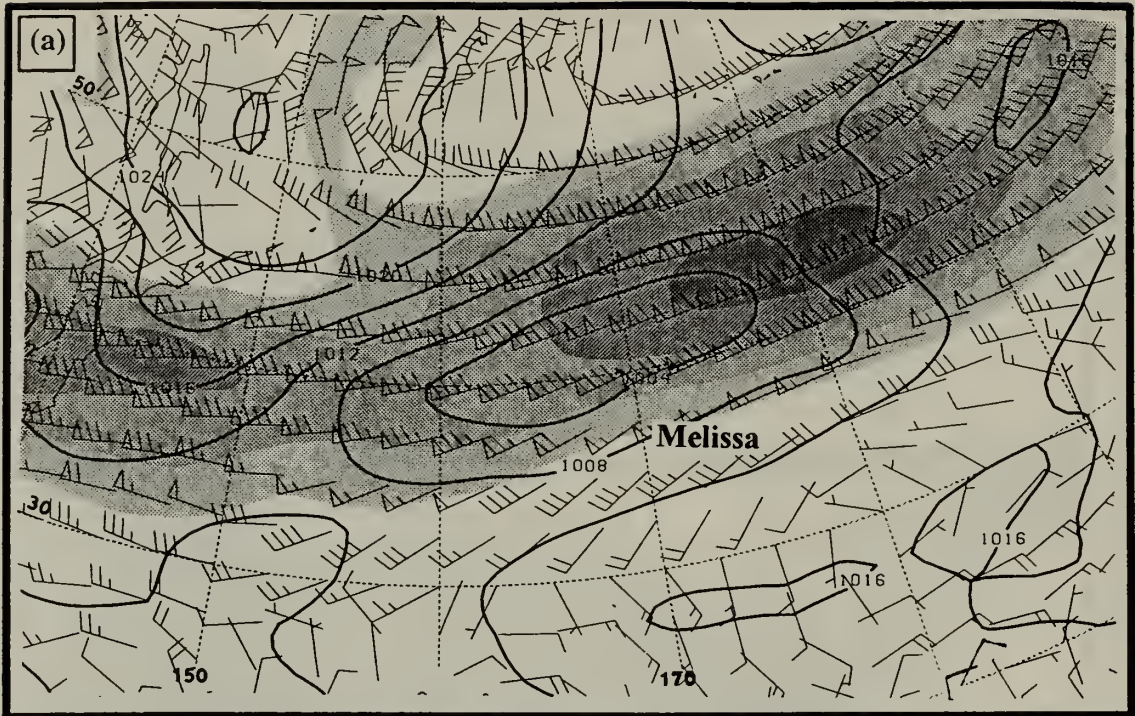
Fig. 24. As in Fig. 15, except for STY Melissa at (a) 0000 UTC 22 September
and (b) 0000 UTC 23 September 1994.

east beneath the left-exit region of that same jet streak (Fig. 24b), and ultimately deepened 32 mb in 48 h to 970 mb.

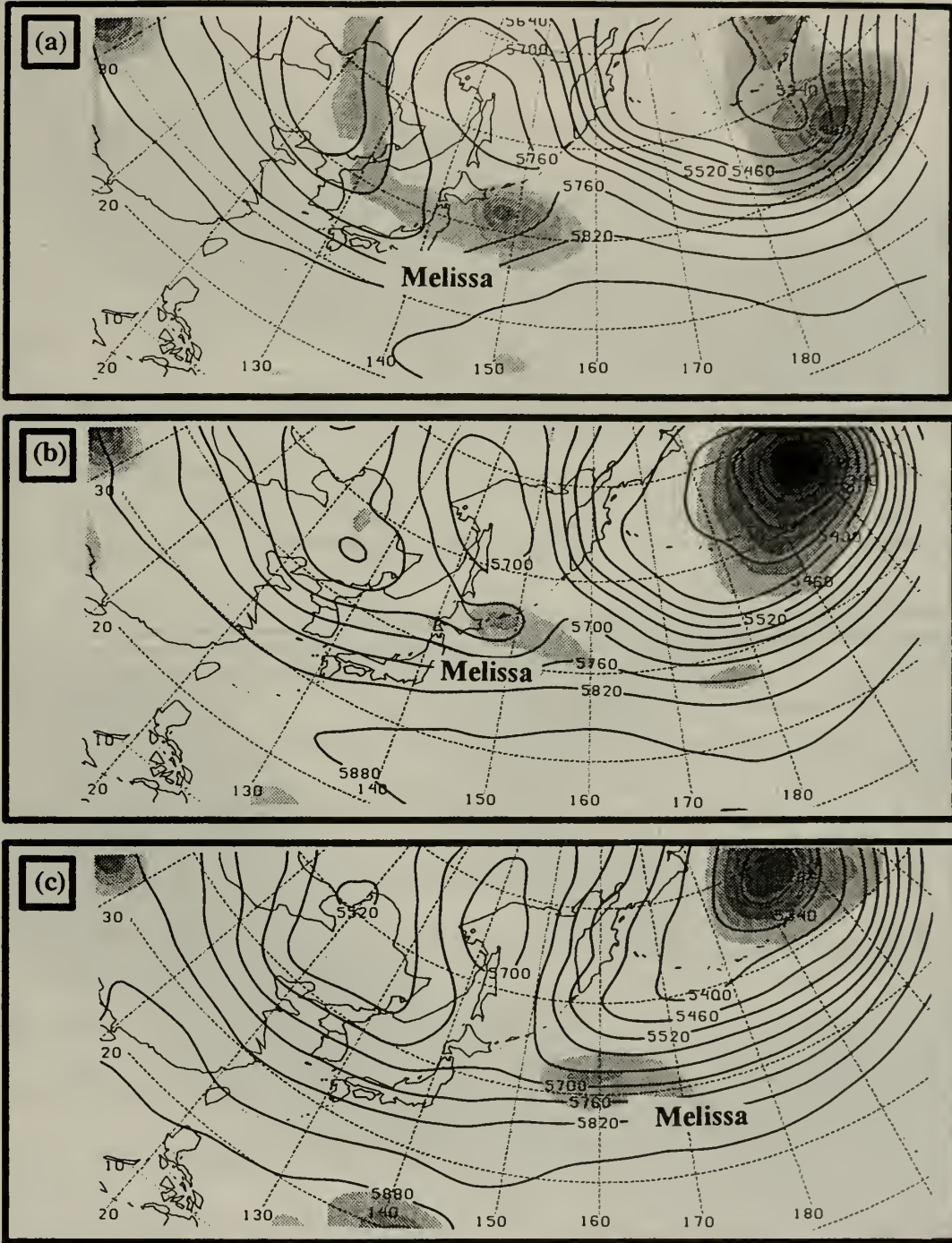## C.   INTENSITY CHARACTERISTICS OF CASES OF ET

After completion of transformation and re-intensification, the average minimum SLP achieved by all cases of ET (excluding dissipators) was 986 mb. Five storms achieved a central SLP below 980 mb: Melissa (970 mb), Oscar (958 mb), Orson (977 mb), Tom (974 mb), and Yates (978 mb). In these intense cases, gale-force (above 35 kt) and storm-force (above 50 kt) wind areas that verified in NOGAPS analyses were significant even when compared to those of a TC of average size and intensity. In particular, the maximum winds associated with these intense cases of ET are located at outer radii, far from the center of the storm. By contrast, the maximum winds of a TC would be expected to be located within the eyewall rainbands of the TC inner core. The location of maximum winds is further evidence that these storms are now baroclinic, extratropical cyclones.

The large area of gale- and storm- force winds associated with STY Oscar at 0000 UTC 16 September is depicted in Fig. 25a. Compare this with Fig. 25b, which illustrates similarly-sized areas of gale- and storm- force winds are associated with the later stage of Oscar as a 958 mb, mid-latitude cyclone. In the lower-left corner of Fig. 25b is the gale- and storm- force wind areas associated with TY Polly, which are more than twice as large as in the four cases depicted in Figs. 26a-d. However, note in Fig. 26c the total area of gale-force winds produced by Tom, and that the total area of gale-force winds and above in each of these cases is still quite large (on the order of 75-100,000 n mi^2). It is interesting to compare these results to those obtained from NSCAT and ERS-1/2 scatterometer data. An ERS-1/2

51
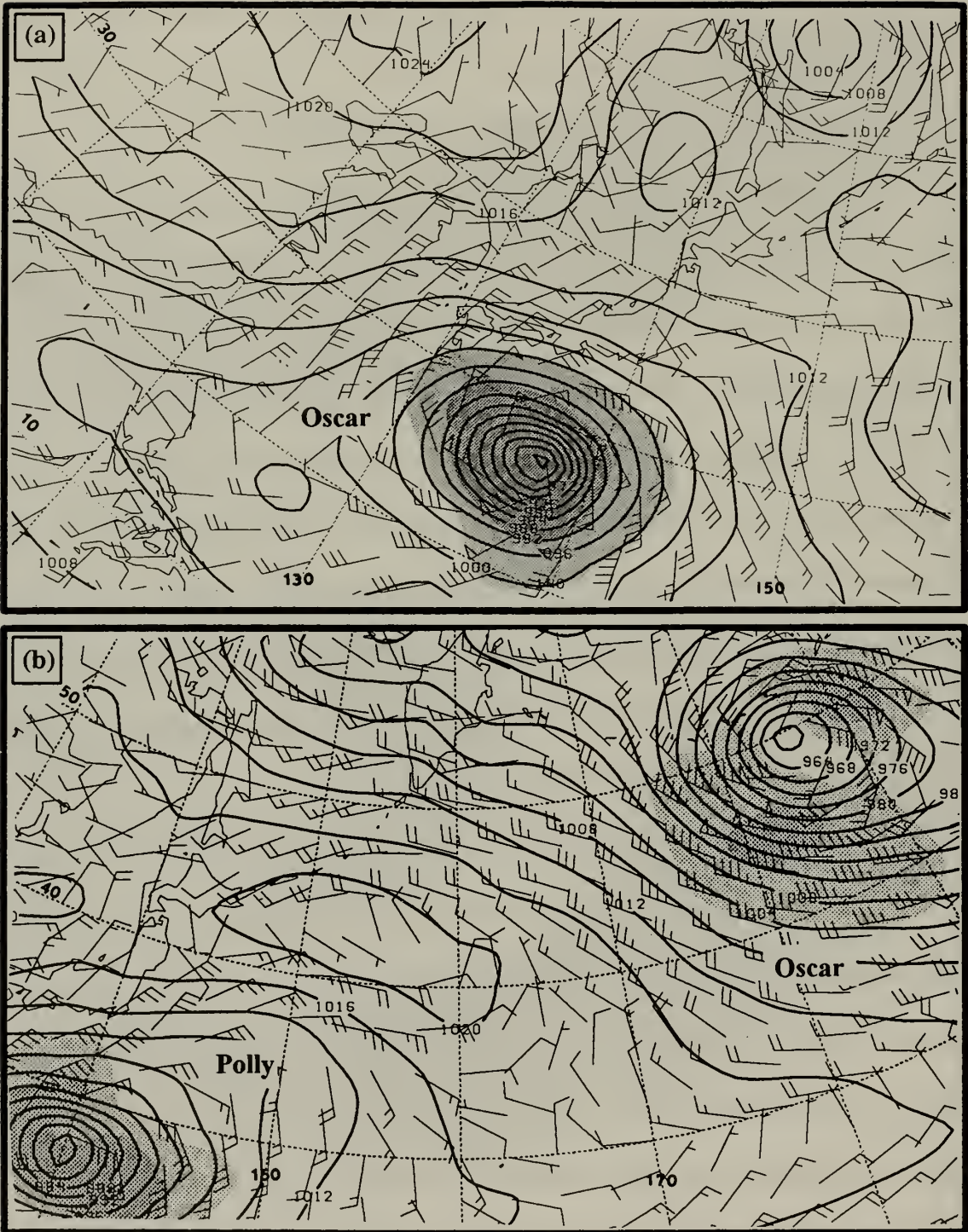
Fig. 25. Gale- and storm-force winds (kt) in NOGAPS analyses depicted by gray shades in the case of (a) STY Oscar at 0000 UTC 16 September, and (b) TY Polly and Oscar after ET at 1200 UTC 19 September 1995. Solid contours (4 mb interval) are SLPs.
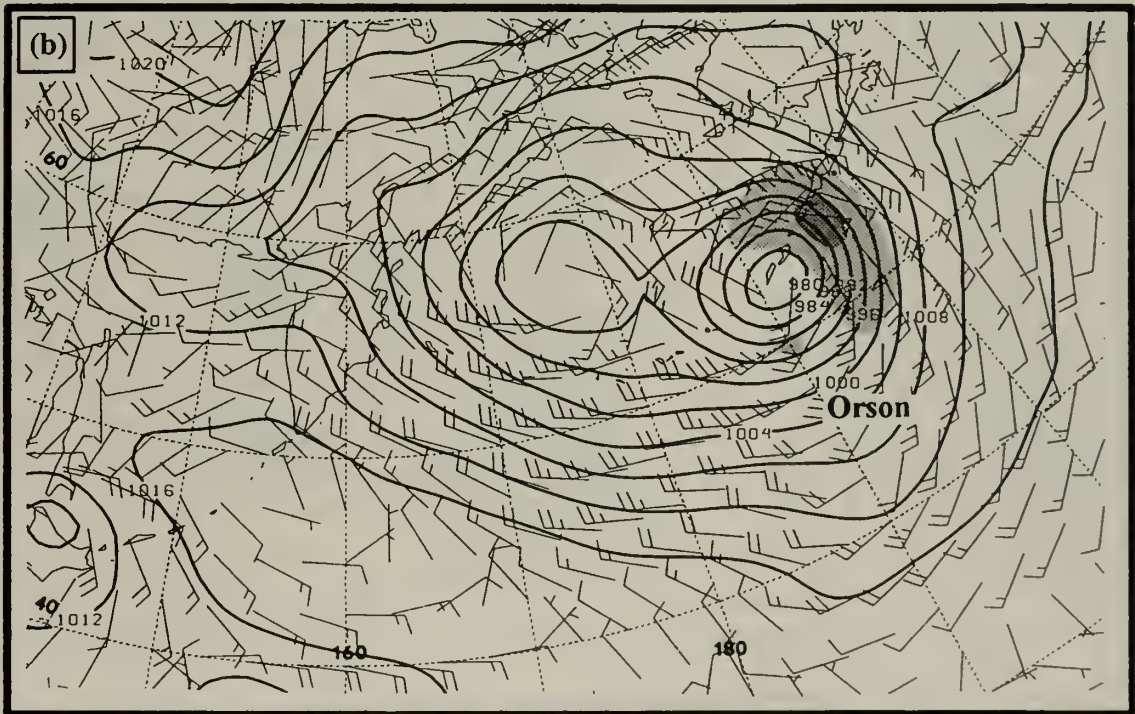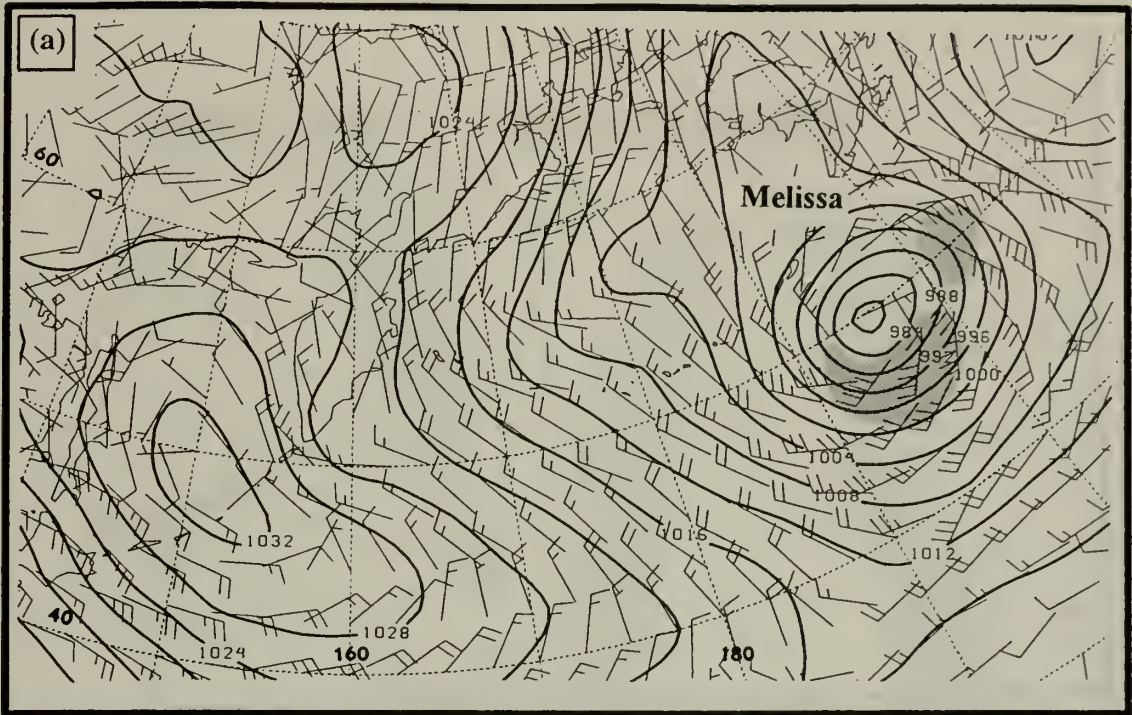
Fig. 26. As in Fig. 25, except for (a) Melissa after ET at 1200 UTC 23 September 1994, and (b) Orson after ET at 1200 UTC 5 September 1996.

53
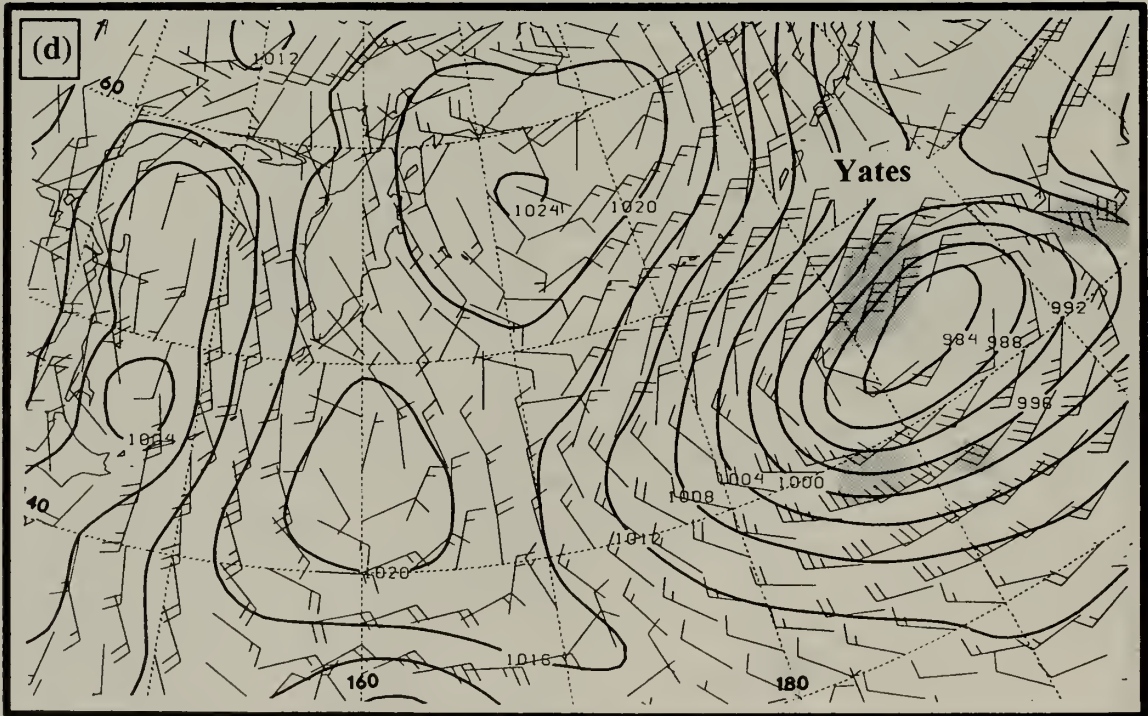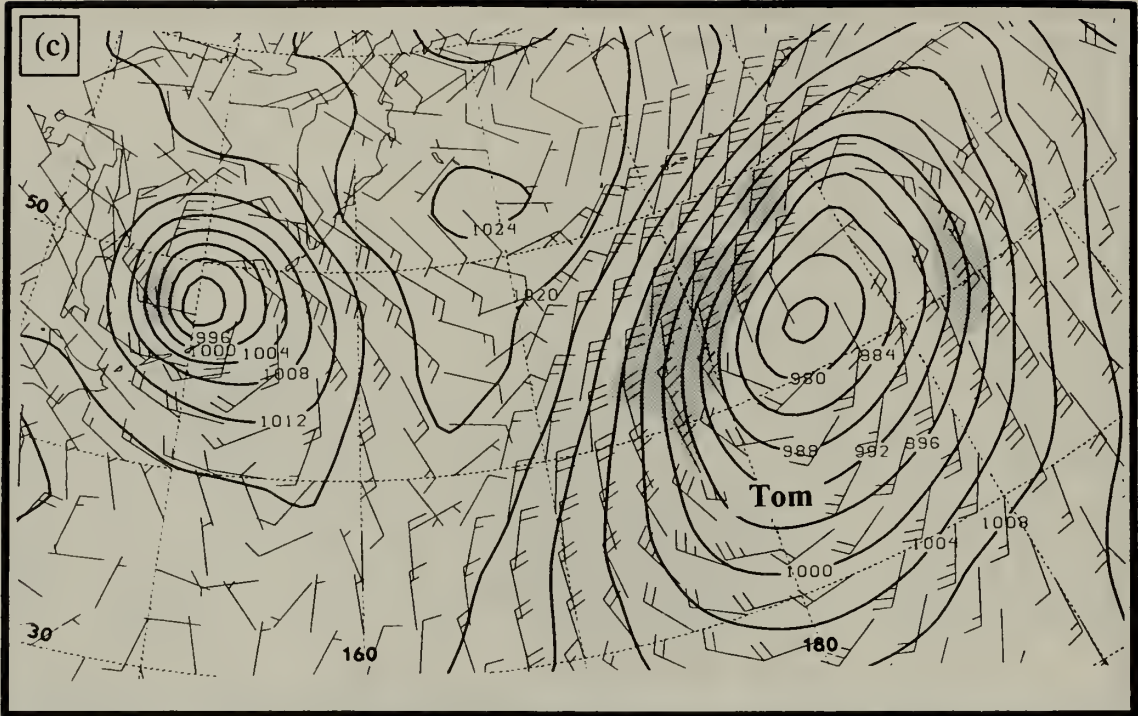
Figs. 26c-d (continued). As in Fig. 25, except for (c) Tom after ET at 0000 UTC 24 September 1996, and (d) Yates after ET at 1200 UTC 4 October 1996.
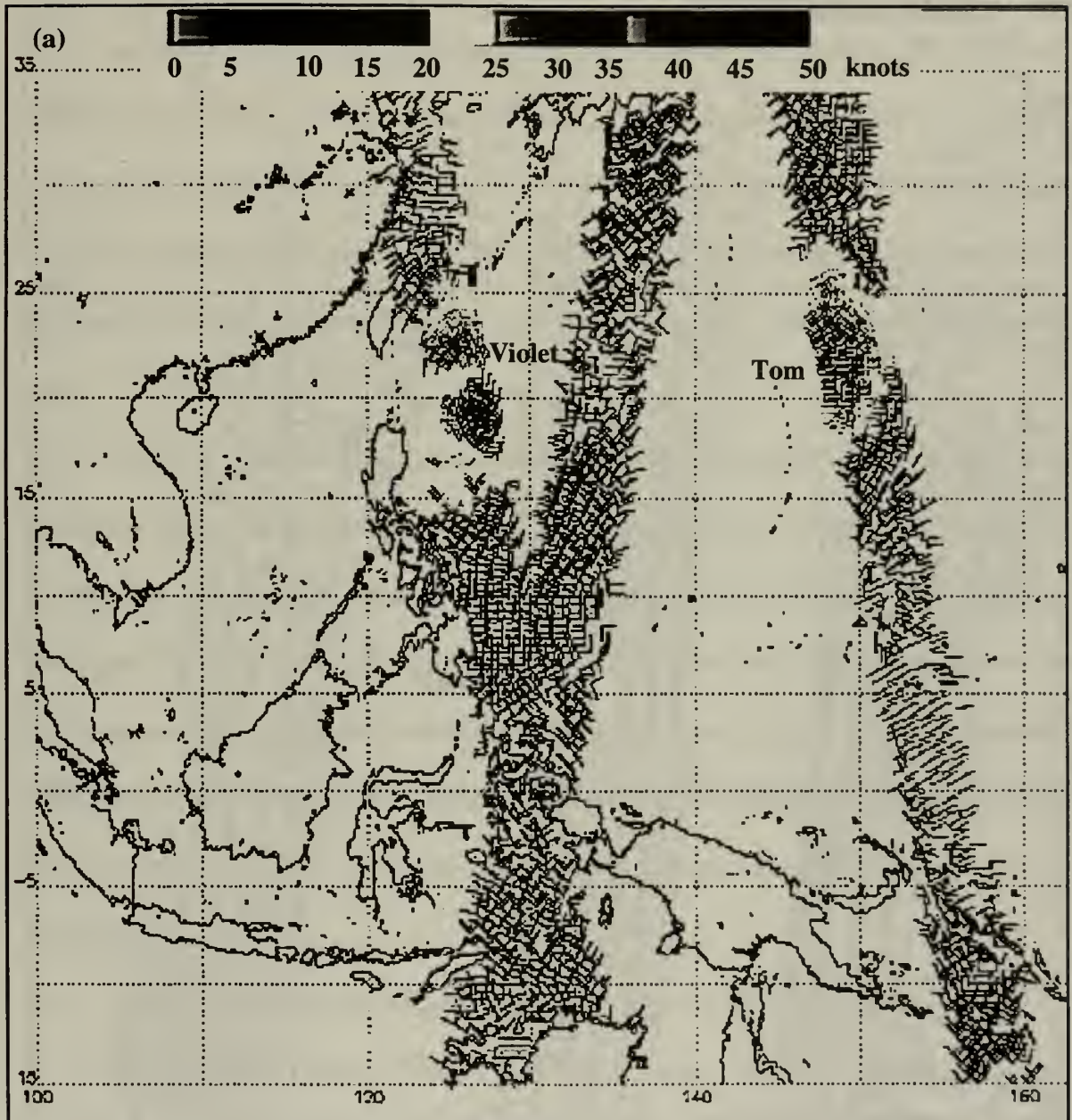
Fig. 27a. Surface wind analysis of TS Tom obtained from ERS1/2 scatterometer composite valid 1700 UTC 16 September 1996.

55
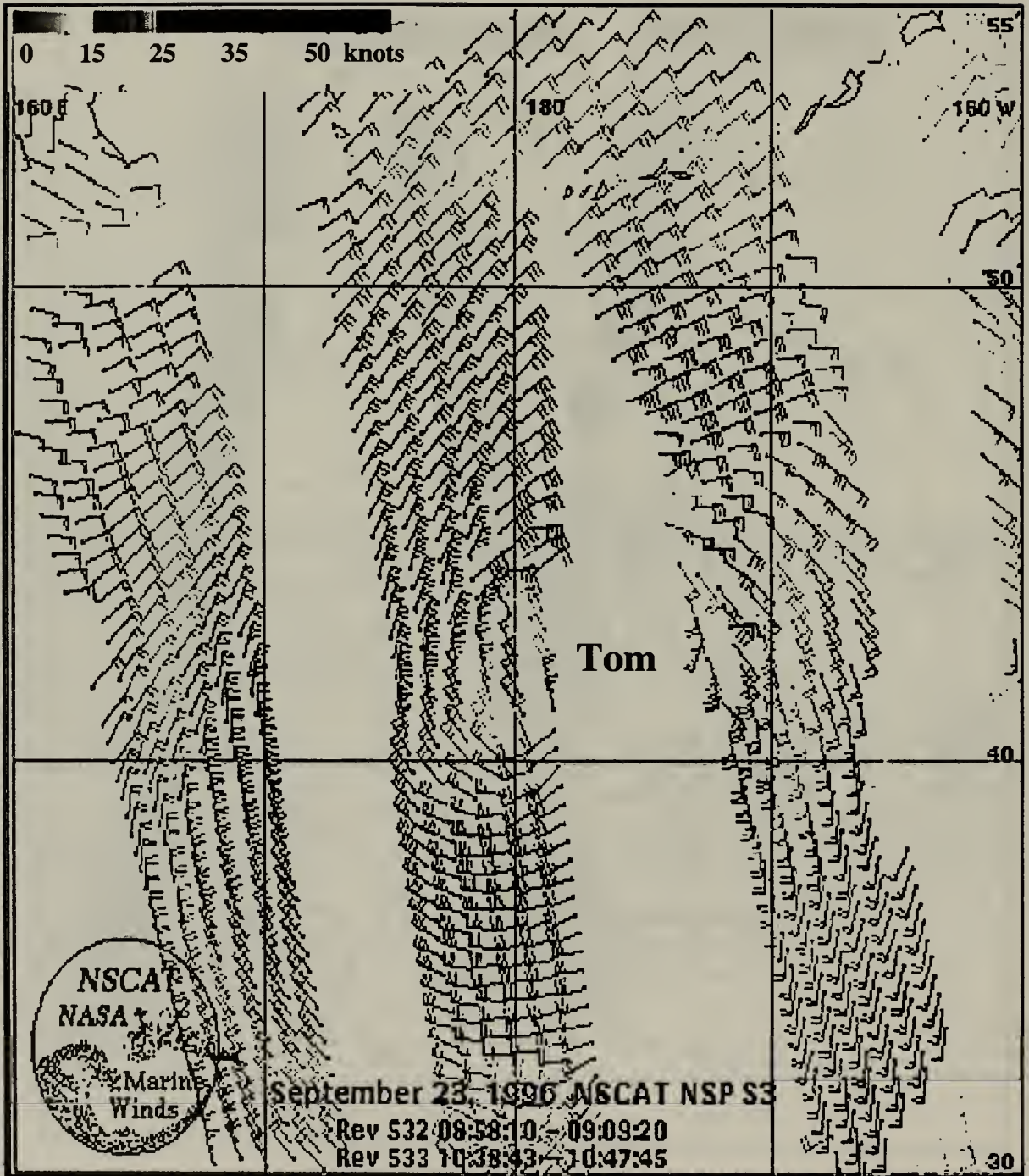
Fig. 27b. Surface wind analysis of Tom during ET obtained from NSCAT scatterometer composite valid 1047 UTC 23 September 1996.

scatterometer composite for 1700 UTC 16 September 1996 (Fig. 27a) depicts the wind structure of TS Tom during the mature TC stage. As expected, the highest surface wind speeds are concentrated at the inner core of the TC and decrease with distance from the storm center. By contrast, the wind structure of Tom just prior to completing ET in an NSCAT scatterometer composite (Fig. 27b) valid 1047 UTC 23 September clearly shows a much larger area of gale-force winds than the NOGAPS analysis in Fig. 26c, and also illustrates that the maximum winds are located well away from the storm center, with weaker winds at inner radii.

Thus, the re-intensification of storms following ET represent significant hazards to maritime interests, and are capable of causing widespread damage and loss of life. In the most extreme case, the gale- and storm-force wind areas produced by ET rivaled that of some of the largest TCs. Furthermore, NOGAPS analyses and forecasts may badly underestimate the areal extent covered by gale- and storm-force wind areas produced by ET. This demonstrates the value of scatterometer data in alerting forecasters to disseminate expanded gale warnings in spite of the small (if at all) area of gale-force winds depicted in NOGAPS analyses and forecasts.

D.   CHARACTERISTIC 500-MB PATTERNS IN CASES OF ET

As described in Chapter I, Harr et al. (1996; hereafter referred to as H96) used EOFs and PC analysis to determine that ET was influenced by the mid-latitude 500-mb circulation pattern into which a transforming TC was translating. The data set of H96 included cases of ET from 1 July through 31 October during 1990-1995; recently, cases of ET in the same period during 1996 were added by Prof. Harr. In H96, NOGAPS 500-mb height fields were

analyzed using EOFs at the first synoptic time after JTWC's last warning for the entire ET data set, including 25 of the 26 cases that occurred during 1994-1996. The case of Seth (October 1994) was omitted since insufficient data existed to perform the EOF analysis.

The 500-mb heights were converted to d-values by subtracting the standard atmosphere 500-mb height value of 5570 m. These d-values are available on a 2.5° latitude/longitude relocatable grid of 425 gridpoints over a domain of 17° latitude by 25° longitude. This grid is always positioned over the transition location, which is defined as the position of the TC at the first synoptic time following the last warning issued by JTWC, such that it is located at 7° latitude, 13° longitude from the lower left corner of the domain. The time mean d-value at each grid point over the 25 storm sample was not removed to allow for any characteristic 500-mb patterns that might be the result of seasonal (summer or autumnal) circulation variability. In addition, the time series of d-values at each gridpoint were not normalized with respect to the standard deviation, which allows the higher latitude grid points with larger d-value variance than lower latitude gridpoints to have an influence on the EOF spatial patterns. This latitudinal variation in d-values may not be too large because the domain only covered 17° of latitude, and only the summer and early autumn period is included.

The first EOF spatial pattern derived has the largest mode of variability in the 500-mb circulation for this specific ET data set, which includes only 25 cases from 1994-96. Thus, these patterns are "empirical" rather than mathematically defined functions such as sines and cosines that are used to represent spatial variations in Fourier analysis. The second spatial pattern is orthogonal to the first pattern and explains the second largest fraction of the total

58

variance for the data set. This process of deriving spatial patterns continues until 425 patterns that explain all of the variability in the data set are completed. Also, coefficients (PC amplitudes) that define the relative contributions of each of the spatial patterns in the data set for each ET case are calculated. Thus, 25 PC amplitudes, corresponding to the 25 cases of ET during 1994-1996, were obtained from the full data set for each mode. The 25 maps of d-values during ET can be reconstructed by summing the entire set of 425 PC amplitudes times the corresponding spatial patterns. Since it is known that the leading modes in terms of the largest amplitude PC values contain the major signal in the sample, and the small amplitude PC values probably represent noise, a definition that isolates these predominant modes is desired.

The first three modes together explained 63% of the total variance, while the first 25 EOFs together explained 99% of the variance. H96 determined that the first two modes described seasonal summer and autumn 500-mb circulation patterns during ET. The third mode (EOF-3) described variations of these typical seasonal patterns, in which the EOF-3 positive (negative)[5] mode has a primary 500-mb low northwest (northeast) of the transition location (Fig. 28). Furthermore, the EOF-3 positive (negative) pattern has a larger (smaller) amplitude 500-mb subtropical ridge to the east of the transition location. Each of the 25 cases of ET can therefore be compared to these two EOF-3 patterns based on its PC sign and

---

[5]When Harr modified his EOF analyses to include cases of ET during 1996, all PC amplitude scores for EOF-3 that were previously negative became positive, and vice versa. For this reason, the present synoptic descriptions of EOF-3 positive and negative patterns is opposite that of H96, and opposite of the description presented here in Chapter I. To avoid confusion, EOF-3 patterns will be categorized hereafter as described in relation to the full data set (1990-1996).

(a) EOF-3 Positive   (b) EOF-3 Negative
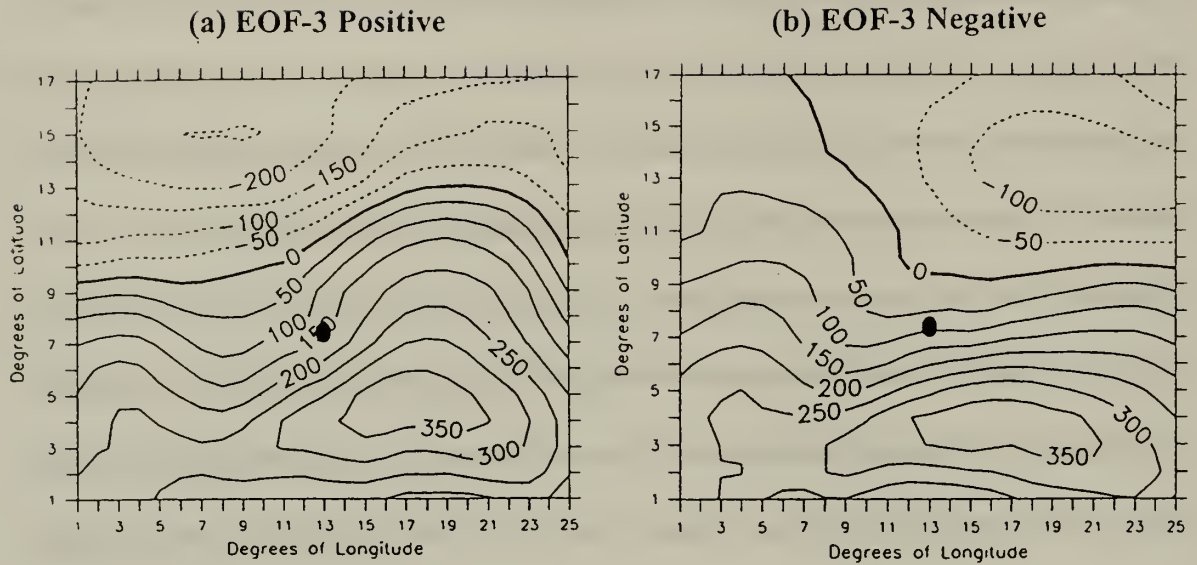
Fig. 28. Average 500-mb d-value patterns based on a composite of cases that have EOF-3 PC scores (a) greater than one standard deviation above the mean, and (b) greater than one standard deviation below the mean. Solid (dashed) lines depict positive (negative) d-value contours, and the heavy black dot denotes the transition location (adapted from Harr et al. 1996).

amplitude. Cases of ET that have EOF-3 PC amplitude one standard deviation above (below) the mean are classified as strongly EOF-3 positive (negative) cases. Individual examples of strongly positive EOF-3 and strongly negative EOF-3 cases are depicted in Fig. 29. Notice the basic similarity of these individual patterns with the composited fields in Fig. 28.

For the EOF-3 cases defined as either positive or negative, their tracks during ET were plotted based on JTWC best track positions (until JTWC discontinued reporting the position of the storm after it became extratropical), and NOGAPS analyses (when best track positions were no longer continued for that particular TC). The tracks of the 10 EOF-3 positive and 15 EOF-3 negative storms are depicted in Figs. 30 and 31 respectively. For the

(a) Carlo, 0000 UTC 27 October 1996 **(b) Dan, 1200 UTC 12 July 1996**
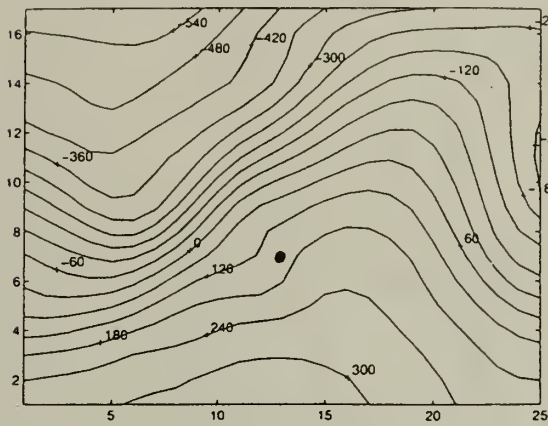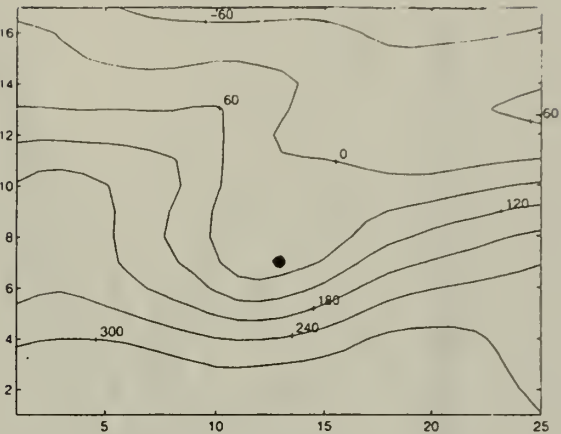
Fig. 29. The 500-mb d-values (m) for (a) EOF-3 positive case of Carlo, October 1996, and (b) EOF-3 negative case of Dan, July 1996 (Harr et al. 1996).

most part, the EOF-3 positive cases have a more meridional track, while the EOF-3 negative cases followed a relatively zonal path. This suggests that EOF-3 patterns at the beginning of ET can be used to characterize future tracks.

Table 3 is a summary of the PC amplitude at the first synoptic time after JTWC's last warning, and the subsequent peak intensity after transformation and re-intensification, for each of the 25 ET cases that occurred from 1 July through 31 October during 1994-1996. The average peak intensity (minimum SLP) for EOF-3 negative (positive) storms is 983.3 mb (991 mb), so that the EOF-3 negative cases subsequently deepen more. Notice that for the eight cases of ET with a minimum SLP below 986 mb after transformation and re-intensification, seven cases are EOF-3 negative and only one (Tom, September 1996) is EOF-3 positive. This suggests that the intensity of storms produced by ET can be related to the
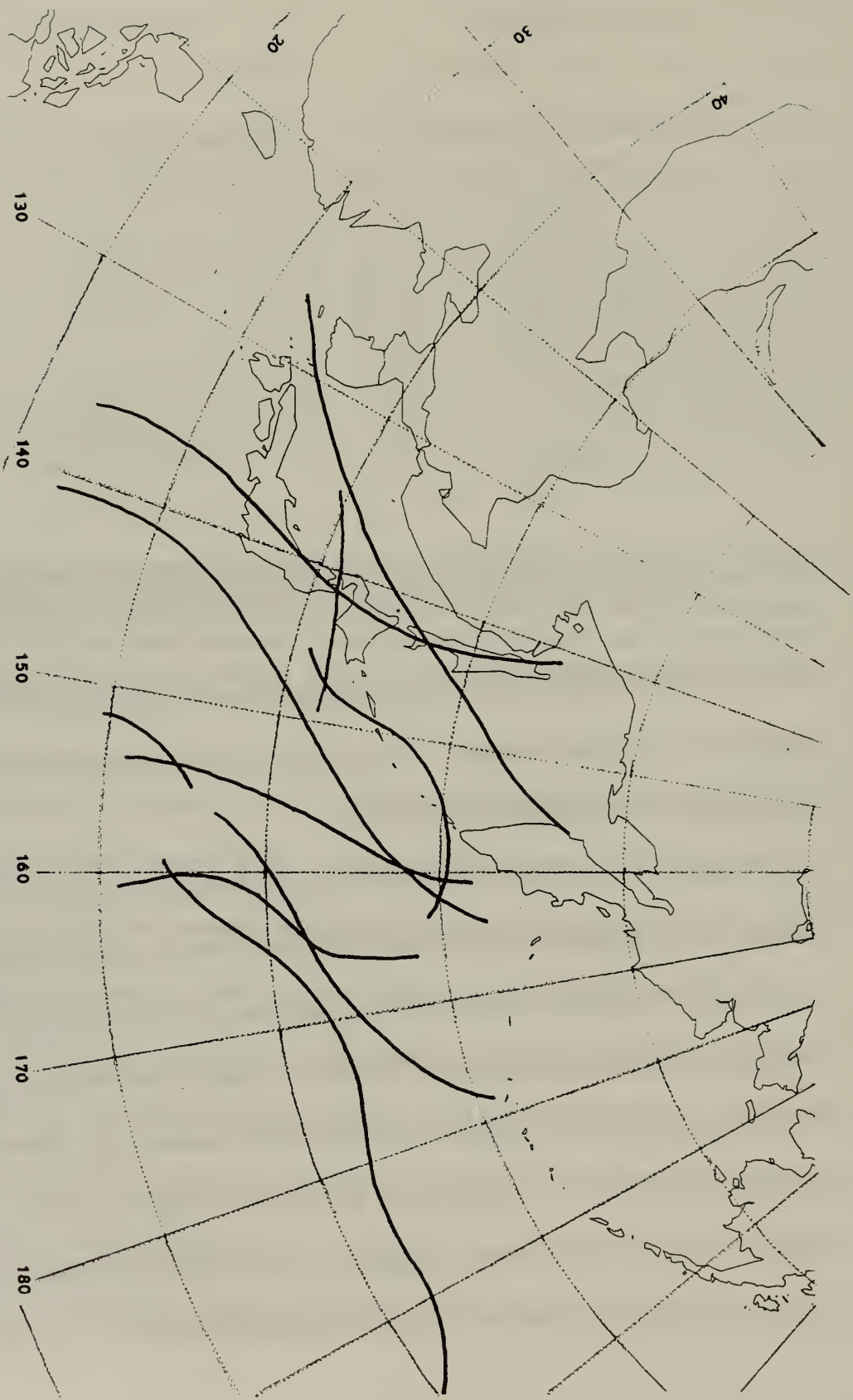
Fig. 30. Tracks of cases of ET from 1 July to 31 October during 1994-1996 that were classified as EOF-3 positive.

62
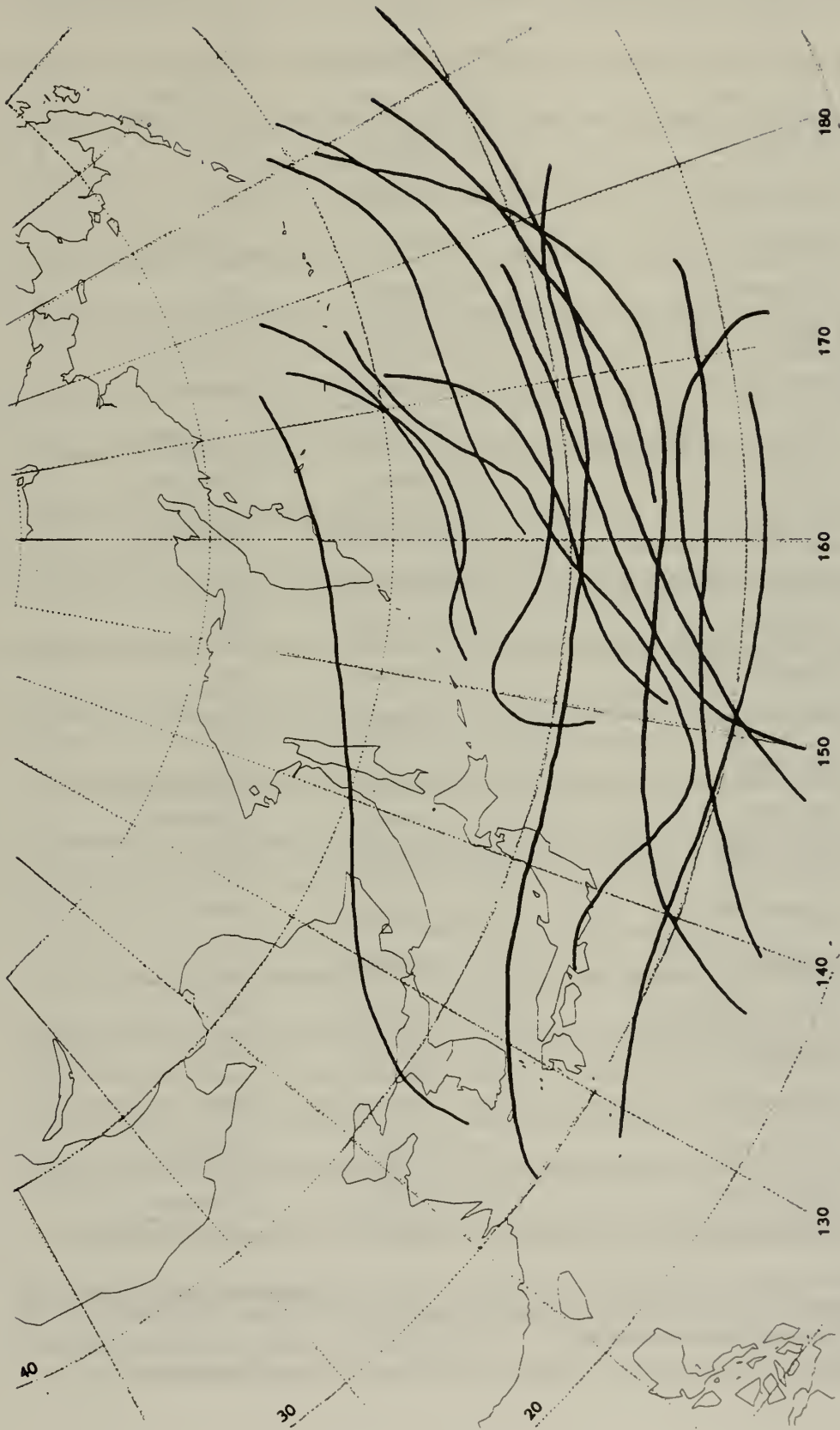
Fig. 31. As in Fig. 30, except for EOF-3 negative cases.

63

Case	Month and Year of transition	PC Amplitude	Peak Intensity (mb)
Zeke	July 1994	-1171.8 (negative)	990
Brendan	August 1994	-435.6 (positive)	Dissipated
Ellie	August 1994	-834.3 (negative)	994
Ivy	September 1994	-26.0 (positive)*	995
Kinna	September 1994	283.0 (positive)	Dissipated
Melissa	September 1994	-984.8 (negative)	970
Nat	September 1994	-340.6 (positive)	Dissipated
Orchid	September 1994	-251.9 (positive)	994
Pat/Ruth	September 1994 after merger	-1344.0 (negative)*	Dissipated
Faye	July 1995	-520.2 (positive)	Dissipated
Janis	August 1995	-1335.9 (negative)	Dissipated
Oscar	September 1995	-1869.0 (negative)*	958
Polly	September 1995	-1255.4 (negative)	986
Ryan	September 1995	-1133.3 (negative)	985
Ward	October 1995	-1180.2 (negative)	1002
Dan	July 1996	-1589.8 (negative)*	986
Eve	July 1996	-956.6 (negative)	Dissipated
Joy	August 1996	-188.2 (positive)	1002
Kirk	August 1996	-1352.0 (negative)*	990
Orson	September 1996	-1113.3 (negative)	977
Tom	September 1996	-539.3 (positive)	974
Violet	September 1996	-274.1 (positive)	990
Yates	October 1996	-806.7 (negative)	978
Zane	October 1996	-802.4 (negative)	Dissipated
Carlo	October 1996	1302.2 (positive)*	Dissipated

Mean PC Amplitude score = -718.1   Standard Deviation = 621.1   Average intensity = 986 mb

Table 3. The EOF-3 PC amplitudes at the first synoptic time after JTWC's last warning and minimum central SLP (peak intensity) after re-intensification of cases of ET during 1 July through 31 October 1994-1996. Cases with an asterisk in the PC amplitude column are considered to be strongly positive or negative as the amplitude exceeds the mean +/- one standard deviation. Cases that did not re-intensify are listed as having dissipated.

EOF-3 pattern into which they transition during transformation, and that EOF-3 negative storms are more likely to deepen explosively during re-intensification. In the lone EOF-3 positive case that deepened below 986 mb (Tom), the PC amplitude at the first synoptic time after JTWC's last warning is well within one standard deviation of the mean. Furthermore, the 500-mb d-value analysis (Fig. 32a) indicates a strong circulation is still associated with Tom as it is transforming, and a peripheral anticyclone is directly to the east of the transition location. The primary low is to the northeast, just out of the domain. No other case in the entire ET data set had such a strong circulation at the transition location, or as vigorous a peripheral anticyclone associated with it. This suggests the case of Tom at the first synoptic time after JTWC's last warning might not have been representative of the same stage of transformation as for the other EOF-3 negative cases with subsequent deepening below 986 mb. Just 24 h later, the 500-mb pattern changed such that Tom was upstream of a primary low to the north and east, with a flattened subtropical ridge and no indication of the peripheral anticyclone (Fig. 32b), which is more representative of the EOF-3 negative pattern associated with Dan in Fig. 29b.

At least in these cases, the EOF-3 pattern at the time of the TC transition appears to determine the characteristic track and intensity of the resultant mid-latitude cyclone. A TC that transitions into an EOF-3 negative (positive) pattern tends to follow a more zonal (meridional) track during transformation and is more (less) likely to have deeper SLP than the mean intensity of cases that completed transition. Therefore, examination of mid-latitude 500-mb circulation in NOGAPS analyses and forecasts will enable a forecaster to understand the subsequent intensity and track following commencement of ET. If the transitioning TC
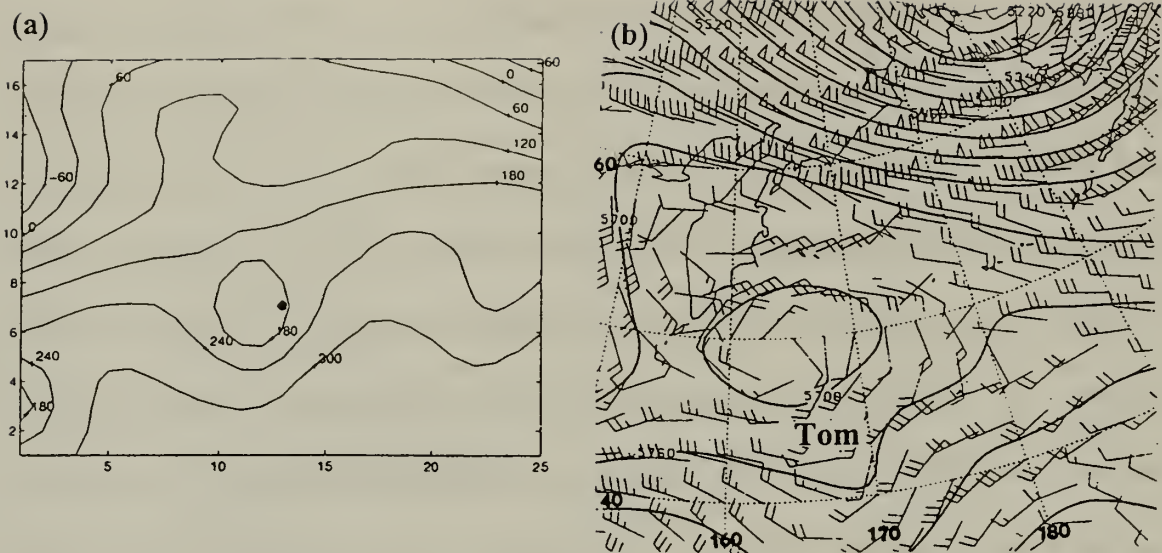
Fig. 32. (a) As in Fig. 28, except for Tom at 1200 UTC 20 September 1996. In (b), 500-mb NOGAPS analysis at 1200 UTC 21 September 1996. Solid lines represent 500-mb heights, winds are in kt.

is south and east of the primary 500-mb low, with a relatively large amplitude subtropical ridge to the east (EOF-3 positive as in Fig. 28a), it should be expected that cyclone that evolves from the remnants of this TC will translate meridionally and achieve average intensity at best. If the TC is west and south of the primary 500-mb low, with a low amplitude ridge to the east (EOF-3 negative as in Fig. 28b), a more zonal track with more vigorous re-intensification should be expected.

It is suggested that storms in an EOF-3 negative pattern were able to deepen more vigorously because their mostly zonal track afforded them ample opportunity to interact with the upper-tropospheric flow and couple vertically with regions in the 200-mb circulation that were more favorable for re-intensification. This reasoning is consistent with the cases of re-

66

intensification described in Chapter III.B. Each of these cases were able to interact with the 200-mb mid-latitude circulation over a period of 48 h or more during and after transformation, until they subsequently re-intensified beneath areas of divergence in the 200-mb flow and achieved a central SLP below 986 mb. All but one of these eight were EOF-3 negative during transformation, and the exception in the case of Tom may not have actually been as far along in the transformation stage as the other seven cases until 24 h later, when the pattern had changed to EOF-3 negative. Therefore, these TCs had more zonal tracks and sufficient time to translate in phase with upper-tropospheric flow favorable for re-intensification during their transition, which permitted more rapid and deeper extratropical cyclogenesis. In contrast, cases that were EOF-3 positive during transformation only briefly interacted with the 200-mb circulation before they translated north of the jet axis and became cut-off within a 500-mb long wave trough. Thus, these cases were unable to couple with the divergent regions associated with jet streaks or diffluent troughs. Therefore, evolution of the mid-latitude upper-tropospheric flow, together with the length of time with favorable coupling in the vertical between the surface and upper-tropospheric circulation, determined to a large extent the progress and outcome of ET.

IV. FORECAST ERRORS ASSOCIATED WITH ET

The NOGAPS 500-mb height anomaly correlation scores over the North Pacific region from 20°N to 80°N and 120°E to 180° were examined for the cases of ET during 1996 to determine what contribution ET may have had to scores below the first standard deviation. In August 1996, consistently low 500-mb anomaly correlation scores (Fig. 33) on the 4th and the 17th, respectively, are found at the times corresponding to the 24-h, 48-h, 72-h, and 96-h forecasts of Joy and Kirk. Joy (Fig. 34) was transforming at 0000 UTC 4 August. The 48- and 72-h NOGAPS 500-mb forecasts essentially predicted that Joy would dissipate (Fig. 34a and b), while the 24-h forecast predicted that Joy would be weaker (Fig. 34c) at 500 mb than depicted in the analysis valid 0000 UTC 4 August (Fig. 34d). By contrast, at 1200 UTC 6 August the surface circulation of Joy (not shown) was overforecast by NOGAPS leading up to the completion of merger. Kirk (Fig. 35) maintained its surface circulation despite having begun to merge at 500 mb with a pre-existing low at 0000 UTC 17 August. The 72-, 48-, and 24-h NOGAPS forecasts all predicted Kirk would be deeper at the surface, and have a stronger 500-mb circulation (Fig. 35 a through c), than the verifying analysis (Fig. 35d) at 0000 UTC 17 August. In summary, the 1996 cases of ET (Joy and Kirk) that merged with a pre-existing mid-latitude low both produced significant error in NOGAPS 500-mb forecasts as demonstrated by low 500-mb anomaly correlation scores. Furthermore, NOGAPS consistently overforecast the deepening of SLP and size of the surface circulations of both Joy and Kirk for the 24-h period leading to the completion of merger.

69
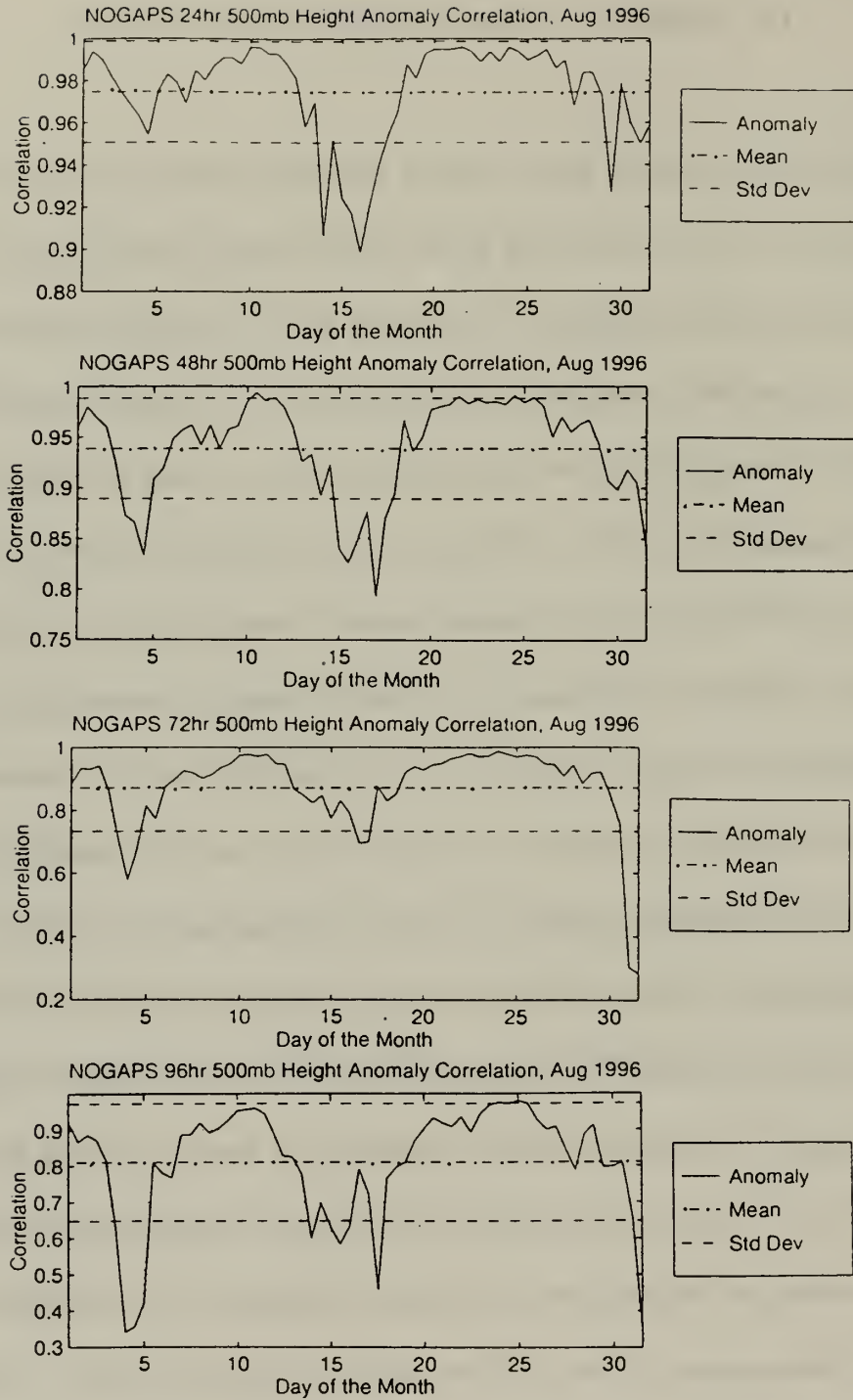
Fig. 33. The NOGAPS 500-mb anomaly correlation scores (daily, solid; monthly mean, dash-dot; mean +/- one standard deviation, dashed) during August 1996 for 24-,48-,72-, and 96-h forecasts (top to bottom).
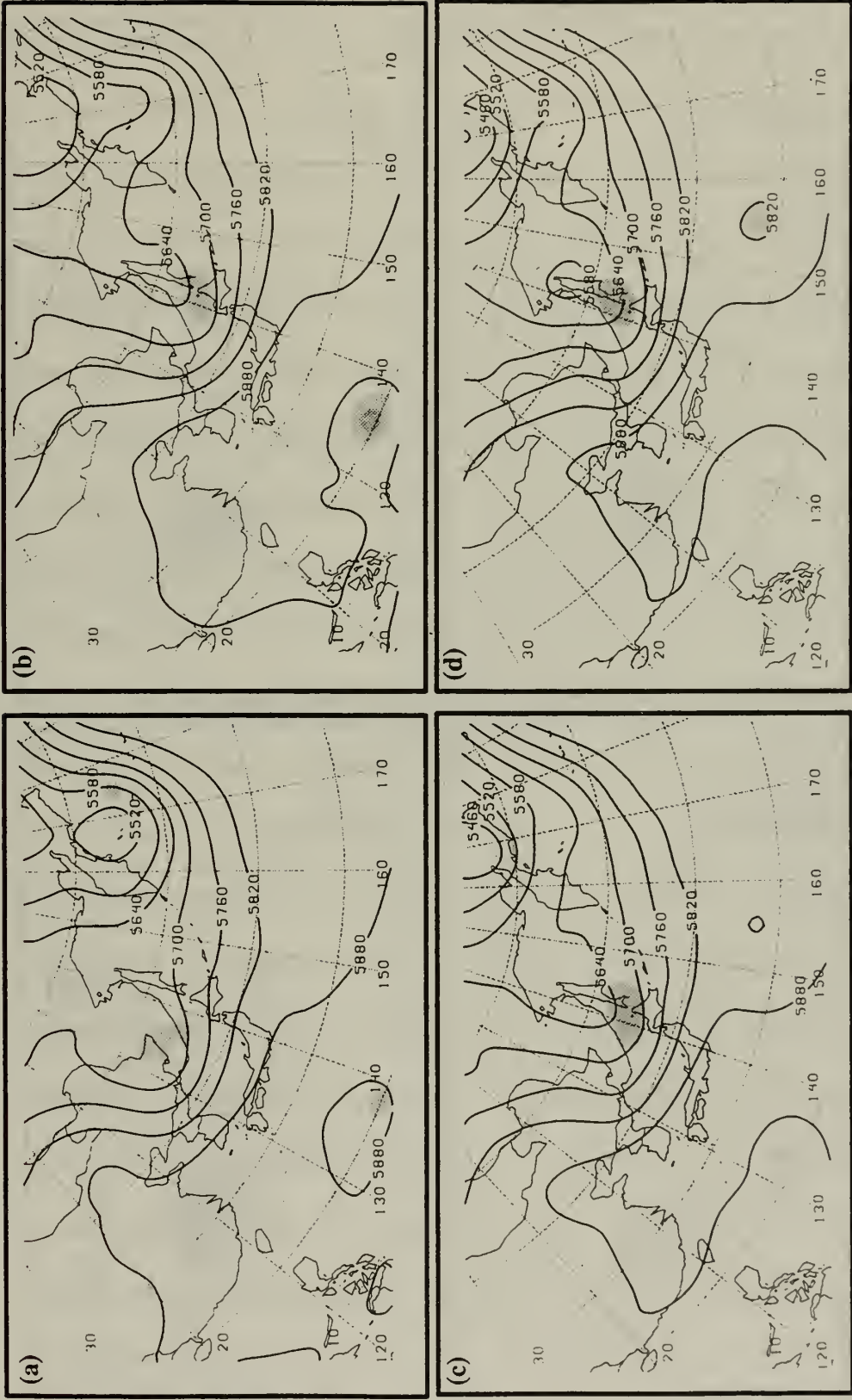
Fig. 34. Transformation of Joy depicted in NOGAPS (a) 72-h forecast, (b) 48-h forecast, (c) 24-h forecast, and (d) verifying analysis for 0000 UTC 4 August 1996. The 500-mb height contours (solid, 60 m) are shown with superposed SLPs at 4-mb intervals indicated by gray shades decreasing from 1004 mb.

71
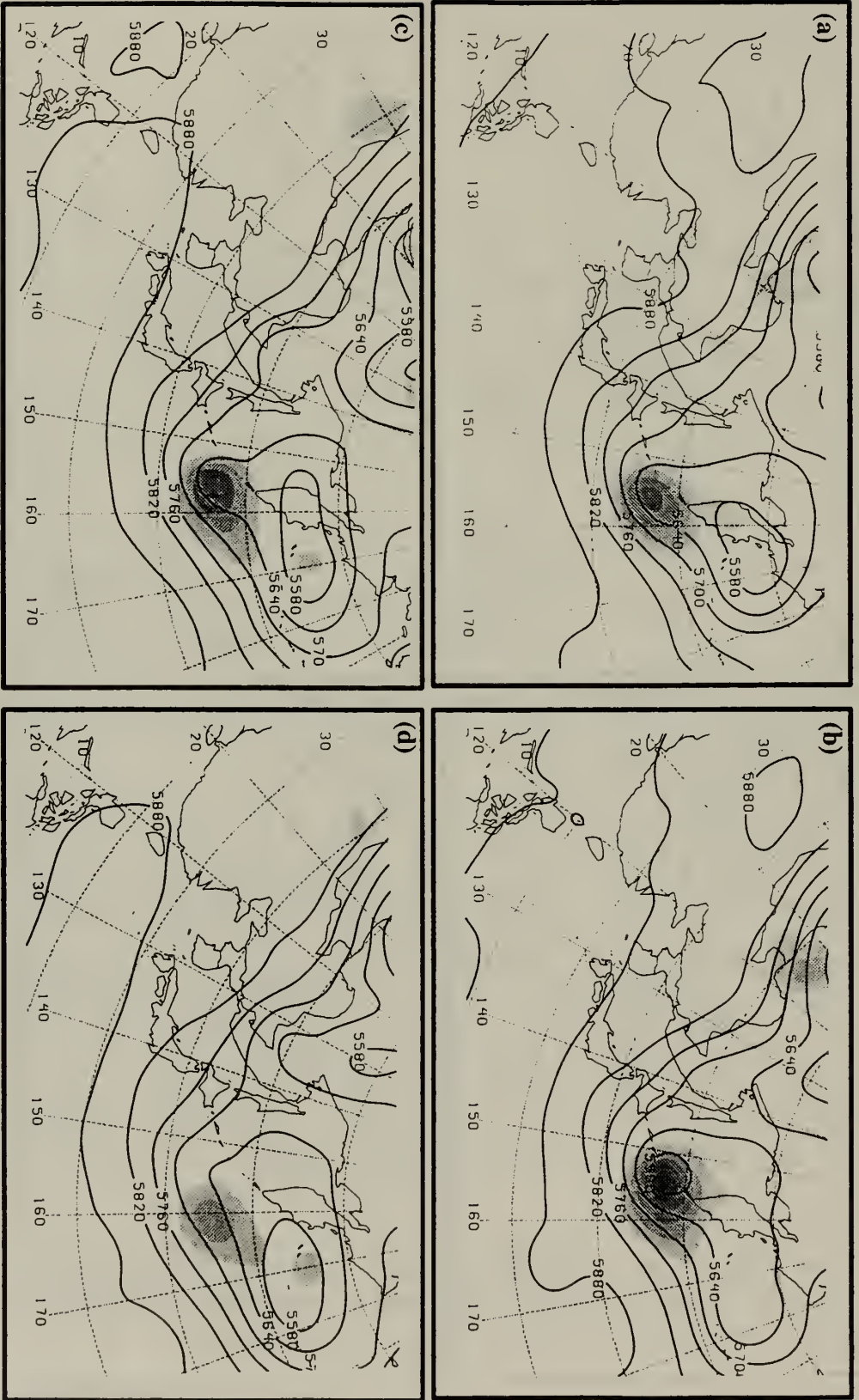
Fig. 35. As in Fig. 34, except for Kirk on 0000 UTC 17 August 1996.

72

No other 1996 cases demonstrated consistent negative impact on 500-mb NOGAPS anomaly correlation scores for a single day at all forecast times. Rather, some cases seemed to be well forecast. For example, Tom (September 1996) transformed during a period of NOGAPS 500-mb anomaly correlation scores that were one standard deviation above the mean at 24-, 48-, 72- and 96-h. Although 500-mb heights associated with this transformation were well forecast, the SLP was not. Therefore, the remaining five non-dissipating 1996 cases were examined to reveal surface track error and SLP error associated with NOGAPS forecasts of ET. Although NOGAPS generally forecast the correct track in these five cases, the forecast position lagged behind the verification position by 100 to 200 n mi. Starting with the synoptic time closest to or coincident with designation by JTWC as extratropical and continuing for the next 60 h, NOGAPS 24-, 48- and 72-h SLP forecast errors were calculated (Fig. 36) for these cases (Dan in July, Orson, Tom and Violet in September, and Yates in October). Since these are all deepening cyclones, negative errors in SLP values indicate an overforecast, i.e., too deep of a SLP. Positive errors in SLP indicated forecasts where NOGAPS underforecast the deepening of the storm. Notice in Fig. 35 the distinct tendency for NOGAPS to overforecast the SLP deepening for up to 42 h after JTWC designated the storm to be extratropical. Then, NOGAPS badly underforecast the SLP over the next 18 h. This tendency was especially demonstrated in three rapidly deepening cases of 1996 (Orson, Tom and Yates), with overforecasts of -4 to -8 mb, followed by underforecasts during re-intensification of 12 to 16 mb. Although not included in Fig. 36, the other two rapidly deepening cases of the 1994-96 data set (Melissa in September 1994 and Oscar in September 1995) had similar NOGAPS SLP forecast errors as did Orson, Tom, and Yates during 1996.
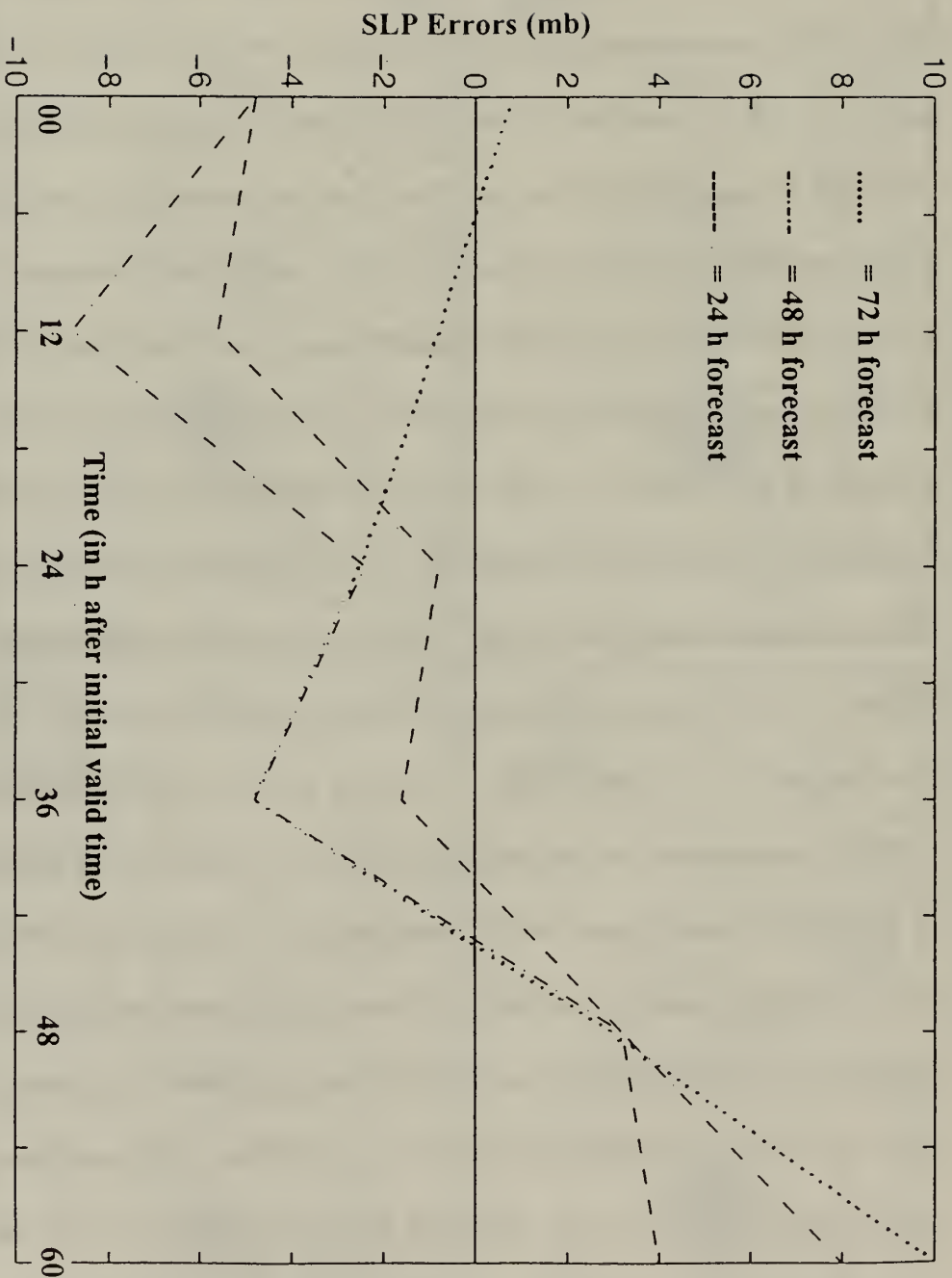
Fig. 36. The NOGAPS SLP forecast errors (24-h, dashed; 48-h, dash-dot; 72-h, dotted) for the five non-dissipating cases of ET during 1996. Time shown in h starting with first synoptic time either after or coincident with JTWC's designation of the storm as extratropical.

The implication is that during the period of transformation preceding rapid deepening cases, the SLPs are likely to be overforecast by NOGAPS. Once re-intensification begins, NOGAPS severely underforecasts the explosive development of these storms. That NOGAPS severely underforecasts the rapid deepening of explosive extratropical cyclogenesis is not surprising, but this change from overforecasts to underforecasts was not anticipated. In these cases of explosive re-intensification, a forecaster relying on NOGAPS could be misled by the tendency of NOGAPS to overforecast ET as transformation is completed, and subsequently predict that the storm will continue to be less deep than depicted by NOGAPS forecasts in the next model run. Then, as re-intensification is about to begin, the forecaster might not be prepared for the rapid deepening that follows, and might fail to anticipate re-intensification at a time when NOGAPS is likely to underforecast it significantly. Therefore, forecasts of the strength and size of the mid-latitude cyclones that results from ET are liable to be even worse than forecast by NOGAPS.

Given the destructive potential of these cases as demonstrated in Chapter III.C, forecasters must be aware of this potential error tendency associated with NOGAPS so that cases of rapid re-intensification can be better predicted. Unfortunately, there is no characteristic SLP forecast error that can be used to distinguish between rapidly deepening and non-rapidly deepening cases of ET before re-intensification. Therefore, forecasters must use satellite imagery and 200-mb NOGAPS analyses to first determine if rapid re-intensification is possible. An additional tool might be the classification of the storm as either

EOF-3 negative or EOF-3 positive during transformation, since storms in the EOF-3 negative pattern during transformation are more likely to deepen rapidly. Then, forecasters must closely monitor the progress of re-intensification, and if rapid deepening is forecast, realize that NOGAPS is likely to severely underforecast its intensity.

V. DISCUSSION AND SUMMARY

It has been demonstrated that the conceptual model of MS is inadequate to describe these 26 definitions of ET during 1994-96. The definitions of compound and complex transitions by MS do not reflect observations of ET in satellite imagery or in the NOGAPS analyses. Furthermore, the MS conceptual model fails to account for or describe a whole class of transitions that do not fit these strict, exclusive definitions. Because the conceptual model of MS is based on surface pressure patterns only, it fails to acknowledge the role of the mid- or upper-tropospheric circulations in ET. Lastly, this model does not describe and is not consistent with the present understanding of the thermodynamics and dynamics that govern ET.

Based on the evidence and conceptual model presented in Chapter III.A, it is proposed that ET is composed of two distinct stages--a *transformation* (Fig. 8b), and then a *re-intensification*. Cases that do not re-intensify are described as having failed ET, and are defined to be dissipators. Almost all (24 of 26) cases of ET in this study appear to have completed transformation in the same basic manner, as evidenced by satellite imagery and NOGAPS analyses. The two exceptions from this common transformation appearance were cases that made landfall, where topographic effects, and larger friction combined with the drier inflowing air over land, made the dissipation process more rapid. Therefore, a conceptual model of the cloud signatures was proposed to describe the process of transformation during ET over the ocean (Fig. 8). The process of transformation is described in terms of thermodynamic and dynamic changes based on NOGAPS analyses. A key

assumption is that high lower-troposphere I^2 values of a mature TC must decrease before transformation can begin. Until then, the TC should exhibit high resistance to radial motions and should be expected to resist direct momentum interaction with surface fronts and troughs. Indeed, these surface features were not observed in this sample to intersect, or cut through the TC.

At some point in its poleward track, the TC will begin to draw colder, drier air into its surface circulation. This ingestion typically occurs to the south and east of the storm center, with the air stream originating either from behind a cold front, from a continental source, or from oceanic regions with low sea-surface temperatures (SSTs). This inflow of cold, dry air is proposed to be the reason for the first stage in the transformation from a TC to a mid-latitude cyclone, which is the observed decrease in deep convection to the south and east of the center of the TC (Fig. 8b). The decrease in energy supply, as represented by the asymmetry in deep convection, weakens the TC warm-core, with subsequent reduction in lower-tropospheric winds and a decrease in lower-tropospheric I^2 values. During the stage when the IR satellite imagery revealed decreased convection south and east of the TC center, the corresponding NOGAPS analyses had increasing SLP and decreasing surface winds. The conceptual model implies that this diminished resistance to radial deflections permits an accelerated intrusion of cold, dry air, which further reduces lower-tropospheric I^2 values and hastens the decay of the TC. Formation of a dry slot that spreads in time (Fig. 8c) follows this systematic decrease in deep convection in the southeast quadrant. The corresponding NOGAPS analyses showed continued increase in SLP with further weakening of surface winds, and a change from a closed 500-mb circulation to an open wave.

The next stage in the conceptual model based on IR satellite imagery is that nearly all deep convection ceases to the south and east of the TC, and an overrunning-type cloud shield is present on the poleward side. The corresponding NOGAPS analyses indicate completion of transformation as expected from the thermal wind relationship (3.1), the wind speeds then increase with height from the surface to 500 mb, rather than decrease with height as in the earlier TC stage.[6]

This sample of ET cases included a variety of initial TC intensities and the transformed baroclinic cyclone remnants had a variety of intensities. Since all cases of ET over the ocean appeared to transform similarly in IR imagery, it is not evident that satellite imagery interpretation will be an effective tool for determining the intensity of a storm during transformation.

Following the first stage of transformation of the TC into a baroclinic low, the second stage involves either a re-intensification, or a further decrease in intensity or dissipation. It is hypothesized that a source of upper-level divergence or PVA is required if this extratropical cyclone is to re-intensify through the Petterssen "Type-B" extratropical cyclogenesis model. Based on the evidence provided in Chapter III.B, it is proposed that the second stage re-intensification depends almost exclusively on the nature of the mid-latitude 200-mb circulation. If the transformed baroclinic circulation becomes phased properly with jet streaks or diffluent troughs in the 200-mb flow, and thus become vertically coupled with areas of

---

[6]Molinari et al. (1995) describe a scenario where decreased inner-core convection is responsible for weakening the TC upper-tropospheric anticyclone, which makes the TC more susceptible to upper-level shear and leads to transition.

divergence in the upper troposphere, a re-intensification will follow according to the Petterssen "Type-B" extratropical cyclogenesis model. Each case of ET in this sample that subsequently re-intensified did indeed become coupled in the vertical with a region in the 200-mb circulation that implied upper-tropospheric divergence, and therefore supported cyclogenesis. Those cases that did not re-intensify following ET transformation either lacked favorable 200-mb support, or were located beneath a region of 200-mb convergence. These storms failed ET and simply dissipated.

It was also demonstrated that the outflow from a large TC may affect the mid-latitude 200-mb circulation to produce an environment that is even more favorable for eventual re-intensification following the transformation stage of ET. Furthermore, this interaction of the outflow of a large TC with a mid-latitude jet stream may also impact the re-intensification of the remnants of another TC downstream that had also experienced transformation. In these special cases, if it is close enough, the outflow of the western (upstream) TC produced an environment at 200 mb that is more favorable for the re-intensification of the eastern (downstream) storm that had also undergone the ET transformation stage.

The re-intensification stage is defined to be complete when the mid-latitude cyclone has reached its peak intensity (minimum SLP). The whole process of ET, from beginning of transformation to end of re-intensification, took an average of 92 h to complete. ET can take as little as 42 h (as it did in the case of Violet in September 1996) or as long as 180 h (as in the case of Melissa in September 1994) to complete. Not including the dissipators in this sample, the 11 storms that transformed within 600 n mi of land completed ET in an average of 75 h, while the six that completed ET over open ocean completed ET in an average of 123

h. It is possible that increased baroclinity near the coast of Asia and Japan, together with drier inflow from over the Asian continent, played a role in the more rapid completion of ET in cases that transformed close to shore. The re-intensified storms in the second stage of ET can, in extreme cases, be quite dangerous. In Chapter III.C, both NOGAPS analyses and scatterometer winds were used to illustrate that large areas of gale-force winds were associated with the five most intense cases of ET during 1 July through 31 October 1994-1996. The most intense case (Oscar) produced areas of gale- and storm-force winds that were about as large as were associated with its STY stage about four days earlier.

These ET cases have also been classified by Prof. Pat Harr according to characteristic 500-mb patterns into which a transforming TC is translating. A *meridional* transition is defined to occur when the transforming TC moves into an EOF-3 positive 500-mb pattern with a primary low to the northwest and a high amplitude subtropical ridge to the east. A *zonal* transition is defined to occur when the transforming TC moves into an EOF-3 negative 500-mb pattern with a primary low to the northeast and a low amplitude subtropical ridge. Based on these definitions and the discussion in Chapter III.D, meridional (zonal) transitions tend to have meridional (zonal) tracks and are less (more) likely to re-intensify vigorously and become deep, powerful mid-latitude cyclones.

Finally, some cases of ET are demonstrated to negatively impact the 500-mb anomaly correlation score of the NOGAPS forecasts in the North Pacific sector, i.e., producing significant forecast errors during the second stage of ET. Two types of NOGAPS forecast errors occurred frequently during ET. First, the NOGAPS model tended to overforecast ET cases in which the transformed TC remnants appeared to merge with a pre-existing mid-

latitude trough. That is, the NOGAPS model erroneously predicted that the transformed TC would become too deep and too large at the surface and at 500 mb during the re-intensification stage of ET. It is possible that this error is caused by continued use of TC synthetic observations in NOGAPS during the latter part of transformation. These synthetic observations could force NOGAPS to overforecast the intensity of the transforming storm. Second, the NOGAPS model poorly handled those ET cases that resulted in the most powerful, rapidly deepening extratropical cyclones. In these cases, NOGAPS overforecast their intensity during the latter part of the transformation stage, then severely underforecast their re-intensification. Although the NOGAPS model generally forecast well the paths of storms undergoing ET, it was occasionally behind the actual position.

The implications of these results for forecasters are significant. First, the new proposed definition of ET departs significantly from the conceptual model of MS. ET is described as a process that is not instantaneous, but occurs in two stages and involves distinctly different thermodynamic and dynamic processes than are implied in the MS conceptual model. This description of ET is three-dimensional and recognizes that the upper- and mid-troposphere contribute significantly to ET during both stages. An attempt to force all cases into the conceptual model of MS revealed many deficiencies and required a very loose interpretation. In the new proposed conceptual, model the definitions of the transformation stage and the re-intensification stage described well all cases of ET over open ocean in this 1994-96 sample. Most importantly, this description of ET in terms of two distinct stages and two distinct synoptic 500-mb patterns during the transformation stage appear to be consistent with the thermodynamic and dynamic processes that are believed to

be responsible for ET. That is, these definitions are consistent with observations of ET in satellite imagery and NOGAPS analyses from which may be inferred the physical processes that occur during ET.

It is believed that the discussion in Chapters III and IV can provide forecasters with rules of thumb that might improve the accuracy of the forecasts during the two stages of ET. A suggested first step is to begin with the systematic approach to TC track forecasting of Carr and Elsberry (1994). Forecasters should closely follow the evolution of a TC as it progresses from the Poleward pattern/Poleward-Oriented region (P/PO) toward a Poleward pattern/Accelerating Westerlies region (P/AW), or from a Standard pattern/Weakened Ridge into a Standard pattern/Accelerating Westerlies region (S/AW). These transitions should be closely monitored for eventual commencement of ET. Although not observed in this sample, storms in a Gyre pattern/Poleward-Oriented or Accelerating Westerlies region (G/PO or G/AW) or in a Multiple pattern/Accelerating Westerlies region (M/AW) may also experience ET.

The conceptual model (Fig. 8) for interpreting satellite imagery of transformation can be used together with NOGAPS analyses that show systematic decrease in SLP, surface wind, and increase in 500-mb heights. As transformation progresses, the forecaster should notice the appearance of a 500-mb open wave, and a wind maximum to the southeast of the TC in 500-mb analyses. Finally, as SLP and surface winds continue to decrease, wind speeds should increase from the surface to 500 mb, which indicates through the thermal wind relationship in (3.1) that the transformation is nearly complete and that the storm is acquiring a cold core.

As the transformation continues, forecasters must also be aware of the character of the 500-mb and 200-mb flow patterns into which the TC is translating. The position of any primary lows relative to the location of the transforming TC, as well as the strength of the subtropical ridge to the east, should be assessed to determine whether a meridional or zonal transition should be anticipated. This information should enable forecasters to make an initial prediction of the track and likely intensity of the storm after completion of ET. Close scrutiny of upper-tropospheric analyses and forecasts should permit forecasters to identify and predict ET cases likely to deepen more vigorously based on the location of jet streaks and diffluent troughs.

Forecasters must also be aware of when NOGAPS is likely to either overforecast or underforecast the re-intensification stage of ET. Forecasters should anticipate that NOGAPS may first overforecast, then underforecast the progress of ET in cases of rapidly deepening storms as described earlier. They should remain vigilant and constantly monitor satellite imagery and NOGAPS surface, 500-mb and 200-mb analyses to assess model accuracy and determine any NOGAPS model trend toward overforecasting, while remembering that once the transformation stage is completed, that error trend may be reversed. Thus, the forecaster will be prepared if NOGAPS suddenly underforecasts explosive extratropical cyclogenesis during the re-intensification stage.

There are many areas of future research that could be conducted as a result of this study. A quantitative diagnosis of cases with significant NOGAPS forecast errors is needed to determine their cause, so that improvements in the model or in the initial condition specification might be suggested. This effort should also determine the impact, if any, of

synthetic TC observations on NOGAPS overforecasts during the transformation stage of ET. Incorporating more cases of ET into the current data set and conducting diagnostic case studies should provide a better test for the validity of the definitions of transformation and re-intensification stages of ET presented herein. Examination of water vapor imagery should reveal the progress of dry air intrusion into the TC during transformation. Additional case studies will establish whether the characteristic 500-mb patterns identified through EOF analysis of the present sample will apply in indicating the subsequent tracks and intensities during those cases of ET. Additional research could determine the role of upper-level shear in ET. Diagnostic case study could be used to determine quantitatively the effect a large TC might have on mid-latitude upper-tropospheric flow, and whether a large TC can build its own upper-level support for re-intensification. Finally, real-time implementation of the forecaster rules of thumb described above could be evaluated for their effectiveness in improving forecasts and warnings during ET.

LIST OF REFERENCES

Brand, S., and C. P. Guard, 1978: Extratropical storm evolution from tropical cyclones in the western North Pacific Ocean. Tech. Rep. TR 78 02, Naval Environmental Prediction Research Facility (Now NRL-Monterey), 20 pp.

Carr, L. E., III, and R. L. Elsberry, 1994: Systematic approach to tropical cyclone track forecasting. Part I. Approach overview and description of meteorological basis. Tech. Rep. NPS-MR-94-002, Naval Postgraduate School, Monterey, CA 93943, 96 pp.

DiMego, G. J., and L. F. Bosart, 1982: The transformation of tropical storm Agnes into an extratropical cyclone. Part I: The observed fields and vertical motion computations. *Mon. Wea. Rev.,* **110,** 385-411.

Foley, G. R., and B. N. Hanstrum, 1994: The capture of tropical cyclones by cold fronts off the west coast of Australia. *Wea. Forecasting,* **9,** 577-592.

Harr, P. A., R. L. Elsberry, P. M. Klein, T. F. Hogan, and W. M. Clune, 1996: Impacts of the extratropical transition of tropical cyclones on midlatitude circulation systems. *Preprints, 15th Conference on Weather Analysis and Forecasting,* Norfolk, VA, Amer. Met. Soc., Boston, MA 02108, 509-512.

JTWC, 1994: Annual Tropical Cyclone Report, Joint Typhoon Warning Center, COMNAVMARINAS PSC 489 Box 12, FPO AP 96536-0051, 337 pp.

JTWC, 1995: Annual Tropical Cyclone Report, Joint Typhoon Warning Center, COMNAVMARINAS PSC 489 Box 12, FPO AP 96536-0051, 289 pp.

Klein, P. M., P. A. Harr, and R. L. Elsberry, 1997: Extratropical transition of western north Pacific tropical cyclones. *Preprints, 22nd Conference on Hurricanes and Tropical Meteorology,* Ft. Collins, CO, Amer. Met. Soc., Boston, MA 02108, 364-365.

Matano, H., and M. Sekioka, 1971: Some aspects of the extratropical transformation of a tropical cyclone. *J. Meteor. Soc. Japan,* **49,** 736-743.

Molinari, J., S. Skubis, and D. Vollaro, 1995: External influences on hurricane intensity. Part III: Potential vorticity structure. *J. Atmos. Sci.,* **52,** 3593-3605.

Sinclair, M. R., 1993: Synoptic-scale diagnosis of the extratropical transition of a southwest Pacific tropical cyclone. *Mon. Wea. Rev.,* **121**, 941-960.

Willoughby, H. E., 1979: Forced secondary circulation in hurricanes. *J. Geophys. Res.,* **84**, 3173-3183.

INITIAL DISTRIBUTION LIST

9.   Commander. 1
     Naval Meteorology and Oceanography Command
     1020 Balch Boulevard
     Stennis Space Center, MS 39529-5005

10. Commanding Officer 1
     FLENUMMETOCCEN
     7 Grace Hopper Avenue Stop 4
     Monterey, CA 93943-5501

11. Superintendent 1
     Attn: Dr. Tim Hogan
     Naval Research Laboratory
     7 Grace Hopper Avenue Stop 2
     Monterey, CA 93943-5502

12. Chief of Naval Research. 1
     800 N. Quincy Street
     Arlington, VA 22217

13. Commanding Officer. 1
     NAVPACMETOCCEN
     Box 113
     Pearl Harbor, HI 96860-5050